Theoretical Aspects of Isotope Effects on Nuclear Shielding

CYNTHIA J. JAMESON

Department of Chemistry, University of Illinois at Chicago, Chicago, Illinois, USA

H. JÖRG OSTEN

Academy of Sciences of the GDR, Central Institute of Physical Chemistry, Berlin, German Democratic Republic

I. INTRODUCTION

Isotope shifts have long been observed in high resolution NMR in the gas phase, in liquids and in solutions. There are large shifts associated with the mass dependence of rate constants for chemical reactions or changes in

ANNUAL REPORTS ON NMR SPECTROSCOPY
VOLUME 17 ISBN 0-12-505317-7

conformational structure. We do not consider these equilibrium or kinetic isotope effects, only intrinsic isotope effects. The review by Batiz-Hernandez and Bernheim[1] and the more recent one by Hansen[2a] in this series include most of the published data up to 1982. There is also a recent discussion of ^{13}C isotope shifts by Forsyth.[2b] Here we review the theory underlying the interpretation of isotope shifts in NMR. The interpretation of isotope shifts involves a consideration of the vibrational and rotational averaging of nuclear shielding. For this reason the isotope shift is intimately related to the observed temperature dependence of nuclear shielding in the gas phase in the zero-pressure limit. These two measurable properties share the same electronic factors - the change in shielding with bond extension or bond angle deformation.

We follow the notation introduced by Gombler[3] for the isotope shift observed for nucleus A upon substitution of the neighbouring ^{m}X isotope in the molecule with the heavier $^{m'}X$ isotope:

$$ {}^{n}\Delta A(^{m'/m}X) = \frac{\nu_A(A\,{}^{m'}X\cdots) - \nu_A(A\,{}^{m}X\cdots)}{\nu_A(A\,{}^{m}X\cdots)} \qquad (m' > m) \qquad (1a) $$

where $\nu_A(A\,{}^{m'}X\cdots)$ is the resonance frequency of the A nucleus in the molecule having the heavier $^{m'}X$ isotope which is n bonds away from the observed nucleus. The molecules $(A\,{}^{m'}X\cdots)$ and $(A\,{}^{m}X\cdots)$ are isotopomers. The isotope shift can also be written in terms of the nuclear shielding difference:

$$ {}^{n}\Delta A(^{m'/m}X) = \sigma^{A}(A\,{}^{m}X\cdots) - \sigma^{A}(A\,{}^{m'}X\cdots) \qquad (1b) $$
$$ = \sigma - \sigma^{*} $$

where the asterisk applies to the heavy isotopomer. Just as for spin–spin couplings, this notation becomes ambiguous when A and X are atoms in cyclic compounds in which there are at least two paths connecting the observed nucleus and substituted atom. In this case the observed quantity is an isotope shift corresponding to two or more bond paths.

There are several general observations which have been made about magnitudes and signs of isotope shifts:[1]

(i) Upon substitution with a heavier isotope the NMR signal of the nearby nucleus usually shifts towards lower frequencies (higher shielding). Thus, as defined in equation (1), isotope shifts are generally negative in sign.

(ii) The magnitude of the isotope shift is dependent on how remote the isotopic substitution is from the observed nucleus. Although there are exceptions, one-bond isotope shifts are larger than two-bond or three-bond isotope shifts.

(iii) The magnitude of the shift is a function of the observed nucleus and reflects its chemical shift range.

(iv) The magnitude of the shift is related to the fractional change in mass upon isotopic substitution.

(v) The magnitude of the shift is approximately proportional to the number of equivalent atoms which have been substituted by isotopes. In other words, isotope shifts exhibit additivity.

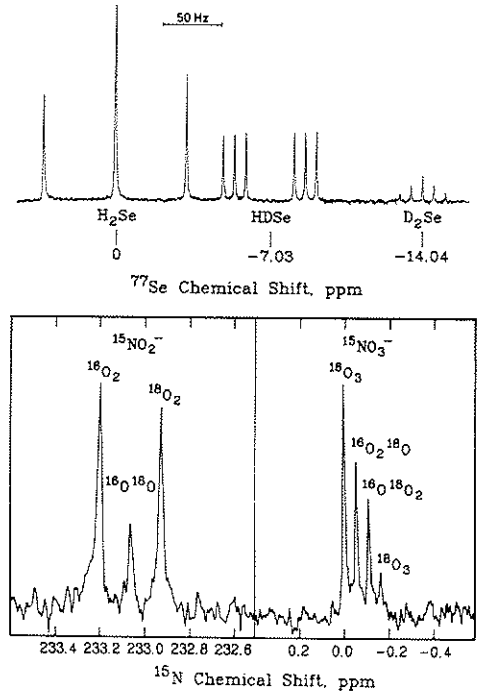

FIG. 1. ^{77}Se FT NMR spectrum of a mixture of H_2Se, HDSe and D_2Se, and ^{15}N spectra of $^{18/16}O$ derivatives of NO_2^- and NO_3^-. From references 4 and 5, respectively, with permission.

Examples of isotope shifts in Fig. 1 illustrate these trends. The ^{77}Se shifts on D substitution in H_2Se are proportionately large (−7.02 ppm per D) compared to ^{17}O shifts on D substitution in H_2O (−1.54 ppm per D), reflecting the large chemical shift range of ^{77}Se compared to ^{17}O. ^{15}N shifts in NH_3 on D substitution (−0.65 ppm per D) are large compared to that for ^{15}N on ^{18}O substitution in NO_2^- (−0.138 ppm) showing the more favourable fractional mass changes in D substitution compared to O substitution. Figure 1 also clearly shows the additivity of isotope shifts; the isotope shift is proportional to the number of substituted atoms, giving rise to

spectra exhibiting equal spacing of characteristic peaks for each isotopomer. We shall discuss the theory underlying these general observations.

There are some less general trends which have been observed, correlating isotope shift with molecular structure.

(a) One-bond isotope shifts tend to increase with increasing bond order[6-8] and decreasing bond length[3] between the observed nucleus and the substituted atom.

(b) The magnitudes of isotope shifts in similar bonds increase with the magnitude of the spin–spin coupling between the observed nucleus and the substituted atom.[9-11]

(c) The magnitudes of one-bond isotope shifts correlate with the chemical shift of the observed nucleus, i.e. the less shielded nuclei have larger isotope shifts.[11-13]

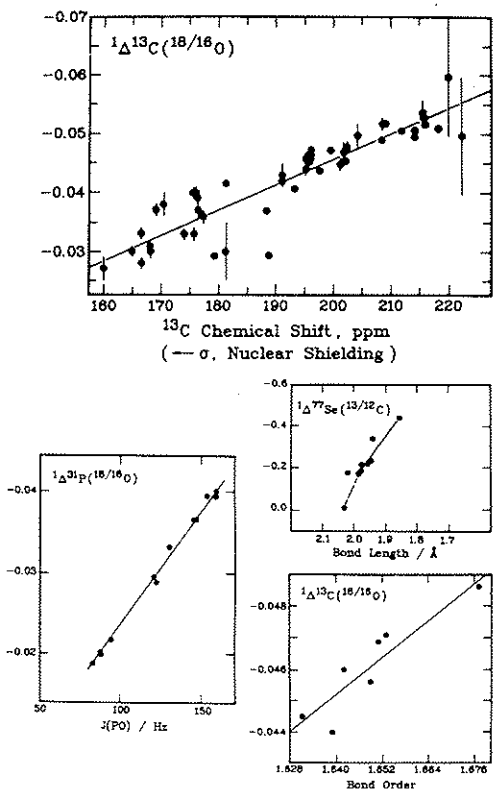

FIG. 2. Correlations between one-bond isotope shifts and various indices of the chemical bond: bond order, bond length, spin–spin coupling, nuclear shielding. From references 12, 10, 3 and 6, with permission.

(d) There is a lone pair effect on the isotope shifts. A nucleus with a σ lone pair tends to have a larger isotope shift in comparison with a related bond in which there is no lone pair on the observed nucleus; for example, the isotope shift for ^{15}N in NH_3 (−0.65 ppm per D) with one lone pair may be compared to that in NH_4^+ (−0.307 ppm per D) with zero lone pairs, or ^{15}N in NO_2^- can be compared with ^{15}N in NO_3^- (see Fig. 1).[14]

(e) The isotope shift tends to be larger when electronegative substituents are introduced at the nuclear site.[8]

Trends (a)–(c) are demonstrated in Fig. 2. These trends are interesting and require interpretation with a suitable theory. It is important to know which aspects of isotope shifts are due to dynamical factors (to rovibrational averaging) and which aspects can be attributed to electronic factors (changes in nuclear shielding with bond extension or bond angle deformation). If the theory can sort out the former, isotope shifts can be used to extract the latter, thus providing chemically interesting information which would make the isotope shift an easily measurable index of the chemical bond.

II. ROVIBRATIONAL EFFECTS ON NUCLEAR SHIELDING

The effects of intramolecular dynamics (vibration and rotation) on nuclear shielding were theoretically predicted by Ramsey[15] and have been observed in two ways. First, there is an observable temperature dependence of the resonance frequency even for the "isolated" molecule (apart from the temperature dependence due to intermolecular interactions).[16] Second, there is an observable shift upon isotopic substitution of neighbouring nuclei. Both are effects of differences in averaging over nuclear configuration as the molecule undergoes vibration and rotation. The temperature dependence of nuclear shielding is observed in the dilute gas phase, where the average shielding can be written as a virial expansion in the gas density ρ,

$$\sigma(T, \rho) = \sigma_0(T) + \sigma_1(T)\rho + \sigma_2(T)\rho^2 + \cdots \quad (2)$$

The intermolecular effects are contained in the density dependent terms.

The nuclear shielding in an "isolated" molecule, $\sigma_0(T)$, is actually observed as the nuclear shielding in the limit of pressure approaching zero. Yet, the pressure must be high enough so that collisional interactions cause a given molecule to pass through a representative number of thermally accessible vibrational and rotational states in a time that is short compared to the reciprocal of the NMR frequency difference between nuclei in different rovibrational states. Thus, mathematically speaking, one does not extrapolate the results to a true zero pressure, but to a pressure so low that collisional deformation of the molecule no longer contributes to σ, while there are still

enough collisions to provide the required rate of transition between vibrational and rotational states.

The observed isotropic nuclear shielding of a nucleus in an isolated molecule, $\sigma_0(T)$, is a statistical average of the nuclear magnetic shielding tensor over all possible orientations of the molecule in the magnetic field. It is also an average over all possible rovibrational states of the molecule weighted according to the fraction of molecules occupying that state at ti t temperature. Thus, the value of the shielding of a nucleus in a gas sam e extrapolated to zero density at a given temperature is a weighted avera of the values characteristic of each occupied state.

The average shielding for a given rovibrational state is different for ea a of several isotopically related species because the masses enter into e solution of the vibrational–rotational hamiltonian. Thus, the thermal aver e shielding $\sigma_0(T)$ is different for the isotopomers. These differences e measured as isotope shifts. It has been found that mass effects on in - molecular interactions (except in hydrogen-bonding or complex-formati.) are not significant, i.e. the mass dependence of $\sigma_1(T)$ in equation (2) is small.[17] Therefore, even isotope shifts measured in condensed phase can sometimes be interpreted as the differences between $\sigma_0(T)$ values of the isotopically related species.

A. Basic principles

The Born–Oppenheimer approximation allows us to consider the nuclear motion in rotation and vibration separately from the electronic motion. Within the Born–Oppenheimer approximation, we can consider a shielding surface which gives the values of nuclear shielding at rigidly fixed nuclear configurations. The interpretation of the experimentally observed nuclear magnetic shielding then involves the two surfaces, the potential energy surface and the nuclear shielding surface, with simultaneous averaging on both surfaces. Figure 3 shows the proton shielding surface[18] and the potential energy surface of the H_2^+ molecule.[19] The shielding surface gives the ^1H nuclear shielding calculated with the relativistic theory for fixed nuclear configurations. For a given rovibrational state, there will be a characteristic average shielding which can be evaluated from the vibrational and rotational wavefunctions and the nuclear shielding function such as the one shown in the figure. The vibrational levels of the HD^+ and D_2^+ isotopomers (which have lower vibrational frequencies than H_2^+) sit lower in the potential well and thus will give different average values of proton shielding. In this case the shielding surface is known for a wide range of nuclear configurations. For most systems, however, there is very limited information, the shielding surface being calculated for just a few points in the vicinity of r_e. For semirigid molecules that we often observe in NMR (excluding molecules

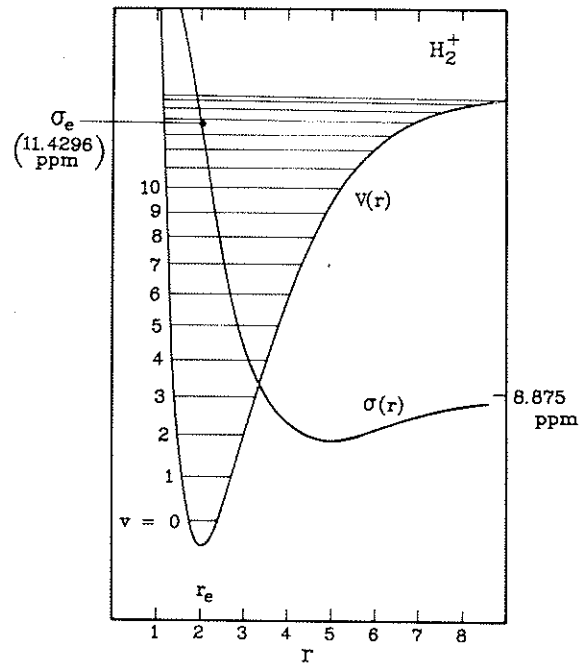

FIG. 3. The ^1H shielding surface and the potential energy surface for $^1H_2^+$. From references 18 and 19, with permission.

which are fluxional or which undergo low frequency torsion), the motions involved in the averaging take place in a small pocket of the potential energy surface close to the equilibrium configuration. Therefore this corresponds to averaging over small displacements on the shielding surface. Then it makes physical sense to expand the nuclear shielding in terms of the normal coordinates Q_s (a concept of significance only for small displacements):

$$\sigma = \sigma_e + \sum_s \left(\frac{\partial \sigma}{\partial Q_s}\right)_e Q_s + \frac{1}{2}\sum_{s,r}\left(\frac{\partial^2 \sigma}{\partial Q_r \partial Q_s}\right)_e Q_r Q_s + \cdots \qquad (3)$$

where the shielding derivatives are taken at the equilibrium configuration. The application of this equation to a general molecular electronic property (not just nuclear shielding) for a general molecular type (an asymmetric rotor) as well as for specific types (spherical tops and symmetric tops) has been formulated.[20–22] Normal coordinates are a logical choice for this expansion since methods of evaluating the average values $\langle Q_s \rangle$, $\langle Q_r Q_s \rangle$ are well known in vibrational spectroscopy. However, the derivatives of the nuclear shielding with respect to the normal coordinates are not invariant under isotopic substitution. For the purpose of discussing the isotope shift

it is more convenient to expand the shielding in terms of internal displacement coordinates:

$$\sigma = \sigma_e + \sum_i \left(\frac{\partial\sigma}{\partial \mathcal{R}_i}\right)_e \mathcal{R}_i + \frac{1}{2}\sum_{i,j}\left(\frac{\partial^2\sigma}{\partial\mathcal{R}_i\,\partial\mathcal{R}_j}\right)_e \mathcal{R}_i\,\mathcal{R}_j + \cdots \tag{4}$$

where $\mathcal{R}_i$ stands for the bond displacements (Δr_i) and the bond angle deformations ($\Delta\alpha_{ij}$).

The theoretical interpretation of isotope shifts in NMR therefore involves the mass-independent electronic quantities such as

$$(\partial\sigma/\partial\mathcal{R})_e = (\partial\sigma/\partial\Delta r)_e, (\partial\sigma/\partial\Delta\alpha)_e, \ldots$$

which describe the change in nuclear shielding with bond extension or angle deformation, and the mass-dependent thermal averages $\langle\mathcal{R}_i\rangle^T$ which are $\langle\Delta r\rangle^T, \langle\Delta\alpha\rangle^T, \ldots$ and $\langle\mathcal{R}_i\,\mathcal{R}_j\rangle^T$ which are $\langle(\Delta r)^2\rangle^T, \langle(\Delta\alpha)^2\rangle^T, \langle\Delta r\,\Delta\alpha\rangle^T, \ldots$. The isotope shift is given by

$$\sigma - \sigma^* = \sum_i \left(\frac{\partial\sigma}{\partial\mathcal{R}_i}\right)_e [\langle\mathcal{R}_i\rangle^T - \langle\mathcal{R}_i\rangle^{T*}] + \frac{1}{2}\sum_{i,j}\left(\frac{\partial^2\sigma}{\partial\mathcal{R}_i\,\partial\mathcal{R}_j}\right)_e [\langle\mathcal{R}_i\,\mathcal{R}_j\rangle^T - \langle\mathcal{R}_i\,\mathcal{R}_j\rangle^{T*}] + \cdots \tag{5}$$

B. Effect of vibration and rotation on the internuclear distance

1. The vibrational average bond extension

In order to be able to evaluate $\langle\mathcal{R}_i\rangle^T, \langle\mathcal{R}_i\,\mathcal{R}_j\rangle^T, \ldots$ etc. we need a potential surface in which the vibrational motion of the molecule takes place. The known derivatives of this surface are the quadratic, cubic, etc. force constants. Normal coordinate analysis with the quadratic force constants gives the solutions to the harmonic problem whch are the harmonic frequencies (ω), the normal coordinates (Q), and the L matrix.[23] The internal displacement coordinates $\mathcal{R}_i = \Delta r_i, \Delta\alpha_{ij}$, etc. can be expressed in terms of these normal coordinates as follows:

$$\mathcal{R} = \mathbf{L}Q \tag{6}$$

where $\mathbf{L}$ is a tensor which contains the transformation coefficients between the curvilinear internal coordinates and various powers of Q. The vibrational part of Δr_i is then

$$\Delta r_i = \sum_r L_i^r Q_r + \frac{1}{2}\sum_{r,s} L_i^{rs} Q_r\,Q_s + \frac{1}{6}\sum_{r,s,t} L_i^{rst}\,Q_r\,Q_s\,Q_t + \cdots \tag{7}$$

Thus the vibrational average $\langle\Delta r\rangle_{vib}$ can be expressed in terms of $\langle Q_r\rangle$, $\langle Q_r\,Q_s\rangle$, etc. The analytical expressions for elements of the $\mathbf{L}$ tensor are given by Hoy *et al.*,[24] in which the linear terms L_i^r are identical to the elements L_{ir} of the L matrix. Equation (7) is exact, but in practice of course the series must be truncated; in general it converges well, each term being smaller than the preceding by a factor of about 10 for typical vibrational amplitudes.[25]

If the calculation is confined to the terms of the second order in equation (7), it is necessary to use the wavefunctions of the first order for obtaining the expectation values of Q_r, whereas it is sufficient to use zero-order wavefunctions for those of $Q_r\,Q_s$.[26] The quantum mechanical hamiltonian for a vibrating rotor has been derived by Wilson and Howard[27] and developed by Nielsen and others.[28,29] There are several equivalent approaches in calculating the desired expectation values from the hamiltonian. Perturbation theory methods and the contact transformation method lead to identical results. The expectation values of only totally symmetric coordinates Q_s are required:

$$\langle Q_s\rangle = -\left(\frac{h}{4\pi^2 c}\right)^{\frac{1}{2}} \omega_s^{-\frac{3}{2}}\left[3k_{sss}(v_s+\tfrac{1}{2}) + \sum_r{}' k_{srr}(v_r + g_r/2)\right] \tag{8}$$

where ω_s are the normal frequencies and k_{srr} are the cubic force constants, both in wavenumbers. g_r denotes the degeneracy of the r-th vibration. $\langle Q_r\,Q_s\rangle = 0$ if $\omega_r \neq \omega_s$ and

$$\langle Q_s^2\rangle = \left(\frac{h}{4\pi^2 c\omega_s}\right)(v_s+\tfrac{1}{2}) \tag{9}$$

These two expressions, equations (8) and (9), represent the expectation values for $\langle Q\rangle$ and $\langle Q^2\rangle$ for one given vibrational level v_s. In an NMR experiment we observe only the average values over all vibrational states for a given temperature:

$$\langle v_s + g_s/2\rangle^T = \frac{\sum_{v_s} g_s(v_s+g_s/2)\exp[-E(v_s)/kT]}{\sum_{v_s} g_s \exp[-E(v_s)/kT]} \tag{10}$$

If we assume harmonic energy levels in evaluating the thermal average in equation (10), the infinite sums are calculable in closed form:[30]

$$\langle v_s + g_s/2\rangle^T = (g_s/2)\coth(hc\omega_s/2kT) \tag{11}$$

A second approach is that of Bartell.[31] The quantum mechanical law of motion applied to a wave packet is given, in Cartesian coordinates, by

$$m\frac{d^2\langle x\rangle}{dt^2} = -\left\langle\frac{\partial V}{\partial x}\right\rangle \tag{12}$$

In our molecular applications the system will be in stationary states or an

equilibrium distribution among stationary states. Since the space average displacement $\langle x \rangle$ is independent of time in such a system, it follows that the space average force is zero, or

$$\langle \partial V/\partial x \rangle = 0 \tag{13}$$

Equation (12) is the molecular quantum mechanical analogue to the Ehrenfest theorem.[32] We use the Cartesian displacement coordinates, rather than internal coordinates, because the latter do not necessarily form a complete set of coordinates. For the same reason it is not always possible to use the set of symmetry coordinates. We adopt local molecular Cartesian frames such that the z_i-axis lies along the direction of the A–X_i bond at its equilibrium position and the x-axis is on the plane X_i–A–X_j and perpendicular to z_i. Now we can express the internal displacement coordinates in terms of the Cartesian displacement coordinates:

$$\Delta r_i = \Delta z_i + [(\Delta x_i)^2 + (\Delta y_i)^2]/2r_i + \cdots \tag{14a}$$

$$\Delta \alpha_{ij} = \frac{\Delta x_i}{r_i} + \frac{\Delta x_j}{r_j} - \frac{\Delta x_i \, \Delta z_i}{r_i^2} - \frac{\Delta x_j \, \Delta z_j}{r_j^2} + \cdots \tag{14b}$$

Using equation (14) we are able to calculate the derivatives of the internal coordinates with respect to Δz_k, for example:

$$(\partial \Delta r_i/\partial \Delta z_k) = \delta_{ik} + \cdots \tag{15a}$$

$$(\partial \Delta \alpha_{ij}/\partial \Delta z_k) = -\frac{\Delta \alpha_{kj}}{2r_k}\delta_{ik} = -\frac{\Delta \alpha_{ik}}{2r_k}\delta_{jk} \tag{15b}$$

where δ_{ij} is the Kronecker delta.

We obtain from a potential function in internal coordinates, by applying equation (13), a set of coupled equations which connect the desired mean bond displacements $\langle \Delta r_i \rangle$ and mean bond angle deformations $\langle \Delta \alpha_{ij} \rangle$ with the mean square amplitudes (MSA) of the internal coordinates in a linear way, whereas the coefficients are functions of the quadratic and cubic force constants and geometry parameters.[31,33–35,14] These MSA's (which include non-vanishing cross products) are related to the mean square normal coordinates $\langle Q^2 \rangle$ in the usual way:[36]

$$\langle \mathcal{R}_i \, \mathcal{R}_j \rangle \approx L \langle Q^2 \rangle \tilde{L} \tag{16}$$

Equation (7) can be written as[25,37]

$$\langle \Delta r \rangle = \langle \Delta z \rangle + [\langle (\Delta x)^2 \rangle + \langle (\Delta y)^2 \rangle]/2r_e + \cdots \tag{17}$$

in the same local Cartesian coordinate system as equation (14a). $\langle \Delta z \rangle$ can be identified with $\sum_r L_i^r \langle Q_r \rangle$, which represents the part of the average displacement that is along the equilibrium bond axis. Unlike a diatomic molecule, nuclear motions perpendicular to this z-axis occur in a polyatomic molecule, so we need to add $[(\Delta x)^2 + (\Delta y)^2]/2r_e$ which can be identified with $\frac{1}{2}\sum_s L_i^{ss} \langle Q_s^2 \rangle$. Thus we see in equation (7) that the first term, the average displacement parallel to the equilibrium bond axis, arises from the average displacement in the totally symmetric coordinate due to cubic anharmonicity; the next term, containing the mean square perpendicular amplitudes, involves only the harmonic potential constants and arises from the non-linear nature of the transformation from interatomic distances to normal coordinates.

Fowler[38] has shown that Bartell's approach is mathematically equivalent to the perturbation approach. However, Bartell's method has the advantage of being useful in a convenient form when the cubic force constants are not available. As originally proposed by Bartell, it has been used with a Urey–Bradley quadratic force field augmented with the cubic terms arising from a Morse anharmonicity for the stretching terms and a suitable model for the non-bonded interactions.

2. *Effects due to molecular rotation: centrifugal stretching*

As a molecule rotates, the atoms tend to move away from the centre of mass. This centrifugal distortion depends only upon the harmonic potential constants to the second-order approximation:[26]

$$\langle Q_s \rangle_{rot} = \frac{1}{8\pi^2 c^2 \omega_s^2} \cdot \sum_\alpha \frac{a_s^{(\alpha\alpha)}}{I_{\alpha\alpha}^{(e)2}} \cdot (v_1^* \, v_2^* \cdots R | (P_\alpha - p_\alpha^*)^2 | v_1^* \, v_2^* \cdots R) \tag{18}$$

where $I_{\alpha\alpha}^{(e)}$ are principal moments of inertia along the α axis in the equilibrium configuration, $a_s^{(\alpha\alpha)}$ are coefficients of the normal coordinate expansion of $I_{\alpha\alpha}$, P_α is the component of the total angular momentum along the α axis, and p_α stands for the vibrational angular momentum. The asterisks denote the angular momentum associated with the degenerate vibrations, and R stands for the overall rotation. The complete expression for $\langle Q_s \rangle$ is then obtained by adding the rotational contribution given by equation (18) to the vibrational contribution given in equation (8). Explicit expressions for $a_s^{(\alpha\alpha)}$ have been derived for specific molecular types,[28] and equation (18) can be written in terms of the rotational quantum numbers for specific molecular types.[26] Averaging over these rotational levels in a similar manner to equation (10) can thus be carried out to give $\langle Q \rangle^T_{rot}$, taking into account the appropriate nuclear spin statistical weights. Except for the H_2 molecule, in which the rotational levels are widely spaced and nuclear spin statistics play an important role in the averaging, the thermal average centrifugal stretching can be calculated classically. The assumption that the spacing of rotational levels is sufficiently small compared with kT

(which is easily satisfied except for the case of extremely low temperatures) allows us to use the law of equipartition of energy for calculating the average value of the angular momentum. If the rotational energy is written in the form

$$E_{\text{rot}} = \sum_{\alpha} (P_\alpha - p_\alpha^*)^2 / 2I_{\alpha\alpha}^{(e)} \tag{19}$$

we obtain

$$\langle (P_\alpha - p_\alpha^*)^2 \rangle^{\text{T}} = kTI_{\alpha\alpha}^{(e)} \tag{20}$$

$$\langle Q_s \rangle^{\text{T}}_{\text{rot}} = \frac{kT}{8\pi^2 c^2 \omega_s^2} \sum \frac{a_s^{(\alpha\alpha)}}{I_{\alpha\alpha}^{(e)}} \tag{21}$$

Toyama *et al.*[26] have shown that equation (18) can be written alternatively in terms of the usual matrices which arise in a harmonic vibrational analysis, so that equation (21) can be written also as

$$\langle \Delta r \rangle^{\text{T}}_{\text{rot}} = kT\tilde{\mathbf{U}}\mathbf{F}_s^{-1}\mathbf{G}_s^{-1}\mathbf{UB\Omega X} \tag{22}$$

where $\mathbf{\Omega}$ denotes a diagonal matrix with the elements

$$\Omega_{ii}^{(\alpha\alpha)} = \Omega_\alpha = \frac{1}{I_{\beta\beta}^{(e)}} + \frac{1}{I_{\gamma\gamma}^{(e)}}$$

and $\mathbf{X}$ is a vector which has the Cartesian coordinates of the atoms at the equilibrium configuration as its elements. $\mathbf{F}_s^{-1}$ and $\mathbf{G}_s^{-1}$ are the inverse of the usual $\mathbf{F}$ and $\mathbf{G}$ matrices in symmetry coordinates. $\mathbf{U}$ is the transformation matrix from internal into symmetry coordinates and $\mathbf{B}$ is the transformation from Cartesian displacements into internal coordinates.[23] Simple formulae of the thermal averaged centrifugal distortion for some molecular types have been derived.[26,28] For linear triatomics, for example, we obtain:[34]

$$\langle \Delta r_1 \rangle^{\text{T}}_{\text{rot}} = \frac{kT}{8\pi^2 c^2}\left[\frac{L_{11}}{\omega_1^2}\sum \frac{a_1^{\alpha\alpha}}{I_{\alpha\alpha}} + \frac{L_{13}}{\omega_3^2}\sum \frac{a_3^{\alpha\alpha}}{I_{\alpha\alpha}}\right]$$

and (23)

$$\langle \Delta r_3 \rangle^{\text{T}}_{\text{rot}} = \frac{kT}{8\pi^2 c^2}\left[\frac{L_{31}}{\omega_1^2}\sum \frac{a_1^{\alpha\alpha}}{I_{\alpha\alpha}} + \frac{L_{33}}{\omega_3^2}\sum \frac{a_3^{\alpha\alpha}}{I_{\alpha\alpha}}\right]$$

where ω_1 and ω_3 are the two stretching vibrational frequencies, L_{ij} are elements of the L matrix, and the coefficients of the normal coordinates in the moment of inertia, $a_s^{\alpha\alpha}$, can be expressed entirely in terms of measured spectroscopic constants:[28]

$$\begin{aligned} a_1^{xx} &= a_1^{yy} = 2(2B_e/\omega_1)^{\frac{1}{2}}\zeta_{23}^{x}, \qquad a_1^{zz} = 0 \\ a_3^{xx} &= a_3^{yy} = 2(2B_e/\omega_3)^{\frac{1}{2}}\zeta_{21}^{x}, \qquad a_3^{zz} = 0 \end{aligned} \tag{24}$$

where B_e is the rotational constant. The Coriolis constants for the symmetrical case are $\zeta_{23}^{x} = 1$ and $\zeta_{21}^{x} = 0$.

For highly symmetrical molecules the rotational effect on the mean bond length can be expressed in even simpler form, for example:[26,39]
For a CO_2 type molecule

$$\langle \Delta r \rangle^{\text{T}}_{\text{rot}} = \frac{kT}{r_e(F_{11} + F_{12})}$$

For a CH_4 type

$$\langle \Delta r \rangle^{\text{T}}_{\text{rot}} = \frac{3kT}{4r_e F_{11}} \tag{25}$$

For a BF_3 type (planar AX_n)

$$\langle \Delta r \rangle^{\text{T}}_{\text{rot}} = \frac{3kT}{nr_e F_{11}}$$

For a SF_6 type

$$\langle \Delta r \rangle^{\text{T}}_{\text{rot}} = \frac{kT}{2r_e F_{11}}$$

where F_{11} and F_{12} are mass-independent quadratic force constants.

Although the rotational contribution to $\langle \Delta r \rangle^{\text{T}}$ is usually one order of magnitude smaller than the vibrational contribution $\langle \Delta r \rangle_{\text{vib}}^{\text{T}}$, it plays an important role in the temperature dependence of nuclear shielding. At the same time, we will find that the rotational effects play no role (or a negligible one) in the isotope shift. This we can predict already for certain cases by examining equations (25). Since these equations involve only mass-independent terms, there will be no rotational contribution to the isotope shift if isotopic substitution preserves the symmetry of the molecule, as in going from CH_4 to CD_4 (but not in CH_4 to CH_3D).[39]

III. ISOTOPE SHIFTS IN DIATOMIC MOLECULES

The general theoretical approach used in the interpretation of isotope shifts in particular and rovibrational effects on nuclear shielding in general has been given in the previous section. However, since some complications arise only in polyatomic molecules, there is some advantage to be gained in understanding isotope shifts in diatomic molecules first.

A. Calculation of isotope shifts in diatomic molecules

For a diatomic molecule it is convenient to expand the shielding as a power series in the reduced coordinate $\xi = (r - r_e)/r_e$. For a particular

molecular state characterized by vibrational and rotational quantum numbers v and J,

$$\langle\sigma\rangle_{vJ} = \sigma_E + (d\sigma/d\xi)_e\langle\xi\rangle_{vJ} + \tfrac{1}{2}(d^2\sigma/d\xi^2)_e\langle\xi^2\rangle_{vJ} + \cdots \quad (26)$$

Here $\langle\xi\rangle_{vJ}$, $\langle\xi^2\rangle_{vJ}$, ... are the averages of the reduced coordinate over the vibrational-rotational wavefunction corresponding to the v,J level. The thermal averages $\langle\xi\rangle^T$, $\langle\xi^2\rangle^T$, ... may then be obtained by

$$\langle\xi^n\rangle^T = \frac{\sum_{vJ} g_{vJ}\langle\xi^n\rangle_{vJ}\exp(-E_{vJ}/kT)}{\sum_{vJ} g_{vJ}\exp(-E_{vJ}/kT)} \quad (27)$$

so that the thermal average shielding is

$$\langle\sigma\rangle^T = \sigma_e + (d\sigma/d\xi)_e\langle\xi\rangle^T + \tfrac{1}{2}(d^2\sigma/d\xi^2)_e\langle\xi^2\rangle^T + \cdots \quad (28)$$

The potential energy surface of a diatomic molecule can be written in terms of a Dunham potential or more approximately in terms of a Morse potential. Both have been used in the interpretation of isotope shifts.

The Dunham potential function expresses the potential energy in terms of a Taylor series expansion in ξ:[40]

$$V = a_0\xi^2(1 + a_1\xi + a_2\xi^2 + a_3\xi^3 + \cdots) \quad (29)$$

The potential parameters $a_0, a_1, \ldots$ can be obtained from the expression for the energy levels of a diatomic molecule:

$$E_{vJ} = \sum_{i=0}^{\infty}\sum_{l=0}^{\infty} Y_{il}(v+\tfrac{1}{2})^i[J(J+1)]^l \quad (30)$$

in terms of the spectroscopic constants Y_{il}. The average values $\langle\xi^n\rangle_{vJ}$ can then be obtained by perturbation theory in terms of the potential parameters. Herman and Short have derived the expressions for the average values:[41]

$$\langle\xi^n\rangle_{vJ} = \sum_{i=0}^{\infty}\sum_{l=0}^{\infty} Z_{il}^{(n)}(v+\tfrac{1}{2})^i[J(J+1)]^l \quad (31)$$

where the $Z_{il}^{(n)}$ are expressed in terms of the vibrational frequency ω_e, the rotational constant B_e and the coefficients $a_0, a_1, \ldots$. Once these averages are known, the thermal average shielding can be obtained. This method has been applied to the H_2 molecule by Raynes *et al.*[42] and to H_2, LiH and HF by Ditchfield.[43] Typically, terms up to a_6 in equation (29) are used.

Some typical results are shown in Figs 4 and 5 and in Table 1. These were calculated by Ditchfield using shielding functions obtained from coupled Hartree–Fock calculations at various internuclear separations. The σ values so obtained for a range of ξ values are fitted to a power series in ξ and the derivatives $(d\sigma/d\xi)_e$, $(d^2\sigma/d\xi^2)_e$, ... are obtained. These were used in equation (26) to calculate the values shown in Table 1. The thermal averages calculated in equation (28) are shown in Figs 4 and 5.

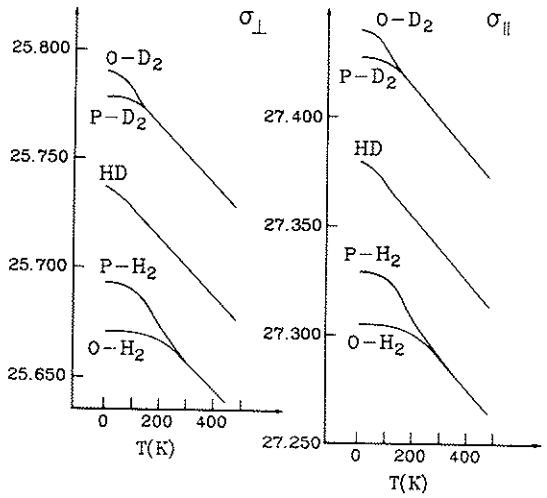

FIG. 4. Calculated shielding components for H or D in H_2, HD and D_2. From reference 43, with permission.

We note in Table 1 that for any given v,J level the ^1H or ^2D shielding in HD is greater than that in H_2; in D_2 it is greater than in HD. The calculated rovibrational effects on the average shielding at 300 K are shown in Table 2. First we note that rovibrational averaging usually leads to deshielding, Li in LiH being the only known exception. Secondly, we note that the third-

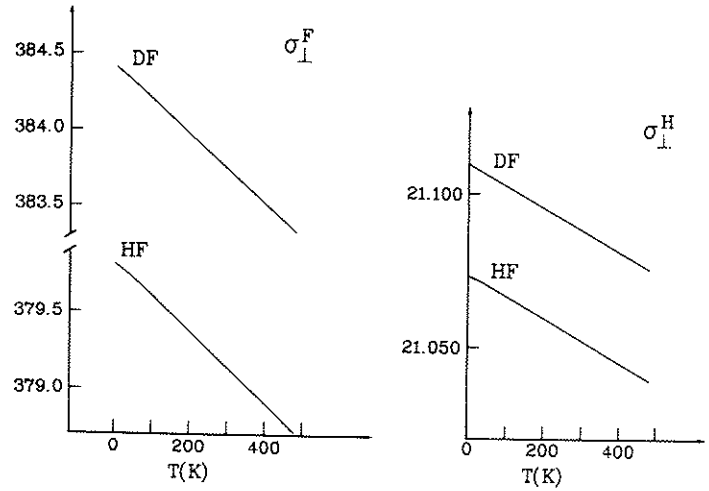

FIG. 5. Calculated shielding components in HF. From reference 43, with permission.

TABLE 1

Rovibrationally averaged shielding tensor components (in ppm) of individual molecular states for ^1H in H_2, HD and D_2, and ^{19}F in HF.[43]

		H_2		HD		D_2		HF	
v	J	$\sigma_\perp^H$	$\sigma_\parallel^H$	$\sigma_\perp^H$	$\sigma_\parallel^H$	$\sigma_\perp^H$	$\sigma_\parallel^H$	$\sigma_\perp^F$	$\sigma_\parallel^F$
at	r_e	26.022	27.706	26.022	27.706	26.022	27.706	395.98	482.12
0	0	25.694	27.330	25.738	27.380	25.790	27.440	379.82	482.10
0	1	25.672	27.306	25.721	27.362	25.779	27.427	379.68	482.10
0	2	25.627	27.257	25.688	27.326	25.756	27.403	379.41	482.10
0	3	25.560	27.185	25.637	27.271	25.723	27.367	379.00	482.10
1	0	25.067	26.608	25.191	26.751	25.339	26.922	344.36	482.07
1	1	25.046	26.585	25.175	26.734	25.328	26.910	344.19	482.07
1	2	25.004	26.539	25.143	26.699	25.307	26.887	343.87	482.07
1	3	24.941	26.470	25.095	26.647	25.275	26.852	343.38	482.07

TABLE 2

The linear, quadratic and higher order rovibrational contributions to the thermal average shielding at 300 K, $\langle\sigma\rangle^{300} - \sigma_e$, in ppm.[43]

Nucl.	Mol.	$(d\sigma/d\xi)_e\langle\xi\rangle$	$\left\{ \begin{array}{l} (d\sigma/d\xi)\langle\xi\rangle + \\ \frac{1}{2}(d^2\sigma/d\xi^2)_e\langle\xi^2\rangle \end{array} \right\}$	up to 6th order
^1H	H_2	−0.5554	−0.3694	−0.3814
^1H	HD			−0.3364
^1H	HF	−0.7021	−0.3721	−0.3911
^2D	DF			−0.2951
^{19}F	HF	−7.42	−11.113	−11.23
^{19}F	DF			−8.161
^1H	LiH	−0.1228	−0.1238	−0.1228
^2D	LiD			−0.0978
^7Li	LiH	+0.1386	+0.0726	+0.0786
^7Li	LiD			+0.0656

TABLE 3

Calculated isotope shifts, in ppm.[43]

Molecule	Nucleus	Calculation	Experiment	Ref.
HD - H_2	^1H	−0.045	−0.036 ± 0.002	44
D_2 - HD	^2D	−0.054	−0.0469 ± 0.0005	45
DF - HF	^{19}F	−3.07	−2.5 ± 0.5	46
DLi - HLi	^7Li	+0.013		

and higher-order terms in equation (28) have very little effect on the thermal average shielding; terms up to quadratic are sufficient to include nearly all rovibrational effects. The calculated isotope shifts at 300 K are shown in Table 3. ^7Li, which shows an unusual temperature dependence, also shows an unusual sign for the D-induced isotope shift.

In order to observe more easily the largest terms which contribute to the above equations and explicitly express their mass dependence, we write only the leading terms, expressed in the measured spectroscopic constants of the molecule. The leading terms in the potential energy are:

$$V(\xi) = (hc\omega_e^2/4B_e)[\xi^2 + a_1\xi^3 + \cdots] - hcB_eJ(J+1)[2\xi - 3\xi^2 + \cdots] \quad (32)$$

where a_1 can also be expressed as

$$a_1 = -[1 + (\alpha_e\omega_e/6B_e^2)] \quad (33)$$

α_e being the vibrational-rotational interaction constant.

An especially useful form of an approximate potential for the diatomic molecule is the Morse function:[47]

$$V = D_e\{1 - \exp[-a(r - r_e)]\}^2 \quad (34)$$

For the Morse potential the ratio $\frac{1}{3}(d^3V/d\xi^3)_e/(d^2V/d\xi^2)_e = -ar_e$ can be identified with a_1, the same a_1 that we have previously defined above. The leading terms in equation (31) are:

$$\langle\xi\rangle_{vJ} = -3(v+\tfrac{1}{2})a_1(B_e/\omega_e) + 4J(J+1)(B_e/\omega_e)^2 \quad (35)$$

$$\langle\xi^2\rangle_{vJ} = 2(v+\tfrac{1}{2})(B_e/\omega_e) \quad (36)$$

These substituted into equation (26) then give the leading terms in the shielding:

$$\langle\sigma\rangle_{vJ} = \sigma_e + (d\sigma/d\xi)_e[-3a_1(B_e/\omega_e)(v+\tfrac{1}{2}) + 4(B_e/\omega_e)^2J(J+1)] + \tfrac{1}{2}(d^2\sigma/d\xi^2)_e 2(B_e/\omega_e)(v+\tfrac{1}{2}) \quad (37)$$

With a classical thermal average for $\langle J(J+1)\rangle^T$ and a further approximation given in equation (11) for $\langle v+\frac{1}{2}\rangle^T$, the thermal average shielding is:[48]

$$\langle\sigma\rangle^T = \sigma_e + (B_e/\omega_e)[(d^2\sigma/d\xi^2)_e - 3a_1(d\sigma/d\xi)_e] \times \tfrac{1}{2}\coth(hc\omega_e/2kT) + (d\sigma/d\xi)_e 4(B_e/hc\omega_e^2)kT \quad (38)$$

Of these quantities, a_1 is mass-independent and the others depend on the reduced mass of the diatomic molecule as follows:

$$\omega_e^* = (\mu/\mu^*)^{\frac{1}{2}}\omega_e$$
$$B_e^* = (\mu/\mu^*)B_e \quad (39)$$
$$\alpha_e^* = (\mu/\mu^*)^{\frac{3}{2}}\alpha_e$$

Furthermore the thermal average $\langle v+\frac{1}{2}\rangle^{T}$ is also mass-dependent since the populations of the vibrational energy levels over which this average is taken depend on the vibrational frequency ω_e. We note that B_e/ω_e^2 is mass-independent, so the rotational contribution to the thermal average shielding in the diatomic molecule is independent of mass.

Therefore the isotope shift is given by

$$\langle\sigma\rangle-\langle\sigma\rangle^{*}=[(d^2\sigma/d\xi^2)_e-3a_1(d\sigma/d\xi)_e](B_e/\omega_e)$$
$$\times\{\coth(hc\omega_e/2kT)-(\mu/\mu^{*})^{\frac{1}{2}}\coth[hc(\mu/\mu^{*})^{\frac{1}{2}}\omega_e/2kT]\} \quad (40)$$

Alternatively, equation (38) and equation (40) can be written in terms of the mean bond displacement $\langle\Delta r\rangle^{T}$ and the mean square amplitude $\langle(\Delta r)^2\rangle^{T}$:

$$\langle\sigma\rangle^{T}=\sigma_e+(d\sigma/d\Delta r)_e\langle\Delta r\rangle^{T}+\tfrac{1}{2}(d^2\sigma/d\Delta r^2)_e\langle(\Delta r)^2\rangle^{T}+\cdots \quad (41)$$

$$\langle\sigma\rangle-\langle\sigma\rangle^{*}=(d\sigma/d\Delta r)_e[\langle\Delta r\rangle-\langle\Delta r\rangle^{*}]$$
$$+\tfrac{1}{2}(d^2\sigma/d\Delta r^2)_e[\langle(\Delta r)^2\rangle-\langle(\Delta r)^2\rangle^{*}]+\cdots \quad (42)$$

where

$$\langle\Delta r\rangle^{T}=\langle\Delta r\rangle^{T}_{rot}+\langle\Delta r\rangle^{T}_{vib} \quad (43)$$

$$\langle\Delta r\rangle^{T}_{rot}=\frac{4B_e r_e}{hc\omega_e^2}kT \quad (44)$$

$$\langle\Delta r\rangle^{T}_{vib}=-(3/2)a_1(B_e/\omega_e)r_e\coth(hc\omega_e/2kT) \quad (45)$$

$$\langle(\Delta r)^2\rangle^{T}_{vib}=(B_e/\omega_e)r_e^2\coth(hc\omega_e/2kT) \quad (46)$$

We note that including only terms up to quadratic allows us to write $\langle\Delta r\rangle^{T}_{vib}=-(3/2)(a_1/r_e)\langle(\Delta r)^2\rangle^{T}$ or, in terms of the Morse parameter:[49]

$$\langle\Delta r\rangle^{T}_{vib}=(3/2)a\langle(\Delta r)^2\rangle^{T} \quad (47)$$

For a harmonic oscillator equation (46) is exact, so we shall refer to the term involving this and the second derivatives of the shielding as the "harmonic vibrational contribution". On the other hand, only for an anharmonic vibration is $a_1\neq 0$, therefore we shall refer to the term involving this and the first derivative of the shielding as the "anharmonic vibrational contribution". The rotational contribution is due to centrifugal stretching. As the molecule rotates, the atoms tend to move away from the centre of mass, thereby contributing to an increase of the mean bond length with increasing rotational energy, or with increasing temperature.

We have calculated the rovibrational corrections to shielding and the isotope shift using equations (38) and (40) and show the rotational (equation (44)), the anharmonic vibrational (equation (45)) and the harmonic vibrational (equation (46)) contributions separately in Tables 4–6 for some

TABLE 4

Rotational, anharmonic vibrational and harmonic vibrational contributions to shielding, $\langle\sigma\rangle^{300}-\sigma_e$, in ppm.[a]

Nucl.	Mol.	Rotational	Anharm. vib.	Harm. vib.	Total
^{1}H	H_2	−0.4238	−0.5342	+0.0669	−0.5096
^{1}H	HD	−0.4238	−0.4619	+0.0578	−0.4464
^{1}H	^{7}LiH	−0.0136	−0.0651	−0.1278	−0.2066
^{1}H	^{6}LiH	−0.0136	−0.0658	−0.1291	−0.2086
^{7}Li	LiH	+0.0380	+0.1816	−0.1035	+0.1160
^{7}Li	LiD	+0.0380	+0.1377	−0.0785	+0.0972
^{1}H	HF	−0.0380	−0.6264	+0.2902	−0.3742
^{2}D	DF	−0.0380	−0.4545	+0.2106	−0.2819
^{19}F	HF	−0.3840	−6.3280	−2.8728	−9.5847
^{19}F	DF	−0.3840	−4.5916	−2.0845	−7.0599
^{13}C	$^{13}C^{16}O$	−0.1594	−1.6432	−0.2285	−2.0311[b]
^{13}C	$^{13}C^{18}O$	−0.1594	−1.6018	−0.2227	−1.9839[b]
^{17}O	$^{12}C^{17}O$	−0.1846	−1.9213	−0.2760	−2.3819[b]
^{17}O	$^{13}C^{17}O$	−0.1846	−1.8775	−0.2697	−2.3319[b]
^{15}N	$^{15}N^{14}N$	−0.2108	−2.4825	−0.8529	−3.5462
^{15}N	$^{15}N_2$	−0.2108	−2.4393	−0.8381	−3.4881

[a] This work, using equation (38).

[b] This may be compared with results of calculations by Raynes and Stanney[55] which are, respectively, −2.23, −2.17, −2.6 and −2.54 ppm.

diatomic molecules. We have used shielding derivatives from the literature for H_2,[42] LiH,[51] HF,[52] CO[53] and N_2.[54]

There are several points worth noting in Table 4. First, as in Table 2, we find that the rovibrational effects lead to deshielding of the nucleus compared to the rigid equilibrium configuration, except in the case of Li in LiH.

TABLE 5

Temperature dependence of nuclear shielding, $\langle\sigma\rangle^{400}-\langle\sigma\rangle^{200}$, in ppm.[a]

Nucl.	Mol.	Rotational	Anharm. vib.	Harm. vib.	Total
^{1}H	H_2	−0.0282	0	0	−0.0282
^{1}H	^{7}LiH	−0.0091	−0.0008	−0.0016	−0.0115
^{7}Li	^{6}LiH	+0.0253	+0.0023	−0.0013	+0.0263
^{1}H	HF	−0.0253	0	0	−0.0253
^{19}F	HF	−0.2560	0	0	−0.2560
^{13}C	$^{13}C^{16}O$	−0.1062	−0.0016	−0.0002	−0.1081
^{17}O	$^{12}C^{17}O$	−0.1231	−0.0020	−0.0003	−0.1254
^{15}N	$^{15}N_2$	−0.1405	−0.0013	−0.0004	−0.1423

[a] This work, using equation (38).

TABLE 6

Anharmonic and harmonic vibrational contributions to the isotope shift, in ppm.[a]

Nucl.	Mol.	Anharm.	Harm.	Total	Expt.	Ref.
^{1}H	HD - H_2	−0.0723	+0.0090	−0.0632[b]	−0.036 ± 0.002	44
^{1}H	^{7}LiH - ^{6}LiH	−0.0007	−0.0013	−0.0020		
^{7}Li	LiD - LiH	+0.0438	−0.0250	+0.0188		
^{1}H	DF - HF	−0.1719	+0.0796	−0.0923		
^{19}F	DF - HF	−1.7364	−0.7883	−2.5248	−2.5 ± 0.5	46
^{13}C	$^{13}C^{18}O$ - $^{13}C^{16}O$	−0.0414	−0.0058	−0.0472[c]	−0.0476 ± 0.0016	50
^{17}O	$^{13}C^{17}O$ - $^{12}C^{17}O$	−0.0438	−0.0063	−0.0501	−0.110 ± 0.001	50
^{15}N	$^{15}N_2$ - $^{15}N^{14}N$	−0.0432	−0.0148	−0.0581	−0.0601 ± 0.002	141

[a] This work, using equation (40).

[b] For isotopomers of H_2 the classical treatment of rotation leads to significant error. A proper average taking into consideration the nuclear spin statistics gives better results: −0.047,[56] −0.042,[42] −0.045.[43]

[c] This may be compared with −0.06 ppm obtained from calculations including cubic terms.[55]

Second, the anharmonic vibration contribution is the largest one of the three in every molecule (except for LiH) and the rotational contribution is the smallest (except for H_2). Third, neglect of the harmonic vibrational contribution leads to error. Differences in shielding between pairs of isotopically related molecular species give the isotope shifts in Table 6. There is no rotational contribution to the isotope shift in the diatomic molecule. The relative contributions of the anharmonic and harmonic vibrational effects vary so that neglect of the harmonic contribution in calculating the isotope shift can lead to error. The largest error would occur in the case of ^{19}F in the DF-HF system, in which the harmonic vibrational contribution is 31% of the observed isotope shift.

On the other hand, the temperature dependence of the shielding depends nearly entirely on rotation, with vibrational effects accounting for 0-2%. This is easily understood by consulting equation (38). The linear temperature dependence dominates the change of the average shielding with temperature, especially for these diatomic molecules which have very strong bonds characterized by high vibrational frequencies. The $(hc\omega/2kT)$ term is large, for which the coth function is very nearly constant and equal to 1.0. For weaker bonds such as in F_2 and ClF, the rotational contribution still dominates the temperature dependence of the shielding although the anharmonic vibration contribution to the temperature dependence becomes significant.[57] A significant rotational contribution to the temperature dependence means that the term in the first derivative determines the observed temperature dependence in a gas in the limit of zero pressure. A single parameter fit to such data then yields empirical values of $(d\sigma/d\Delta r)_e$.

Ditchfield has noted that for the diatomic molecules H_2, HF and LiH the contributions to the temperature dependence of shielding from second and higher derivatives of shielding are altogether too small to affect the observed temperature dependence in the zero-pressure limit to a measurable extent.

B. The dynamic factor in isotope shifts

In order to be able to discuss general trends in isotope shifts, we need to be able to see what factors determine the isotope effect on $\langle\Delta r\rangle_{vib}$ and $\langle\Delta r^2\rangle$.

1. Estimation of $\langle\Delta r\rangle - \langle\Delta r\rangle^*$

From equation (45) we see that by making use of the implicit mass dependence of B_e and ω_e (equation (39)) we can write

$$\langle\Delta r\rangle - \langle\Delta r\rangle^* = -(3/2)a_1 r_e\{(B_e/\omega_e)\coth(hc\omega_e/2kT) - (\mu/\mu^*)^{\frac{1}{2}}(B_e/\omega_e)\coth[hc(\mu/\mu^*)^{\frac{1}{2}}\omega_e/2kT]\} \quad (48)$$

There are several approximations which can be invoked to simplify this expression further:

(i) if $\coth(hc\omega_e/2kT)$ is very close to 1.0 and $\coth[hc(\mu/\mu^*)^{\frac{1}{2}}\omega_e/2kT]$ is also very close to 1.0, i.e. for high vibrational frequencies, then $\langle\Delta r\rangle - \langle\Delta r\rangle^*$ reduces simply to

$$\langle\Delta r\rangle - \langle\Delta r\rangle^* \approx [1-(\mu/\mu^*)^{\frac{1}{2}}]\langle\Delta r\rangle \quad (49)$$

Similarly

$$\langle(\Delta r)^2\rangle - \langle(\Delta r)^2\rangle^* \approx [1-(\mu/\mu^*)^{\frac{1}{2}}]\langle\Delta r^2\rangle \quad (50)$$

(ii) $[1-(\mu/\mu^*)^{\frac{1}{2}}]$ can be further approximated by $(\mu^*-\mu)/2\mu^*$ so that

$$\langle\Delta r\rangle - \langle\Delta r\rangle^* \approx \langle\Delta r\rangle\left(\frac{\mu^*-\mu}{2\mu^*}\right) = \langle\Delta r\rangle\frac{1}{2}\left(\frac{m'-m}{m'}\right)\left(\frac{m_A}{m_A+m}\right) \quad (51)$$

$$\langle(\Delta r)^2\rangle - \langle(\Delta r)^2\rangle^* \approx \langle(\Delta r)^2\rangle\left(\frac{\mu^*-\mu}{2\mu^*}\right) = \langle(\Delta r)^2\rangle\frac{1}{2}\left(\frac{m'-m}{m'}\right)\left(\frac{m_A}{m_A+m}\right) \quad (52)$$

where m_A is the mass of the observed nucleus A and the isotopes m' and m of the other nucleus X in the diatomic molecule.

2. The concept of the reduced isotope shift

Although equation (52) is only an approximate one, it is still a nice simple formula which allows us to separate out most (not all) of the mass dependence of the isotope shift.

$${}^{1}\Delta A({}^{m'/m}X) = \langle\sigma\rangle - \langle\sigma\rangle^* \approx \left\{\begin{matrix}(d\sigma/d\Delta r)_e\langle\Delta r\rangle + \\ \frac{1}{2}(d^2\sigma/d\Delta r^2)_e\langle(\Delta r)^2\rangle\end{matrix}\right\}\cdot\frac{1}{2}\left(\frac{m'-m}{m'}\right)\left(\frac{m_A}{m_A+m}\right) \quad (53)$$

If we define a reduced isotope shift as

$$^1\Delta^R(A, X) \equiv {}^1\Delta A({}^{m'/m}X)\left(\frac{m'-m}{m'}\cdot\frac{1}{2}\frac{m_A}{m_A+m}\right)^{-1} \tag{54}$$

then

$$^1\Delta^R(A, X) \approx (d\sigma/d\Delta r)_e\langle\Delta r\rangle + \tfrac{1}{2}(d^2\sigma/d\Delta r^2)_e\langle(\Delta r)^2\rangle \tag{55}$$

This definition has the advantage of allowing us to compare isotope shifts of the same nucleus under different isotopic substitutions, for example the $^{37/35}$Cl-induced ^{19}F isotope shift with the $^{2/1}$H-induced ^{19}F isotope shift in ClF and HF respectively. The mass factors have been explicitly removed, leaving a reduced isotope shift which contains primarily electronic information (not entirely since $\langle\Delta r\rangle$ and $\langle(\Delta r)^2\rangle$ are still mass-dependent).

Furthermore, within this approximation the reduced isotope shift gives the rovibrational corrections to shielding at that temperature,

$$\langle\sigma^A\rangle^{300} - \sigma_e{}^A \approx {}^1\Delta^R(A, X). \tag{56}$$

3. *Estimation of* $\langle\Delta r\rangle$

If we make the approximation of including only the linear term in equation (55), the reduced isotope shifts can be implemented in the determination of the derivatives $(d\sigma/d\Delta r)_e$ or for the prediction of magnitudes of isotope shifts from known or estimated derivatives. To do this we need to be able to estimate $\langle\Delta r\rangle$. For diatomic molecules this is not a problem since there are usually enough known spectroscopic constants to calculate $\langle\Delta r\rangle$ without using estimates. To apply this reduced isotope shift concept to polyatomic molecules we need to be able to estimate $\langle\Delta r\rangle$ for a bond in a polyatomic molecule. Thus we use the known spectroscopic constants for many diatomic molecules to verify how good this estimation method is.

We have already seen in equation (47) that, for diatomic molecules,

$$\langle\Delta r\rangle_{vib}{}^T = (3/2)a\langle(\Delta r)^2\rangle^T \tag{47}$$

If the harmonic approximation is used for $\langle(\Delta r)^2\rangle$ it is possible to express $\langle\Delta r\rangle_{vib}$ as[58]

$$\langle\Delta r\rangle_{vib} \approx \left(\frac{3h}{8\pi}\right)(-F_3F_2^{-3})\mu^{-1/2} \tag{57}$$

where

$$F_3 \equiv (1/3)(\partial^3V/\partial r^3)_e \qquad F_2 \equiv (\partial^2V/\partial r^2)_e$$

and the temperature dependence has been suppressed. Herschbach and Laurie found that F_3 and F_2 are approximately exponential functions of internuclear distance, each described by a family of curves which are

determined by the location of the bonded atoms in rows of the periodic table.[59]

$$(-1)^nF_n = 10^{-(r_e-a_n)/b_n} \tag{58}$$

Thus we write

$$\langle\Delta r\rangle_{vib} \cong (3h/8\pi)\mu^{-\frac{1}{2}}10^{-D} \tag{59}$$

where

$$D \equiv (r_e-a_3)/b_3 - 3(r_e-a_2)/2b_2 \tag{60}$$

10^{-D} has units of (energy)$^{-1/2}$. The constant in equation (59) is 19.35×10^{-3} if μ is in amu, and the a_2, b_2, a_3 and b_3 are reproduced in Table 7. A comparison of equation (59) with the $\langle\Delta r\rangle_{vib}$ calculated at 300 K using

TABLE 7

Herschbach–Laurie parameters.[59]

Row		a_2	a_3	b_2	b_3	Row		a_2	a_3	b_2	b_3
H	1	1.54	1.58	0.64	0.48	2	4	2.63	2.70	0.96	0.73
H	2	1.80	1.85	0.69	0.59	2	5	2.71	2.81	1.09	1.09
H	3	1.98	2.01	0.95	0.74	3	3	2.70	2.77	1.12	0.89
H	4	2.08	2.07	0.96	0.74	3	4	2.66	2.76	1.48	1.19
H	5	2.06	2.12	0.78	0.90	3	5	2.73	2.83	1.31	1.05
1	1	1.73	1.78	0.47	0.39	4	4	2.85	2.95	0.94	0.70
1	2	2.02	2.10	0.53	0.48	4	5	2.84	2.93	1.09	0.78
1	3	2.15	2.26	0.60	0.55	H	3T	1.82	1.92	1.04	0.86
1	4	2.36	2.41	0.76	0.57	H	4T	1.83		0.75	
1	5	2.47	2.48	0.87	0.68	H	5T	1.77		0.47	
2	2	2.40	2.48	0.70	0.61	1	3T	1.98		0.44	
2	3	2.54	2.57	0.98	0.72	1	4T	2.15		0.52	

equation (45) and the known spectroscopic constants of a large set of diatomic molecules[60] shows good overall agreement for $\langle\Delta r\rangle_{vib}$ values from 3 to 25×10^{-3} Å.[58] What this means is that it is possible to estimate $\langle\Delta r\rangle$ for a diatomic molecule by knowing only the bond length. Similarly

$$\langle(\Delta r)^2\rangle = (h/4\pi)\mu^{-1/2}10^{+d} \tag{61}$$

where $d \equiv (r_e-a_2)/2b_2$. 10^{+d} has units of length $\times$ energy$^{-1/2}$.

Thus the reduced isotope shift can be expressed as

$$^1\Delta^R(\Delta, X) = \frac{h\mu^{-1/2}}{8\pi}[3\times10^{-D}(d\sigma/d\Delta r)_e + 10^d(d^2\sigma/d\Delta r^2)_e] \tag{62}$$

C. The electronic factor in isotope shifts: the change in shielding with bond extension

We have seen that the dynamic factor in isotope shifts is largely predictable and transferable for a given bond, e.g. C–F, from one molecule to the next. This means that the isotope shift carries primarily electronic information. This is shown by the correlation in Fig. 2. The change in shielding with bond extension is as much an index of the chemical bond as is the spin–spin coupling or the chemical shift. Therefore we shall consider in this section what is known about this index from theoretical and experimental sources.

1. The change in ^1H shielding with internuclear separation in H_2^+

The shielding in the H_2^+ molecule has been fully characterized over the entire range of internuclear separations by Hegstrom,[18] with relativistic calculations; it is represented in Fig. 3. We note several points about the behaviour of the ^1H shielding in this molecule. First, the shielding at the equilibrium configuration is greater than the diamagnetic shielding of the separated atoms, which is also found for ^{19}F in ClF but is unusual otherwise. In most diatomic molecules the nuclear shielding at the equilibrium separation, σ_e, is less than the diamagnetic shielding of the separated atoms. Second, the shielding decreases with bond extension away from equilibrium. This is typical for diatomic molecules. Only Li in LiH has shown exceptional behaviour.[43,51] This indicates that, if H_2^+ is at all typical, the minimum in the shielding function occurs at nuclear separations significantly greater than that at the equilibrium geometry. In Fig. 3 we have also sketched the potential energy curve $V(r)$ and the vibrational levels. With these we can readily see that vibrational averaging leads to deshielding and that the ^1H shielding in H_2^+ would decrease with increasing temperature as the higher vibrational levels become more populated. The mean bond displacement for HD^+ is less than that for H_2^+, leading to the correspondingly higher average shielding for ^1H in HD^+ compared to H_2^+, i.e. an isotope shift of the usual sign.

2. Derivatives of the perpendicular and parallel components of nuclear shielding in a diatomic molecule

We can illustrate $(d\sigma_\perp/d\Delta r)_e$ and $(d\sigma_\parallel/d\Delta r)_e$ for ^1H and ^{19}F in HF by means of a shielding density difference map.[61] The shielding density describes the contributions to shielding from various regions in the electronic distribution in the molecule in the same way that a charge density map shows the electronic distribution itself. The shielding density for the equilibrium HF geometry can be subtracted from the shielding density for the extended HF geometry, giving the density difference maps shown in Fig.

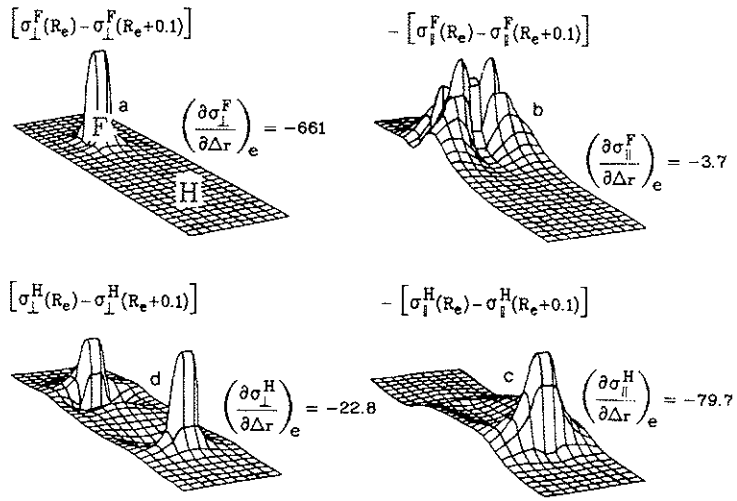

FIG. 6. Shielding density difference maps for ^{19}F and ^1H in the HF molecule upon bond extension, individually scaled. For comparison, extrema are: (a) $^{19}F(\perp)$ 116.46, -10^{-3}; (b) $^{19}F(\parallel)$ −0.076, 0.0128; (c) $^1H(\parallel)$ −0.333, 0.0124; (d) $^1H(\perp)$ 1.884, −2.003 (at H) and 1.123, −1.972 (at F), in arbitrary units. From reference 61, with permission.

6. These may be viewed as mappings of the distribution of $(d\sigma/d\Delta r)_e$, i.e. they show which regions of electronic distribution contribute to the change in shielding as the bond is extended. These are individually scaled so as to show the features of the $(d\sigma_\perp/d\Delta r)_e$ and $(d\sigma_\parallel/d\Delta r)_e$ density surfaces. The maximum values for each surface are shown in the figure caption. The derivatives obtained with this particular calculation (coupled Hartree–Fock calculation with gauge origin at F, using the Lie–Clementi basis set for HF) are also shown in the figure.

There are several points of interest in Fig. 6. First, the perpendicular component of the ^{19}F shielding in HF has a much larger derivative than the parallel component, whereas the derivatives of the parallel and perpendicular components have comparable magnitudes for ^1H shielding. The reason for this becomes apparent when it is recalled that $\sigma_\parallel$ is purely diamagnetic (for any gauge origin along the line of centres) whereas $\sigma_\perp$ has both diamagnetic and paramagnetic contributions. Since the diamagnetic contribution to shielding varies as $1/r$ (where r is the position of the electron relative to the nucleus) whereas the paramagnetic shielding varies as r^{-3}, it is reasonable that the paramagnetic shielding changes more drastically when the bond is extended. Proton shielding, on the other hand, is largely diamagnetic, so the changes with bond extension of the values of $\sigma_\perp$ and $\sigma_\parallel$ are comparable. Second, the ^{19}F shielding change with bond

extension comes from the immediate neighbourhood of the F nucleus with very minor contributions from the other regions in the molecule. On the other hand, the ^{1}H shielding change with bond extension originates not only from the vicinity of the ^{1}H nucleus but also from around the F nucleus, particularly for $(d\sigma_\perp{}^H/d\Delta r)_e$. The paramagnetic contribution to this component originates largely from the p orbitals on F. The changes in the parallel components [$(d\sigma_\parallel{}^H/d\Delta r)_e$ in Fig. 6 (b) and (d) are entirely diamagnetic] corresponding more closely to the charge density redistribution upon bond extension observed by Bader and Bandrauk[62] shown in Fig. 7. Charge is removed from along the internuclear axis and becomes concentrated in the perpendicular region. The quadrupolar character of the charge density difference observed in Fig. 7 is reflected in Fig. 6 (b) and (d) for the $(d\sigma_\parallel/d\Delta r)_e$.

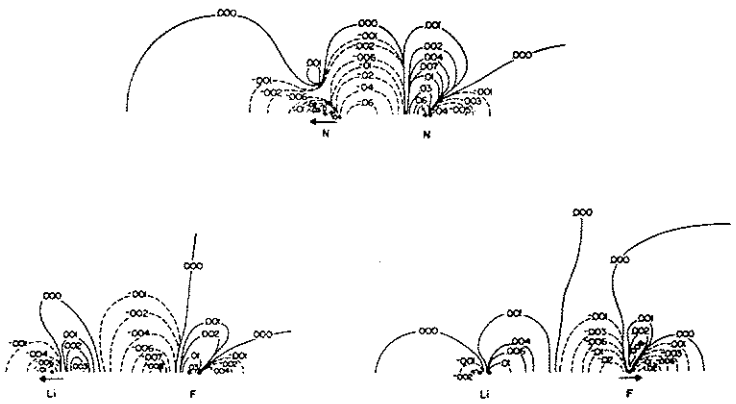

FIG. 7. Charge redistribution upon bond extension in LiF and N_2 molecules. Positive contours correspond to an increase, negative to a decrease in electronic charge density. Displacement of nucleus marked by arrow is 0.132 a.u. for N_2, 0.232 a.u. for LiF. From reference 62, with permission.

The shieldings in diatomic molecules other than H_2^+ have only been calculated for separations very close to the equilibrium one. This allows derivatives of the shielding to be calculated. Some of Ditchfield's calculated derivatives for H_2, HF and LiH are shown in Table 8. He actually reported values up to 6th derivatives for HF and LiH.

The unusual positive $(d\sigma_\perp{}^{Li}/d\Delta r)$ shown in Table 8 leads to an unusual sign of the isotope shift for ^{7}Li. The explanation for this may be seen in Fig. 7; upon bond extension the charge polarization in the vicinity of the Li nucleus in LiF is primarily dipolar. The charge density is removed from the overlap region and builds up immediately in front of the Li nucleus.

TABLE 8

The shielding functions for H_2, HF and LiH, in ppm.[43]

Mol.	Component	σ_e	$(d\sigma/d\xi)_e$	$(d^2\sigma/d\xi^2)_e$
H_2	$\sigma_\perp{}^H$	26.0223	−14.9632	24.0505
	$\sigma_\parallel{}^H$	27.7056	−16.1798	23.0573
HF	$\sigma_\perp{}^H$	21.2063	−20.9333	88.3674
	$\sigma_\parallel{}^H$	44.2187	−73.1549	179.126
	$\sigma_\perp{}^F$	395.981	−605.969	−1998.51
	$\sigma_\parallel{}^F$	482.118	−3.4390	17.4407
LiH	$\sigma_\perp{}^H$	25.3210	−3.9974	−10.6593
	$\sigma_\parallel{}^H$	28.3655	−12.0785	19.5267
	$\sigma_\perp{}^{Li}$	88.9281	15.0629	−41.1407
	$\sigma_\parallel{}^{Li}$	101.605	−6.9587	12.7755

In Ditchfield's shielding calculations on LiH this unusual sign is shown to arise from a decrease in the local paramagnetic currents arising from $\sigma \rightarrow \pi^*$ magnetic field-induced mixing when the bond is extended, which results in an increase in $\sigma_\perp{}^{Li}$, an increase large enough to offset the decreases in the diamagnetic contributions.

3. *Empirical estimates of* $(d\sigma/d\Delta r)_e$

Derivatives of nuclear shielding can also be obtained from experiment. There are three sources: (i) molecular beam data on individual v and J states; (ii) $\sigma_0(T)$ data from dilute gas phase measurements extrapolated to zero pressure; (iii) isotope shifts.

Most molecular beam data provide nuclear spin-rotation constants C_{vJ} for a specific v,J state of the molecule. The relationship which has been established between the electronic part of the spin-rotation constant and the paramagnetic part of nuclear shielding[63,64] then allows the paramagnetic shielding tensor components for a given v,J state of the molecule to be calculated from the spin-rotation constants:

$$C_{vJ}{}^{elec} = k\left\langle \frac{\sigma^p}{R^2} \right\rangle_{vJ} \tag{63}$$

where k involves only fundamental constants. Theoretical calculations of the diamagnetic components are relatively easy since they depend only on the ground state electronic wavefunction. Putting these two parts together then allows the determination of $\langle\sigma\rangle_{vJ}$ from molecular beam data. When molecular beam spectra for more than one v,J state have been analysed, one can write the spin-rotation constants in terms of the same reduced

coordinate as in equation (26):[65]

$$C_{vJ}^{elec} = k \sum_n s_n \left\langle \frac{\xi^n}{R^2} \right\rangle_{vJ} \tag{64}$$

In the analysis of the spin-rotation constant for a given v, the expansion coefficients s_n obtained by fitting several individual C_J^{elec} are related to $(d^n\sigma^p/d\xi^n)_e$. Alternatively, one could write the relation between the paramagnetic shielding and the total spin-rotation constant (not just the electronic part) as:

$$\sigma^p = k(1+\xi)^2 C - b(1+\xi)^{-1} \tag{65}$$

where k and b are known constants in terms of the equilibrium molecular geometry. By differentiating this equation with respect to ξ, $(d\sigma^p/d\xi)_e$ can be found in terms of $(dC/d\xi)_e$. This approach was used for F_2.[66] Using the measured spin-rotation constant,

$$\langle C\rangle/\text{kHz} = -(156.85 \pm 0.10) - (0.0024 \pm 0.0010)J(J+1)$$

one can identify

$$4(dC/d\xi)_e(B_e/\omega_e)^2 = -0.0024 \pm 0.0010 \tag{66}$$

From this one may calculate $(d\sigma^p/d\xi)_e$ for ^{19}F in F_2 as -4080 ppm.

Another experimental source of shielding derivatives is the temperature dependence of shielding measured in the dilute gas phase in the limit of zero pressure. There are temperature dependent intermolecular effects which have to be removed in obtaining the zero-pressure limit. These are density dependent and are linear functions of density in the dilute gas.[16] Therefore, variable temperature measurements in samples of known density can give information on both $\sigma_0(T)$, the shielding in the zero-pressure limit, and $\sigma_1(T)$, the intermolecular shielding coefficient in the virial expansion (equation (2)). The fitting of the experimental data points described by $[\sigma_0(T) - \sigma_0(300)]$ to the $\langle\sigma\rangle^T - \langle\sigma\rangle^{300}$ of equation (38) leads to an empirical estimate of $(d\sigma/d\xi)_e$. Although equation (38) involves two parameters, $(d\sigma/d\xi)_e$ and $(d^2\sigma/d\xi)_e$, only the first derivative can be obtained from experiment. The rotational contribution, which has a linear dependence on temperature as seen in equation (38), dominates the temperature dependence, $\langle\sigma\rangle^{400K} - \langle\sigma\rangle^{300K}$, for example. This is shown very dramatically in Table 5. It is in fact not necessary for the rotational contribution to $\langle\sigma\rangle^{400} - \langle\sigma\rangle^{200}$ to be so overwhelming. A significant rotational contribution when combined with an anharmonic vibrational contribution makes the term in $(d\sigma/d\xi)_e$ dominant over the harmonic vibrational contribution which has the factor $(d^2\sigma/d\xi^2)_e$. Both vibrational contributions have the same dependence on temperature, that of $\langle v+\frac{1}{2}\rangle^T$, and on mass, as seen in equation (40). Thus the relative magnitudes of anharmonic and harmonic contributions to the isotope shift (shown in Table 6) also directly reflect the relative magnitudes of the anharmonic and harmonic contributions to the temperature dependence. We see in Table 6 that, except for LiH, the ratio of anharmonic/harmonic contributions which is the ratio $-3a_1(d\sigma/d\xi)_e/(d^2\sigma/d\xi^2)_e$ is better than 2.2–8. Any rotational contribution to the temperature dependence makes the $(d\sigma/d\xi)_e$ more important. Thus it is usually not possible to extract $(d^2\sigma/d\xi^2)_e$ from $\sigma_0(T) - \sigma_0(300)$ experimental data. At the same time this means that the one-parameter fit to the experimental data gives a good account of $(d\sigma/d\xi)_e$ essentially uncontaminated by $(d^2\sigma/d\xi^2)_e$ contributions.

There is a major problem associated with this source of $(d\sigma/d\xi)_e$, however. The $\sigma_0(T) - \sigma_0(300)$ data result after correcting for the temperature dependence of the reference (such as the substance used for the field-frequency lock). This is a small correction when compared to $\sigma_0(T) - \sigma_0(300)$ for ^{19}F. However, for other nuclei which have relatively small changes in σ_0 with temperature, the errors associated with the temperature dependence of the reference may be as large as the $\sigma_0(T) - \sigma_0(300)$ values themselves. This is found to be the case for ^{13}C in CH_4 and ^{11}B in BF_3. For ^{13}C in CO the reference temperature dependence is of the same order of magnitude as the $\sigma_0(T) - \sigma_0(300)$ for CO itself. This leads to systematic errors not reflected in the reported precision of the data. For ^{13}C in CO we reported a derivative that is too small to reproduce the experimental ^{18}O-induced isotope shift in the ^{13}C spectrum observed.[50] On the other hand, with the theoretical derivatives from Stevens and Karplus, we calculate an isotope shift which is -0.0472, in good agreement with the experimental value -0.0476 ± 0.0016 ppm. Some diatomic molecules for which derivatives have been estimated in this way are ^{13}C in CO $((d\sigma/d\Delta r) = -226)$,[67] ^{15}N in N_2 (-774),[67] ^{19}F in ClF (-2070)[57] and ^{19}F in F_2 (-4530),[57] all in ppm Å^{-1}. There are also some estimates for ^1H in HCl and HBr, but since the temperature dependence of ^1H shielding is very small these are probably not accurate.[68]

A third source of empirical estimates of $(d\sigma/d\xi)_e$ is the isotope shift itself. In those cases in which the ratio $[-3a_1(d\sigma/d\xi)]/(d^2\sigma/d\xi^2)_e$ is 8 or greater, the isotope shift will give a value within 12% (or better) of the true $(d\sigma/d\xi)_e$ if the observed isotope shift is fitted to only the linear part of equation (42). For an unfavourable case, ^{19}F in HF, this ratio is 2.2, which means that the isotope shift will give 145% of the true $(d\sigma/d\xi)_e$. Nevertheless, since the isotope shift is so much easier to measure than the temperature dependence of shielding in the gas phase in the zero-pressure limit, this is a valuable tool for this purpose. Furthermore, it is possible to measure isotope shifts in ions such as CN^-, PO_4^{3-} or NH_4^+, on which it would be very difficult to make gas-phase measurements. Thus, for these types of species the isotope shifts provide useful electronic information which is not

otherwise accessible. Diatomic molecules for which isotope shifts have been used to derive estimates of $(d\sigma/d\Delta r)$ are (-456 ± 15 for ^{13}C and -1150 ± 130 for ^{17}O),[50] CN^- (-473 for ^{13}C and -873 for ^{15}N)[69] and H_2 (-11.5,[58] -12.1 [70]), all in ppm $Å^{-1}$.

Of course a combination of methods (ii) and (iii) would allow both first and second derivatives to be determined from experiment. An attempt to use a combination of (i) and (iii) for H_2 gives inconsistent results.[70]

IV. ONE-BOND ISOTOPE SHIFTS IN POLYATOMIC MOLECULES

A. *Ab initio* calculations: the water molecule

Ab initio methods of calculation have provided some highly accurate estimates of electric and magnetic properties of small molecules. However, almost all these calculations have been performed only at the equilibrium molecular geometries. An accurate calculation of NMR isotope shifts requires reliable quantum chemical calculations of the nuclear shielding surface near the equilibrium configuration. From such calculations it would be possible to obtain derivatives of the shielding with respect to geometry changes. These derivatives multiplied by the differences in the mean bond displacements, mean bond angle deformations, etc. which are obtained as thermal averages over a small part of the potential surface lead to calculated NMR isotope shifts according to equation (5). This has been done so far only for the water molecule. Coupled Hartree–Fock perturbation theory has been used[71] to calculate the ^1H and ^{17}O nuclear shielding surfaces. For equilibrium geometries ($r_{OH} = 0.9572$ Å; angle HOH = 104.52°), the origin of the vector potential of the external magnetic field is placed at the oxygen nucleus, and for non-equilibrium geometries the gauge origin is placed at the site on the Eckart axes that the oxygen nucleus would occupy in the equilibrium configuration of $H_2{}^{16}O$. The distance of the gauge origin from the oxygen nucleus is never more than 0.03 Å.

For the equilibrium configuration the following values of the diamagnetic and the paramagnetic parts of both the proton and oxygen shielding tensor components (all in ppm) are obtained.

For the oxygen shielding:

$$\sigma^d(O) = \begin{pmatrix} 415.311 & 0 & 0 \\ 0 & 417.169 & 0 \\ 0 & 0 & 416.02 \end{pmatrix}$$

$$\sigma^p(O) = \begin{pmatrix} -52.549 & 0 & 0 \\ 0 & -112.641 & 0 \\ 0 & 0 & -105.987 \end{pmatrix}$$

leading to

$$\sigma(O) = \begin{pmatrix} 362.762 & 0 & 0 \\ 0 & 304.529 & 0 \\ 0 & 0 & 309.839 \end{pmatrix} \qquad \sigma^O = 325.710 \text{ ppm}$$

For the proton shielding:

$$\sigma^d(H) = \begin{pmatrix} 31.480 & 0 & 21.497 \\ 0 & 7.701 & 0 \\ 18.026 & 0 & 22.712 \end{pmatrix}$$

$$\sigma^p(H) = \begin{pmatrix} 6.628 & 0 & -7.759 \\ 0 & 14.234 & 0 \\ -12.217 & 0 & 6.712 \end{pmatrix}$$

leading to

$$\sigma(H) = \begin{pmatrix} 38.108 & 0 & 17.738 \\ 0 & 21.935 & 0 \\ 5.809 & 0 & 29.424 \end{pmatrix} \qquad \sigma^H = 29.823 \text{ ppm}$$

The isotropic shielding can be directly compared with experimental values. For the proton shielding they estimated a σ_e value of 30.59 ± 0.02 ppm by combining the experimental value of 30.052 ± 0.0015 ppm[72] with a zero-point vibration correction of -0.54 ppm. For the oxygen shielding the agreement with an experimental value of $\sigma_e = 357 \pm 17$ ppm is less satisfactory. The experimental room temperature gas phase value is 344.0 ± 17.2 with a vibrational correction of -13.6.[73]

The calculation of the shielding surface was performed at forty-eight different nuclear geometries (sixteen of C_{2v} symmetry, thirty-two of C_s symmetry) over a range of $0.65 \text{ Å} < r < 1.25 \text{ Å}$ and $61° < \alpha < 155°$. The functional dependence of the oxygen and the proton shielding on $Я_1$, $Я_2$ and $\Delta\alpha$ has been calculated (Fig. 8). The protons are labelled 1 and 2 and the displacements from the equilibrium geometry are $Я_1$ (positive for an increase in the O–H_1 bond length), $Я_2$ (for the O–H_2 bond length), and $\Delta\alpha$ (positive for an increase in the HOH bond angle). Figure 8(a) shows how the oxygen shielding changes with $\Delta\alpha$ ($Я_1 = Я_2 = 0$). A minimum in the shielding surface near the equilibrium bond angle is close to $\Delta\alpha = +0.02$ rad. The fact that σ^O reaches a minimum at an angle coincident with the energy can be understood by the argument that angle change in either direction from the equilibrium weakens the bonding so that σ approaches its atomic value which is larger than for equilibrium. As is visible from Fig. 8(a), σ^O is sensitive to small bond angle deformations. Figure 8(b) gives a plot of σ^O against S_i, the actual displacement along the bond direction of each of

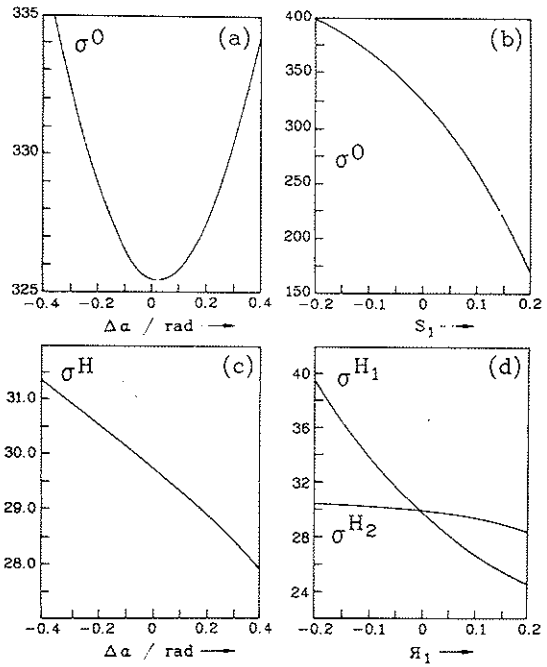

FIG. 8. Nuclear shielding function (in ppm) for H_2O: (a) σ^O *vs.* bond angle change; (b) σ^O *vs.* displacement along the bond direction of each of the two protons; (c) σ^H *vs.* bond angle change; (d) σ^{H_1} and σ^{H_2} *vs.* displacement along O-H_1. From reference 71, with permission.

the two protons. Figure 8(b) also shows that the oxygen shielding is very sensitive to changes in the O-H bond lengths.

The proton shielding as a function of $\Delta\alpha$ and $\mathcal{R}_1$ is given in Fig. 8(c) and (d). The dependence of σ^H on bond angle changes is small compared to bond length changes. An increase in the bond length leads to a decrease in the proton shielding. There are smaller (secondary) effects on σ^H, i.e. the change in $\sigma(H_2)$ due to a change in the other O-H bond ($\mathcal{R}_1$).

From a least-squares fit of their shielding data for different geometries to equation (4), Fowler *et al.* obtained altogether twenty-two independent derivatives of the proton and oxygen nuclear shielding with respect to geometry changes (up to fourth order). Some of these are given below.

For the oxygen shielding:

$$(\partial\sigma^O/\partial\Delta r)_e = -270.9 \text{ ppm Å}^{-1} \qquad (\partial\sigma^O/\partial\Delta\alpha)_e = -27.3 \text{ ppm rad}^{-1}$$

$$(\partial^2\sigma^O/\partial\Delta r^2)_e = -1045.6 \text{ ppm Å}^{-2} \qquad (\partial^2\sigma^O/\partial\Delta\alpha^2)_e = +138.8 \text{ ppm rad}^{-2}$$

For the proton shielding:

$$(\partial\sigma^{H_1}/\partial\Delta r_1)_e = -35.3 \text{ ppm Å}^{-1} \qquad (\partial\sigma^{H_1}/\partial\Delta r_2)_e = -4.6 \text{ ppm Å}^{-1}$$

$$(\partial\sigma^H/\partial\Delta\alpha)_e = -4.0 \text{ ppm rad}^{-1} \qquad (\partial^2\sigma^H/\partial\Delta\alpha^2)_e = -3.0 \text{ ppm rad}^{-2}$$

$$(\partial^2\sigma^{H_1}/\partial\Delta r_1^2)_e = +110.0 \text{ ppm Å}^{-2} \qquad (\partial^2\sigma^{H_1}/\partial\Delta r_2^2)_e = -24.5 \text{ ppm Å}^{-2}$$

The small magnitude of $(\partial\sigma^O/\partial\Delta\alpha)_e$ found in H_2O by Fowler *et al.* as well as by Schindler and Kutzelnigg[74] can be understood in terms of the changes in the bond pair and lone pair electron distributions with bond angle deformation. The lone pair has an important role to play in the ^{17}O shielding (as also in ^{33}S and ^{77}Se shielding in the other bent molecules H_2S, H_2Se, SO_2, SeO_2) because the highest occupied molecular orbital in molecules of this type consists primarily of a lone pair on the central atom, as indicated by theoretical calculations and supported by photoelectron spectral data. The lowest excitation energy corresponds to the magnetic dipole allowed b_1 (lone pair) $\rightarrow a_1$ excitation which therefore makes an important contribution to the paramagnetic term in the shielding according to Ramsey's theory.[64] Figure 9 shows the results of *ab initio* studies in H_2O, in which the bond lengths are held fixed at their equilibrium value and the bond angle is allowed to vary.[75] These diagrams show that, as the nuclei vibrate away from their equilibrium positions, the oxygen orbital lags behind whereas the orbitals centred on H completely follow the H nuclei. Also, the oxygen lone pair p character increases with increasing bond angle. Similar results are obtained for H_2S. The consequences of charge redistribution accompanying bond angle deformation are as follows. The lack of orbital following leads to a small magnitude of $(\partial\sigma^O/\partial\Delta\alpha)_e$. In the limit of complete orbital stasis $(\partial\sigma^O/\partial\Delta\alpha)_e \approx 0$. To a first approximation the increase in p character of the O lone pair with increasing bond angle gives a deshielding contribution, i.e. $(\partial\sigma^O/\partial\Delta\alpha)_e < 0$. This qualitative picture is consistent with the results of Fowler *et al.*, and also with Schindler and Kutzelnigg's $(\partial\sigma^O/\partial\Delta\alpha)_e = -7 \text{ ppm rad}^{-1}$.

The next step in calculating the isotope shifts in the water molecule is the calculation of $\langle\Delta r\rangle$ and $\langle\Delta\alpha\rangle$. Fowler and Raynes[76] used the first method outlined in Section II.B.1. They obtained the oxygen and proton shielding for individual vibrational and rotational states, some of which are shown in Table 9. These shieldings for individual states cannot be measured experimentally because of the short lifetime of a molecule in a particular rovibrational state compared with the relatively long time scale of an NMR experiment. Thus all that can be obtained experimentally is an average value for a given temperature. The two methods described in Section II were employed to obtain the thermal average. Method 1 is a straightforward

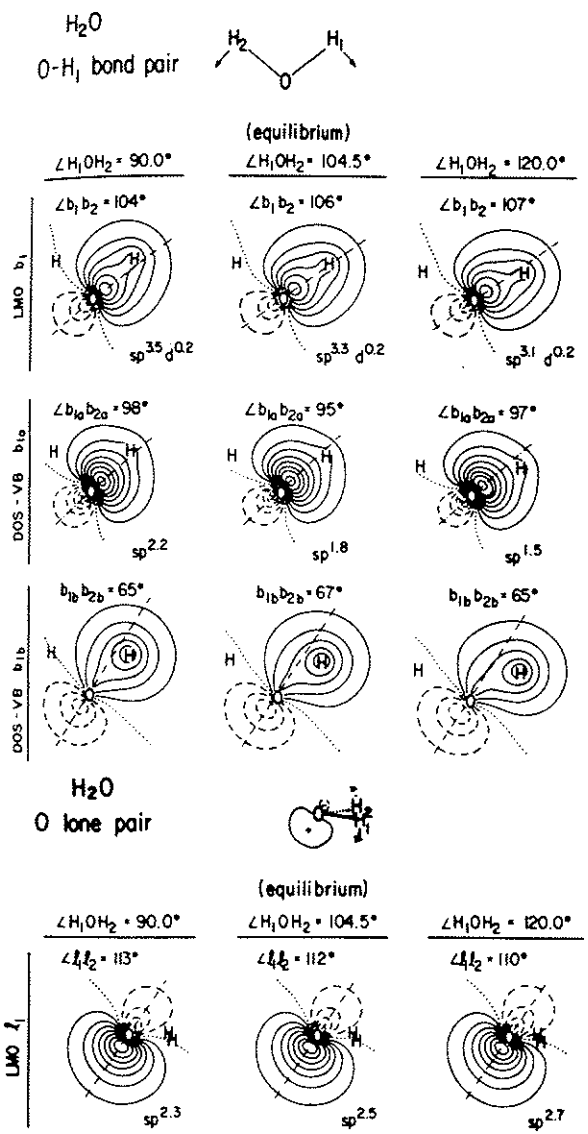

FIG. 9. Charge density maps illustrating bond pair and lone pair "orbital following" in H_2O with change in bond angle. From reference 75, with permission.

TABLE 9

Nuclear shielding σ^H and σ^O for the water isotopomers $H_2{}^{17}O$ and $D_2{}^{17}O$ in low rovibrational states, in ppm.[76]

State					$H_2{}^{17}O$		$D_2{}^{17}O$
v_1	v_2	v_3	J	τ	σ^H	σ^O	σ^O
		at r_e			29.820	325.56	325.56
0	0	0	0	0	29.276	312.44	316.12
0	0	0	1	−1	29.273	312.41	316.10
0	0	0	1	0	29.276	312.38	316.08
0	0	0	1	1	29.274	312.37	316.08
0	1	0	0	0	29.052	313.95	317.34
0	2	0	0	0	28.830	315.25	318.48
1	0	0	0	0	28.923	297.92	305.83
0	0	1	0	0	28.739	297.82	305.54
1	1	0	0	0	28.742	298.85	306.72
0	1	1	0	0	28.541	299.12	306.65

average, thus

$$\langle\sigma\rangle^T = \frac{\sum_{vJ\tau}(2J+1)g_{Ns}\langle\sigma\rangle_{vJ\tau}\exp(-E_{vJ\tau}/kT)}{\sum_{vJ\tau}(2J+1)g_{Ns}\exp(-E_{vJ\tau}/kT)} \tag{67}$$

where $E_{vJ\tau}$ stands for a particular rovibrational energy level and g_{Ns} is a factor which takes account of nuclear spin statistics. This method obviously requires the calculation of a very large number of energy levels (for example rotational levels are calculated as far as $J=25$ and levels more than 5000 cm^{-1} above the zero point levels are excluded).[76]

In practice equation (67) is always a truncated summation over a finite number of rovibrational states. It is found that this sum does not converge very fast; the individual terms can even have alternating signs. In Table 10 the thermal average shieldings of the oxygen and proton in the water molecule obtained with this method and with the coth function (as used in equation (11)) are compared. The results are nearly identical for temperatures normally accessible in NMR spectrometers. For larger molecules it becomes impossible to calculate a sufficient number of rovibrational states in order to use the exact method for the thermal averaging, so the only practical way of calculating expectation values of molecular properties over different rotational and vibrational states for a given temperature is by using the harmonic approximation for the vibrational partition function.

The isotope effects on nuclear shielding in the water molecule are $^1H(^{18/16}O) = -0.002$ ppm $(-0.012 \pm 0.004$ ppm$)$[77] for the oxygen-induced shift on the protons, and $^{17}O(^{2/1}H, ^{2/1}H) = -3.68$ ppm $(-3.08 \pm 0.20$ ppm$)$[78]

for the deuterium-induced shifts on the oxygen nucleus in $D_2{}^{17}O$ compared to $H_2{}^{17}O$ (all at 300 K). The experimental values are given in parentheses. There are no gas phase data for comparison; both measurements were made on liquid phase samples in which hydrogen-bonding will almost certainly have somewhat different effects on different isotopomers.

TABLE 10

The thermal average shielding in water calculated using equation (67) and approximately using the coth function, equation (11).[76]

Temp. (K)	Proton shielding			Oxygen shielding		
	exact		approx.	exact		approx.
	o-$H_2{}^{16}O$	p-$H_2{}^{16}O$	$H_2{}^{16}O$	o-$H_2{}^{17}O$	p-$H_2{}^{17}O$	$H_2{}^{17}O$
0	29.272	29.275	29.275	312.413	312.443	312.443
30	29.272	29.275	29.273	312.394	312.409	312.397
60	29.270	29.271	29.270	312.354	312.356	312.351
100	29.267		29.267	312.296		312.290
150	29.263		29.263	312.216		312.214
200	29.258		29.258	312.139		312.137
250	29.254		29.254	312.061		312.061
300	29.250		29.250	311.983		311.985
350	29.245		29.245	311.906		311.910
400	29.240		29.241	311.830		311.836
450	29.235		29.236	311.755		311.763
500	29.230		29.231	311.681		311.692

The accurate calculation of isotope shifts in any property (bond length, nuclear shielding, etc.) is done by a difference approach, i.e. the property is calculated for both the reference molecule and the isotopically substituted molecule and the difference between them is obtained. This is the approach used in this review exclusively. Another approach is a direct one, in which isotopic substitution is considered as a perturbation of the reference molecule. The mass perturbation appears as a modification to the kinetic energy term in the vibration-rotation hamiltonian. The formulae for this double perturbation method have been derived by Fowler, and a more approximate version of the same approach is given by Mamayev and Sergeyev.[79] Fowler finds that (as expected) the mass perturbation approach works nearly as well as the difference approach when the fractional mass change is small (as for $^{16}O \rightarrow {}^{18}O$) but not so well (giving incorrect signs and magnitudes) when the fractional mass change is large (as for H → D).

B. Calculation of mean bond displacements and mean bond angle deformations

In the following we describe applications of Bartell's approach to different molecular types, starting with some molecules where the force field up to at least cubic terms is known, and then some model potentials for other polyatomic molecules.

1. Triatomic molecules

The best description of the potential energy surface for polyatomic molecules is for linear triatomics, especially one in which many isotopic species provide an abundance of spectroscopic observables from which a least-squares refinement technique gives an anharmonic force field which is the best fit to the data. Of the polyatomic molecules, CO_2 and NNO probably have the most studied potential energy surface from the point of view of vibrational spectroscopy. The anharmonic force fields up to quintic and sextic terms have been obtained from the very large set of vibrational-rotational data belonging to ten isotopic species in the case of CO_2,[80-83] and eleven in the case of NNO.[84-86]

The general force field in terms of the true curvilinear coordinates for the linear triatomic molecule is:

$$\begin{aligned} V = {} & K_{11}\mathcal{R}_1{}^2 + K_{22}\mathcal{R}_2{}^2 + K_{33}\mathcal{R}_3{}^2 + K_{13}\mathcal{R}_1\mathcal{R}_3 \\ & + K_{111}\mathcal{R}_1{}^3 + K_{113}\mathcal{R}_1{}^2\mathcal{R}_3 + K_{133}\mathcal{R}_1\mathcal{R}_3{}^2 + K_{333}\mathcal{R}_3{}^2 \\ & + K_{122}\mathcal{R}_1\mathcal{R}_2{}^2 + K_{223}\mathcal{R}_2{}^2\mathcal{R}_3 + \text{higher order terms} \end{aligned} \tag{68}$$

Here $\mathcal{R}_1$ denotes the displacement coordinate of the Y-X bond, $\mathcal{R}_3$ the displacement of the X-Z bond and $\mathcal{R}_2$ the bond angle deformation $\Delta\alpha$. Applying equation (13) by using the derivatives (14) we obtain

$$\begin{aligned} \langle \Delta r \rangle_{\text{vib}} = -[1/(2K_{11} + K_{13})]\{ & (3K_{111} + K_{113})\langle (\Delta r)^2 \rangle \\ & + 2K_{113}\langle \Delta r_1 \Delta r_3 \rangle + [K_{122} - (1/r)K_{22}]\langle (\Delta\alpha)^2 \rangle\} \end{aligned} \tag{69}$$

for the mean bond displacement due to vibration in CO_2 and two similar, but coupled equations for NNO.[34] Owing to the symmetry of the molecules the mean bond angle deformation must be zero, whereas the mean square amplitude of $\langle (\Delta\alpha)^2 \rangle$ is non-zero. The rotational contribution which can be obtained in a closed form (Section II.B.2) has to be added. Table 11 shows some characteristic results obtained using a harmonic oscillator partition function (equation (11)). The results for $\langle \Delta r_{CO} \rangle^T$ in CO_2 are in excellent agreement with recent electron diffraction data,[87] and with an accurate calculation of $\langle \Delta r \rangle$ by Kohl and Hilderbrandt[88] using variational methods. For example, at 300 K we find the vibrational contribution to $\langle \Delta r_{CO} \rangle^T =$

TABLE 11

Mean bond displacement due to anharmonic vibration and rotation in linear triatomic molecules, all in 10^{-3} Å.[34]

		$\langle\Delta r\rangle^{T}_{vib}$	$\langle\Delta r\rangle^{T}_{rot}$	$\langle\Delta r\rangle^{T}$
$^{13}C^{16}O_2$	250 K	4.4802	0.1718	4.6520
	300 K	4.5031	0.2062	4.7093
	350 K	4.5350	0.2405	4.7755
$^{15}N^{15}N^{16}O$				
$\langle\Delta r_{NN}\rangle^{T}$	250 K	4.9389	0.1425	5.0814
	300 K	4.9868	0.1710	5.1578
	350 K	5.0464	0.1995	5.2459
$\langle\Delta r_{NO}\rangle^{T}$	250 K	5.3217	0.2436	5.5652
	300 K	5.3556	0.2923	5.5479
	350 K	5.4044	0.3410	5.7453

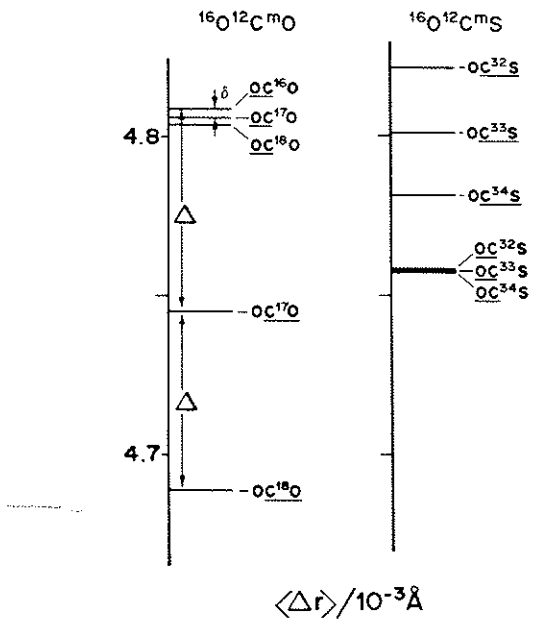

FIG. 10. Mean bond displacements at 300 K in CO_2 and OCS, illustrating the primary effect (Δ), the secondary effect (δ) and the additivity of the effects. From reference 90, with permission.

0.0045 and $\langle\Delta r_{CO}{}^{2}\rangle^{T} = 0.0012$, whereas Kohl and Hilderbrandt obtain 0.0040 and 0.0012, respectively.

In order to study the mass dependence of $\langle\Delta r\rangle^{T}$ we performed the calculation for different isotopomers of a symmetric (CO_2) and a non-symmetric (OCS)[89] linear triatomic molecule.[90] The results are shown in Fig. 10.

For bent triatomic molecules $\langle\Delta\alpha\rangle \neq 0$, so we also have to include the mean bond angle deformations, leading to three coupled equations to be solved. Such calculations were performed for several bent triatomic molecules.[14] The results shown in Table 12 can be summarized as follows. As is generally found for other molecules, vibrational and rotational contributions to the mean bond displacements $\langle\Delta r\rangle$ are positive. As usual an increase in temperature leads to an increase in the mean bond displacements, and for X–H bonds this is dominated by rotational contributions because the higher vibrational frequencies for these molecules lead to a smaller

TABLE 12

Mean bond displacement and mean bond angle deformation at 300 K, isotope effects ($\Delta_{iso} = \langle\Delta r\rangle^{300}_{light} - \langle\Delta r\rangle^{300}_{heavy}$, or $r\langle\Delta\alpha\rangle^{300}_{light} - r\langle\Delta\alpha\rangle^{300}_{heavy}$) and temperature dependence ($\Delta_T = \langle\Delta r\rangle^{400} - \langle\Delta r\rangle^{200}$, or $r\langle\Delta\alpha\rangle^{400} - r\langle\Delta\alpha\rangle^{200}$) for bent triatomic molecules.[14]

		$\langle\Delta r\rangle$			$r\langle\Delta\alpha\rangle$		
		vib.	rot.	total	vib.	rot.	total
H_2O	(10^{-2} Å)	1.915	0.088	2.003	0.218	−0.215	0.003
D_2O	(10^{-2} Å)	1.391	0.087	1.478	0.211	−0.201	0.010
Δ_{iso}	(10^{-3} Å)	5.237	0.006	5.243	0.075	−0.141	−0.066
Δ_T	(10^{-4} Å)	0.085	5.846	5.931	0.083	−14.340	−13.508
H_2S	(10^{-2} Å)	1.836	0.110	1.947	0.129	−0.067	0.062
D_2S	(10^{-2} Å)	1.318	0.110	1.428	0.126	−0.057	0.069
Δ_{iso}	(10^{-3} Å)	5.181	0.002	5.181	0.034	−0.104	−0.070
Δ_T	(10^{-4} Å)	0.309	7.364	7.673	0.249	−4.505	−4.256
H_2Se	(10^{-2} Å)	1.925	0.124	2.049	−0.183	−0.076	−0.260
D_2Se	(10^{-2} Å)	1.373	0.124	1.497	−0.101	−0.071	−0.172
Δ_{iso}	(10^{-3} Å)	5.514	0.001	5.515	−0.826	−0.054	−0.880
Δ_T	(10^{-4} Å)	0.553	8.272	8.825	2.286	−5.101	−2.815
O_2S	(10^{-2} Å)	0.471	0.046	0.516	0.283	−0.179	0.104
$^{18}O_2S$	(10^{-2} Å)	0.454	0.046	0.500	0.282	−0.176	0.106
Δ_{iso}	(10^{-3} Å)	0.171	0.001	0.172	0.015	−0.031	−0.016
Δ_T	(10^{-4} Å)	2.138	3.041	5.179	7.385	−11.965	−4.579

temperature dependence in the $(1/\omega)\coth(hc\omega/2kT)$ terms appearing in the vibrational averaging. The rotational contribution, on the other hand, is linear with temperature. The magnitude of the isotope effect on the bond length at 300 K is dominated by vibratior in all cases.

The vibrational contribution to the mean bond angle deformation, $\langle\Delta\alpha\rangle_{vib}$, is of either sign, i.e. in some of the molecules the average bond angle is greater than the equilibrium value and in others it is smaller. In all cases, however, $\langle\Delta\alpha\rangle_{vib}$ increases algebraically with increasing temperature, the changes with temperature being smaller for the hydrides owing to the greater vibrational frequencies. The rotational contribution to the mean bond angle deformation, $\langle\Delta\alpha\rangle_{rot}$, is negative for all bent triatomics. These findings can be understood in terms of the predominant centrifugal stretching effects arising from the rotation about the principal axis parallel to the line connecting the two end atoms. The isotope effects on $\langle\Delta\alpha\rangle$ upon substitution of the end atoms have different signs, a result of the different mass dependence of the rotational and vibrational contributions. The change with mass of $\langle\Delta\alpha\rangle_{vib}$ is of either sign but always such as to bring the mean bond angle closer to the equilibrium values as the masses of the end atoms increase.

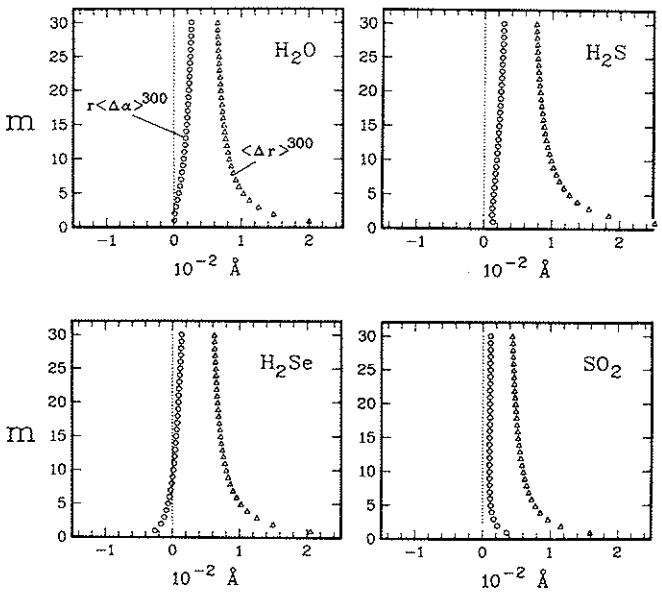

FIG. 11. The mass dependence of $r\langle\Delta\alpha\rangle$ (shown as ○) and $\langle\Delta r\rangle$ (shown as △) in bent triatomic molecules. The masses of the end atoms are varied arbitrarily while keeping the same force field. From reference 14, with permission.

On the other hand, the changes with masses of $\langle\Delta\alpha\rangle_{rot}$ is always of the same sign, the bond angle increasing with increasing mass. Altogether the mass dependence of $\langle\Delta r\rangle$ is stronger than that of $\langle\Delta\alpha\rangle$ in all cases. For example, $[\langle\Delta r_{XH}\rangle-\langle\Delta r_{XD}\rangle]\gg r[\langle\Delta\alpha_{HXH}\rangle-\langle\Delta\alpha_{DXD}\rangle]$ by a factor of 6 to 80. Figure 11 shows the mass dependence of $\langle\Delta r\rangle$ and $\langle\Delta\alpha\rangle$ for selected bent triatomic molecules. These calculations were carried out with arbitrarily assigned masses of 1–30 amu for the end atoms without changing the mass-independent constants in the force field. Figure 11 shows that even in bent triatomic molecules the $\langle\Delta\alpha\rangle$ term is not important for isotope shifts.

2. *The Urey–Bradley model force field approach*

A review by Duncan shows that uniquely determined general harmonic force fields (GHFF) are available for only selected molecules[91] and the general anharmonic force field is known for even fewer molecules. In most cases it is necessary to assume certain model potential functions. It has been shown[92] that a modified Urey–Bradley potential function[93] gives a reasonably good description of molecular vibrations. The Urey–Bradley force field (UBFF) has found its greatest application in the calculation of vibration frequencies of halogenated molecules. The number of independent UB force constants is usually less than that of the GHFF and they show a remarkable degree of transferability. This means that it is possible to use exactly the same set of UB force constants for all halomethanes to be compared, for example, a feature which makes the UB approach especially suitable for application to isotope effects.[11,94,33] The UB field is expressed as[95]

$$V=\sum_i[K_i' r_i\Delta r_i+\tfrac{1}{2}K_i(\Delta r_i)^2]+\sum_{i<j}[H_{ij}' r_{ij}^2\Delta\alpha_{ij}+\tfrac{1}{2}H_{ij}(r_{ij}\Delta\alpha_{ij})^2]$$
$$+\sum_{i<j}[F_{ij}' q_{ij}\Delta q_{ij}+\tfrac{1}{2}F_{ij}(\Delta q_{ij})^2] \qquad (70)$$

where r is the bond length, α the bond angle, q the distance between atoms not bonded directly, and r_{ij} represents $(r_ir_j)^{1/2}$. K', K, H', H, F', F are the bond stretching, angle bending, and repulsive (between non-bonded atoms) force constants. The non-bonded distance coordinate Δq_{ij} can be expressed in terms of Δr_i, Δr_j and $\Delta\alpha_{ij}$ (equation 7 in reference 33).

To take into account the anharmonicity of vibration Bartell[96] suggested the following terms:

$$V_a=-\tfrac{1}{2}\sum_i a_iK_i(\Delta r_i)^3+\tfrac{1}{2}\sum_i\sum_{j\neq i}(1/6q_{ij})F_{ij}^3(\Delta q_{ij})^3 \qquad (71)$$

It seems reasonable to express the stretching part of V as a potential function similar to that of a diatomic molecule, so a Morse function (equation (34)) is used for the stretching anharmonicity.[96] F_{ij}^3, the cubic force constant

appropriate to non-bonded interactions, can be obtained as follows:

$$F^3 = q[\partial^3 V(q)/\partial q^3] \tag{72a}$$

$$V(q) = A\exp(-Bq) - Cq^{-6} \quad \text{for H–X interactions} \tag{72b}$$

$$V(q) = 4\varepsilon[(q_0/q)^{12} - (q_0/q)^6] \quad \text{for X–Y interactions} \tag{72c}$$

The parameters A, B, C, or ε and q_0 are available.[97,98] So far there is no sufficiently good model to describe the bending anharmonicity. Thus we neglect the H^3 terms in equation (71) even if they could become important in certain cases like pyramidal molecules of C_{3v} symmetry.[14]

In order to use Bartell's approach to calculate the mean bond displacements from a UB force field we need the additional derivatives of the non-bonded displacement coordinate Δq_{ij} with respect to the Cartesian displacement coordinates:

$$(\partial \Delta q_{ij}/\partial \Delta z_k) = s_{kj}\delta_{ik} = s_{ik}\delta_{jk} \tag{15c}$$

where δ_{ij} is the Kronecker delta and s_{ij} is a geometry factor:

$$s_{kj} = (r_k - r_j \cos \alpha_{kj})/q_{kj}$$

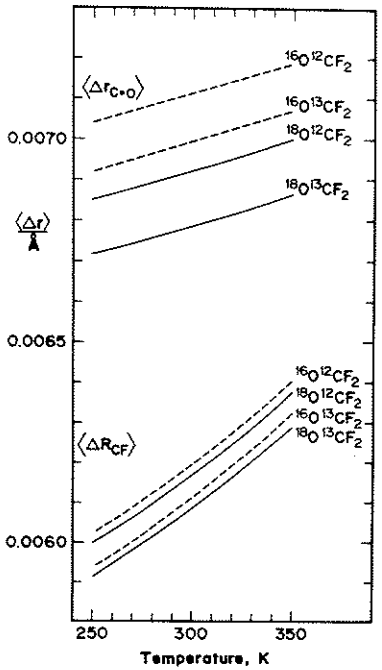

FIG. 12. Mean bond displacement for various isotopomers of $O{=}CF_2$.[33]

Results for the mean bond displacement as a function of temperature for various isotopomers of carbonyl fluoride obtained from such calculations[33] are shown in Fig. 12.

3. *Estimation methods for mean bond displacements*

Although second derivative terms are not negligible in isotope shifts, for the purpose of obtaining estimates of isotope shifts we will consider only the term in the first derivative with respect to bond extension:

$$\sigma - \sigma^* \approx (\partial\sigma/\partial\Delta r)_e[\langle \Delta r \rangle - \langle \Delta r \rangle^*] \tag{73}$$

A method of estimating $\langle \Delta r \rangle$ which can be applied to an arbitrary bond to an end atom in a molecule would be very useful for predicting orders of magnitude of isotope shifts. This would allow one to determine *a priori* whether a particular isotopic substitution would be worthwhile to attempt for a given application. For the majority of molecules insufficient spectroscopic information is available to permit full dynamic calculations, so it is necessary to develop an approximation method in order to estimate the mean bond displacements for these molecules. It appears that stretching cubic constants for polyatomic molecules can be deduced from the bond length in the same way as for diatomic molecules. The Herschbach and Laurie parameters used for such estimation for diatomic molecules (Section III.B.3) are found to describe F_3 for polyatomic molecules as well.[58,59] Therefore we can use equation (59) to predict mean bond displacements in polyatomic molecules if the Morse anharmonic stretching accounts for most of the mean bond displacement.[58]

In Fig. 13 the plots of $\mu^{-1/2}10^{-D}$ *vs.* $\langle \Delta r \rangle_{vib}$ calculated for selected polyatomic molecules are compared with the results for some diatomic molecules.[58] A least-squares fit gives a slope of 22×10^{-3} rather than the 19.35×10^{-3} factor containing the fundamental constants in equation (59). The slope for the polyatomic molecules is somewhat larger because the other contributions due to bending and non-bonded interactions can be significant. Bartell has shown that, for molecules of the AX_n type, the Morse stretching contribution to $\langle \Delta r \rangle$ is only 64% in CH_4,[99] and only about 40% in SF_6.[100] However, equation (59) with a modified factor of 22×10^{-3} for polyatomics gives a satisfactory estimate of $\langle \Delta r \rangle$ from r_e. Therefore we shall use

$$\langle \Delta r \rangle_{vib}/\text{Å} \approx 22\times10^{-3}\mu^{-1/2}10^{-D} \tag{74}$$

where D is given by equation (60).

The rotational contribution to $\langle \Delta r \rangle$ is likewise easily estimated from r_e alone for an AX_n molecule:[99]

$$\langle \Delta r \rangle_{rot} = 2\bar{E}_{rot}/(nF_2 r_e) \tag{75}$$

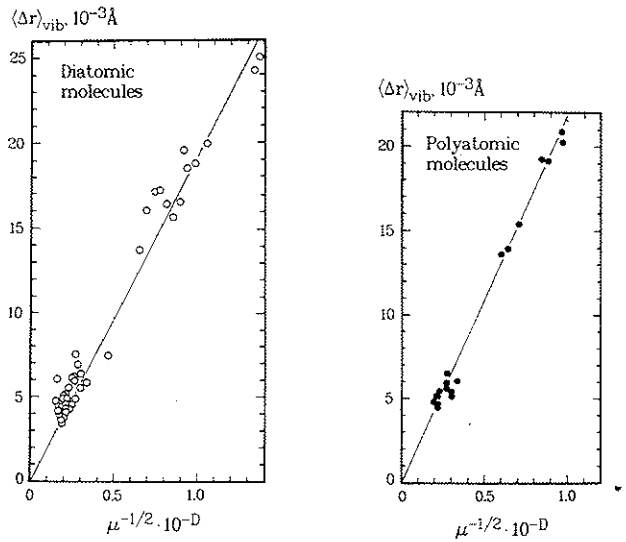

FIG. 13. Test of approximation in equation (47) (straight line, slope = 19.35×10^{-3}), against calculated mean bond displacements for diatomic molecules. The same method is applied to polyatomic molecules; the straight line is a least-squares fit to the data (slope = 22×10^{-3}). From reference 58, with permission.

where $\bar{E}_{rot}$ is the classical average, kT for linear molecules, and $(3/2)kT$ for non-linear ones, and F_2 is expressed according to equation (58). However, we do not even need $\langle\Delta r\rangle_{rot}$ for estimating most isotope shifts. For bent triatomic molecules we already have seen that rotation does not play a significant role in the isotope shifts of the central atom upon end atom substitution. We have shown (Section III.A) that for diatomic molecules there is no rotational contribution to the isotope shift and for symmetrical substitution in molecular types CH_4, BF_3, SF_6, CO_2 there is also no rotational contribution to the isotope shift (Section II.B.2). We will see in Section IV.D that, even in unsymmetrical substitution in CH_4 isotopomers, the rotational contribution plays no role in the D-induced ^{13}C isotope shift. For the isotope shift of the end atom the rotational contribution is also not too important. For example, the dynamical factor relevant to $^2\Delta^1H(^{2/1}H)$ in CH_4-CH_3D is -2.687×10^{-4} Å from rotation and 5.53×10^{-3} Å from vibration, only 5% contribution from rotation. For $^1\Delta^1H(^{17/16}O)$ in $H_2{}^{16}O$-$H_2{}^{17}O$ the dynamical factor is -4.176×10^{-7} Å from rotation and 3.102×10^{-5} Å from vibration, only 1.4% rotational contribution.

C. The reduced isotope shift in polyatomic molecules

From dynamical calculations for different molecular types of different symmetries[33-35,14] we find in general (for any molecular type and any

substitution site) that the change in the mean bond displacement upon isotopic substitution can be expressed as follows:

$$\Delta = \langle\Delta r\rangle - \langle\Delta r\rangle^* = \langle\Delta r\rangle\frac{m'-m}{m'}f(m, m_A, \ldots) \tag{76}$$

The consequences of equation (76) for one-bond isotope shifts in NMR are clear if equation (73) holds (i.e. including only linear terms in the expansion of nuclear shielding in bond displacements). Comparing several isotopic species which differ in one mass m', from the parent species with mass m, we should get a constant value for the ratio $(\langle\Delta r\rangle - \langle\Delta r\rangle^*)/[\langle\Delta r\rangle\times(m'-m)/m']$. Furthermore, if the isotope shift can be approximated by equation (73), we should find $(\sigma-\sigma^*)/[(m'-m)/m'] =$ constant. An excellent test of this is provided by the $^{m'/m}$Se-induced ^{77}Se isotope shifts in diselenides. Gombler[101] measured the isotope shifts in $R_1{}^{77}SeSeR_2$ (R_1, $R_2 = CF_3$, CH_3) for $m = 74$, $m' = 76$, 77, 78, 80, 82 plotted in Fig. 14. Indeed we find a strictly linear behaviour of the isotope shifts $^1\Delta^{77}Se(^{m'/74}Se)$ *vs.* $(m'-m)/m'$ (for $m = 74$) for all four molecules.[90] This seems to indicate that either the interpretation of isotope shifts using equation (73) is sufficient, or all of the dynamic variables $(\langle\Delta r\rangle^2)$, $\langle(\Delta\alpha)^2\rangle$, etc.) on which the shielding

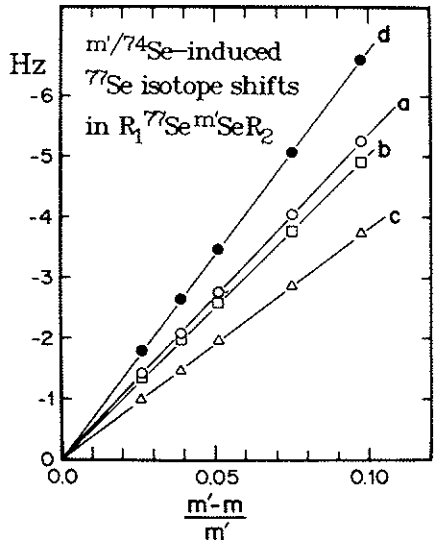

FIG. 14. Effect of selenium isotopes on the ^{77}Se nuclear shielding in the diselenides $R_1{}^{77}Se{}^{m'}SeR_2$. (a) $R_1 = R_2 = CH_3$; (b) $R_1 = R_2 = CF_3$; (c) $R_1 = CF_3$, $R_2 = CH_3$; (d) $R_1 = CH_3$, $R_2 = CF_3$; from experimental results by Gombler.[101] This plot of $^1\Delta^{77}Se(^{m'/74}Se) = \sigma(R_1{}^{77}Se^{74}SeR_2) - \sigma(R_1{}^{77}Se{}^{m'}SeR_2)$ *vs* $(m'-74)/m'$ illustrates the validity of equation (76). From reference 90, with permission.

depends are scaled by $(m'-m)/m'$ upon isotopic substitution. In fact we have found[102] in bent triatomic molecules that $\langle(\Delta\alpha)^2\rangle$, for example, does not scale by $(m'-m)/m'$.

By comparing the mean bond lengths of various isotopomers of several molecular types, we have found[90] a functional form

$$f(m, m_A, \ldots) \approx \frac{1}{2}\frac{m_A}{m_A+m}$$

that can reproduce the primary effect of isotopic substitution on the mean bond displacement for substitution at end atoms:

$$\Delta = \langle\Delta r\rangle - \langle\Delta r\rangle^* \approx \langle\Delta r\rangle \frac{m'-m}{m'} \cdot \frac{1}{2}\frac{m_A}{m_A+m} \tag{51}$$

that is, the same form as we had derived (equation (51)) for diatomic molecules. Thus, for a single substitution of m by m':

$$\begin{aligned} {}^1\Delta A({}^{m'/m}X) &\approx \left(\frac{\partial\sigma^A}{\partial\Delta r_{AX}}\right)_e [\langle\Delta r_{AX}\rangle - \langle\Delta r_{AX}\rangle^*] \\ &\approx \left(\frac{\partial\sigma^A}{\partial\Delta r_{AX}}\right)_e \langle\Delta r\rangle \frac{m'-m}{m'} \cdot \frac{1}{2}\frac{m_A}{m_A+m} \end{aligned} \tag{77}$$

On this basis we can use the same definition for the reduced isotope shift as for diatomic molecules, equation (54), which in this approximation can be identified with

$${}^1\Delta^R(A, X) \approx \left(\frac{\partial\sigma^A}{\partial\Delta r_{AX}}\right)_e \langle\Delta r_{AX}\rangle + \frac{1}{2}\left(\frac{\partial^2\sigma^A}{\partial\Delta r_{AX}^2}\right)_e \langle(\Delta r_{AX})^2\rangle \tag{78}$$

and for 300 K, for a symmetrical AX_n molecule,

$$[\sigma_0{}^A(300\text{ K}) - \sigma_e] \approx n\,{}^1\Delta^R(A, X) \tag{79}$$

Thus we can obtain directly from experimental isotope shifts the same $[\sigma_0(300)-\sigma_e]$ that normally have been obtained from fitting the experimental $[\sigma_0(T)-\sigma_0(300)]$ function to dynamical calculations of $(\langle\Delta r\rangle^T - \langle\Delta r\rangle^{300})$.[103] Note that equation (79) is an approximation because, unlike equation (55) for diatomics, not all the quadratic terms which contribute to the rovibrational corrections to shielding in polyatomic molecules are included.

In Table 13 we present some experimental isotope shifts and the derived rovibrational corrections to the shielding in selected molecules. For CH_4, dynamical calculations including secondary vibrational effects on mean bond displacements,[35] yield for the rovibrational correction to the ^{13}C-shielding −2.985 ppm, to be compared to an estimate of −3.3 ppm. For ^{19}F in HF, calculations lead to −9.58 ppm (this work) shown in Table 4, −9.75 ppm,[104] and −11.23 ppm,[43] to be compared with −10.5 ppm from equation (79).

TABLE 13

The rovibrational correction to shielding, in ppm, and estimates of the derivatives $(\partial\sigma/\partial\Delta r)_e$, in ppm Å^{-1}, directly obtained from reduced isotope shifts (see references 14 and 58).

Nucl.	Mol.	m'/m	$-{}^1\Delta$	$-{}^1\Delta^R$	$[\sigma(300)-\sigma_e]$	$(\partial\sigma/\partial\Delta r)_{est}$
		(a) Highly symmetric molecules ($\langle\Delta\alpha\rangle = 0$)				
^2D	HD	$^{2/1}H$	0.0469	0.2814	−0.2814	−11.5
^{11}B	BH_4^-	$^{2/1}H$	0.138	0.6	−2.4	−26.7
^{13}C	CH_4	$^{2/1}H$	0.192	0.82	−3.3	−39
	CN^-	$^{15/14}N$	0.03 ± 0.005	1.87	−1.87	−380
	CO	$^{18/16}O$	0.0476 ± 0.0016	1.91	−1.91	−470
	CO_2	$^{18/16}O$	0.019	0.76	−1.53	−160
	CS_2	$^{34/32}S$	0.009	1.06	−2.12	−220
^{15}N	NH_4^+	$^{2/1}H$	0.307	1.32	−5.26	−65
	NO_3^-	$^{18/16}O$	0.056	2.16	−6.5	−410
	CN^-	$^{13/12}C$	0.075 ± 0.005	3.51	−3.5	−700
	N_2	$^{15/14}N$	0.0601 ± 0.002	3.49	−3.49	−900
^{17}O	CO	$^{13/12}C$	0.110 ± 0.011	4.88	−4.88	−1190
^{19}F	HF	$^{2/1}H$	2.5 ± 0.5	10.5	−10.5	−675
^{31}P	PO_4^{3-}	$^{18/16}O$	0.019 ± 0.002	0.52	−2.1	−120
^{55}Mn	MnO_4^-	$^{18/16}O$	0.59 ± 0.02	13.7	−55	−2490
^{95}Mo	MoO_4^{2-}	$^{18/16}O$	0.25 ± 0.01	5.26	−21	−1400
^{99}Tc	TcO_4^-	$^{18/16}O$	0.44 ± 0.06	9.2	−37	−2030
^{195}Pt	$PtCl_6^{2-}$	$^{37/35}Cl$	0.167	7.3	−43.8	−2530
	$PtBr_6^{2-}$	$^{81/79}Br$	0.028 ± 0.006	3.18	−19	−1470
		(b) Bent molecules ($\langle\Delta\alpha\rangle \neq 0$)				
^{17}O	H_2O	$^{2/1}H$	1.54	6.52	−13.0	−340
^{15}N	NH_3	$^{2/1}H$	0.65	2.77	−8.3	−140
	NO_2^-	$^{18/16}O$	0.138	5.13	−10.3	−990
^{31}P	PH_3	$^{2/1}H$	0.843	3.48	−10.4	−200
	PCl_3	$^{37/35}Cl$	0.019	1.5	−4.5	−310
	PBr_3	$^{81/79}Br$	0.006	1.72	−5.2	−370
^{77}Se	H_2Se	$^{2/1}H$	7.02	28.4	−56.9	−1540

Another useful application of the reduced isotope shift is in the estimation of a derivative of nuclear shielding from a measured one-bond isotope shift with no other information other than a bond length. We use our empirical method of estimating $\langle\Delta r\rangle_{vib}$ for cases where it is not possible to perform a full dynamical calculation. We can apply this method to the estimation of the shielding derivatives from reported one-bond isotope shifts using

$$(\partial\sigma^A/\partial\Delta r)_e \approx {}^1\Delta^R(A, X)/\langle\Delta r_{AX}\rangle_{vib} \tag{80}$$

Estimates of shielding derivatives using this equation are shown in Table 13. No other information except the bond length was used to obtain these derivatives. It is encouraging that they compare reasonably well with results from *ab initio* and other methods which require much more elaborate experiments or computations. Comparisons with other values are discussed in Section IV.F.

So far we have limited the discussion to molecules with vanishing mean bond angle deformations. We have shown in Section IV.B.1 that, for several bent triatomic molecules, the substitution of another isotope on an end position does not change $\langle\Delta\alpha\rangle$ significantly compared to the change in $\langle\Delta r\rangle$. The same holds for other bent molecules.[14] Fowler[71] has shown that the $\langle\Delta\alpha\rangle$ terms do not contribute significantly to the isotope shift in H_2O. The isotope shift is dominated in all cases by changes in the mean bond displacements rather than the changes in the mean bond angle deformations. This means that we can apply the same definition for a reduced isotope shift as a first order approximation for these molecules too. Table 13 includes some rovibrational corrections for bent molecules calculated in this way. For ^{17}O in H_2O Fowler *et al.* calculate -13.576,[76] to be compared with our estimate of -13.0. The agreement of our estimate with *ab initio* shielding calculations is encouraging.

If the substitution takes place at a non-end atom, we can no longer treat the isotope effect on the bond length like that in a diatomic molecule, because of the complex character of molecular vibrations. For non-end substitutions all contributions to $\Delta\langle\Delta r\rangle$ coming from bending vibrations, for example, are no longer negligible. The change of the mass of one non-end atom has an influence on all bonds connected to this atom, and we find the effect on $\langle\Delta r\rangle$ of an individual bond is always smaller than predicted by equation (51).[102] Nevertheless, for halogen-substituted methanes we can reproduce the effect of $^{13/12}C$ substitution on all bonds by a simple formula, modifying equation (51) only by an additional factor $m/(m+\frac{1}{2}m_A)$.

Equation (76) has another consequence: it allows us to correlate the dynamic factor $[\langle\Delta r\rangle-\langle\Delta r\rangle^*]$ with mean bond displacement in polyatomic molecules. By applying equation (74) or by doing the dynamical calculations for the same bond type, e.g. C–F,[94] we find that $\langle\Delta r\rangle$ increases with increasing bond length. Thus, the dynamic factor alone would lead to an opposite correlation between isotope shifts and bond length from that which is observed (e.g. see Fig. 2). The observations can only be expected if the magnitude of the electronic factor increases with decreasing bond length.

D. The additivity of NMR isotope shifts

One of the theoretically interesting and practically useful aspects of the isotope effect on NMR chemical shifts is the proportionality of the shift to the number of substituted atoms in equivalent positions. The practical

consequence of this is a spectrum with equally spaced peaks, the intensities giving an indication of the relative amounts of each isotopomer in the sample (Fig. 1). For example, the one-bond $^{2/1}H$-induced isotope shift in the ^{13}C spectrum of CH_nD_{4-n} isotopomers results in incremental isotope shifts as n goes from 0 to 4.[105] There are similar observations in other systems such as in PO_4^{3-},[106] $NH_{4-n}D_n^+$,[107] $BH_{4-n}D_n^-$,[108] $NH_{3-n}D_n$,[109] $PH_{3-n}D_n$.[110] Nor is this observation limited to one-bond isotope shifts. For example, the ^{59}Co spectrum of $Co(en)_3Cl_3$ in H_2O/D_2O solution shows 13 equally spaced peaks separated by 5.2 ppm, the peaks corresponding to all members of the isotopic homologous series in which the 12 exchangeable hydrogen atoms per molecule of the cobalt complex are replaced by deuterium atoms.[111] This additivity of the isotope effect on the chemical shift upon substitution in equivalent locations appears to be without exception, and the deviations from additivity usually appear to be small and have been noticed outside of experimental error only in isolated cases. There are some indications of additivity of mass effects in other forms of molecular spectroscopy. The sum of the squares of the vibrational frequencies of members of an isotopic homologous series is linearly related to the number of isotopes substituted, and this relation is valid for symmetry types which are common to all members of the series.[112] The sum of vibrational frequencies in $CH_{4-n}D_n$ is found empirically to depend on the number (n) of the substitutions by the heavy isotope, i.e. the zero-point energies of these molecules are linearly related to n.[113]

In Section IV.B.1 we have shown the mass effects on average nuclear positions in linear triatomic molecules. In the following we examine the origin of the observed additivity of the NMR isotope shift, determine if any systematic deviations from additivity can be expected, and how large they may be. An interesting molecule from the point of view of discussing the additivity of NMR isotope shifts is the methane molecule. The anharmonic force field of methane has recently been refined[114] to fit spectroscopic data from the isotopic species $^{12}CH_4$, $^{13}CH_4$, $^{12}CD_4$, $^{12}CH_3D$, $^{12}CHD_3$, and $^{12}CH_2D_2$. Six of the 13 cubic force constants are determined experimentally and the remaining cubic force constants are fixed at values derived from *ab initio* calculations.[115] We have calculated the mean bond displacements in the methane family $CX_{4-n}Y_n$ (X, Y = H, D, T), with the method described in detail elsewhere,[35] and find that the substitution effects on the vibrational contribution to mean bond displacements are strictly additive. Each substitution of a hydrogen by a deuterium shortens the appropriate bond by nearly the same amount Δ. The mean bond displacements in $^{12}CH_{4-n}T_n$ and $^{12}CD_{4-n}T_n$ exhibit the same strictly linear dependence on n.[35,90] We can express $\langle\Delta r_{CH}\rangle$ and $\langle\Delta r_{CD}\rangle$ in $^{12}CH_{4-n}D_n$ as follows. Let

$$d = \langle\Delta r_{CH}\rangle \text{ in } CH_4 \text{ at } 300\text{ K}$$

$$d-\Delta = \langle\Delta r_{CD}\rangle \text{ in } CD_4 \text{ at } 300\text{ K}$$

where $d = 2.0881 \times 10^{-2}$ Å and $\Delta = 5.5345 \times 10^{-3}$ Å. We find

$$\langle \Delta r_{CD} \rangle = d - \Delta + \delta_D(n) \tag{81a}$$

$$\langle \Delta r_{CH} \rangle = d + \delta_H(n) \tag{81b}$$

Similar relations can be found for the other series of isotopomers.[90] That is, for a given bond, substitution of an isotope involved in this bond had an effect Δ on its own mean bond length (a primary effect on the mean bond displacement); each substitution of an isotope at some other bonds has a much smaller effect δ (a secondary effect).

The rotational contribution (centrifugal stretching) to the mean bond displacement was calculated and is illustrated in Fig. 15 where the sum of all four $\langle \Delta r_i \rangle_{rot}$ is shown to be invariant to n:[90]

$$(4-n)\langle \Delta r_{CH} \rangle_{rot} + n\langle \Delta r_{CD} \rangle_{rot} = 4d_{rot} \tag{82}$$

where $d_{rot} = 5.2 \times 10^{-4}$ Å. The invariance of the centrifugal distortion to isotopic substitution which preserves T_d symmetry is pointed out in Section II.B.2. Here we find that, although there is a rotational effect on each bond,

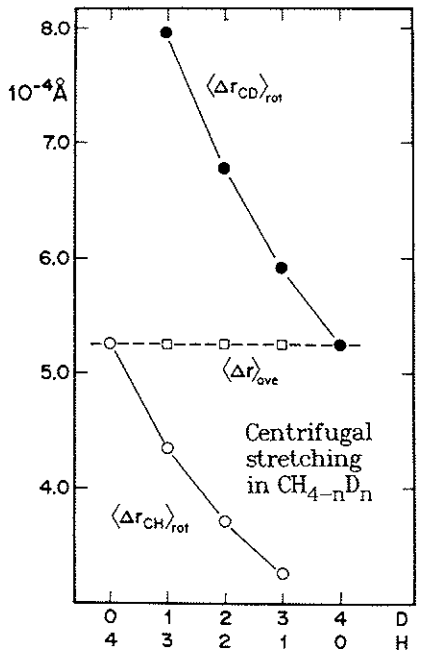

FIG. 15. The rotational contribution to mean bond displacement in the methanes. From reference 90, with permission.

the sum is also invariant, so the centrifugal distortion does not contribute to the isotope shift of the central nucleus.

The vibrational contribution to the isotope shift depends on

$$\sum_i \langle \Delta r_i \rangle_{vib} = (4-n)\langle \Delta r_{CH} \rangle_{vib} + n\langle \Delta r_{CD} \rangle_{vib}$$

$$= 4d - n\Delta + \delta(n) \tag{83}$$

which is nearly linear with n, since $\delta(n) \ll \Delta$. The $^{2/1}$H-induced ^{13}C NMR isotope shift between any two isotopomers of $CH_{4-n}D_n$ can then be expressed, following equation (73), as

$$\sigma^C(CH_{4-n}D_n) - \sigma^C(CH_{4-n'}D_{n'}) = (\partial\sigma^C/\partial\Delta r)_e[(n'-n)\Delta + \delta(n) - \delta(n')]$$

$$\approx (\partial\sigma^C/\partial\Delta r)_e(n'-n)\Delta \tag{84}$$

Equation (84) is the basis for the near additivity of isotope shifts due to substitution at equivalent sites. If we leave out the term $[\delta(n') - \delta(n)]$ which is two orders of magnitude smaller than Δ, we have strict additivity: the magnitude of the shift is proportional to the number $(n'-n)$ of atoms which have been substituted by isotopes.

To test the general validity of the findings in the methanes we briefly return to the linear triatomic molecules. Figure 10 shows the results for single substitution in different isotopomers of CO_2 and OCS,[34] but the conclusions which follow are based on calculations for all possible isotopomers using $^{18/17/16}$O, $^{13/12}$C and $^{34/33/32}$S. As shown in Fig. 10 we find that substitution of a heavier isotope provides a drastic shortening of the average length of the bond directly attached to this isotope by a constant Δ, and as a secondary effect it shortens the other bond by a constant δ, where $\Delta \gg \delta$. We also find an empirical general additivity rule which is valid for all triatomics:

$$\langle \Delta r(^{m'}\mathrm{Y\,A}\,^{n'}\mathrm{X}) \rangle_{av} - \langle \Delta r(^{m}\mathrm{Y\,A}\,^{n}\mathrm{X}) \rangle_{av}$$

$$= [\langle \Delta r(^{m'}\mathrm{Y\,A}\,^{n}\mathrm{X}) \rangle_{av} - \langle \Delta r(^{m}\mathrm{Y\,A}\,^{n}\mathrm{X}) \rangle_{av}]$$

$$+ [\langle \Delta r(^{m}\mathrm{Y\,A}\,^{n'}\mathrm{X}) \rangle_{av} - \langle \Delta r(^{m}\mathrm{Y\,A}\,^{n}\mathrm{X}) \rangle_{av}] \tag{85}$$

where

$$\langle \Delta r \rangle_{av} \equiv \tfrac{1}{2}[\langle \Delta r_{AY} \rangle + \langle \Delta r_{AX} \rangle]$$

Thus, if we include only linear terms, for the shielding of the central atom in the linear triatomics,

$$\langle \sigma \rangle \approx \sigma_e + \left(\frac{\partial\sigma}{\partial\Delta r}\right)_e 2\langle \Delta r \rangle_{av} \tag{86}$$

The additivity of the isotope shift for the central atom which follows from

equations (85) and (86) may be written in the usual notation, for ^{13}C in OCS, for example:

$$^1\Delta^{13}C(^{18/16}O, ^{34/32}S) = {}^1\Delta^{13}C(^{18/16}O) + {}^1\Delta^{13}C(^{34/32}S) \quad (87)$$

Once again, additivity of isotope shifts is predicted on the basis of additivity of mass effects on $\langle \Delta r \rangle$.

Although the secondary isotope effects on the mean bond displacements are small, the term $[\delta(n') - \delta(n)]$ in equation (84) provides a theoretical basis for deviations from strict additivity of isotope shifts. If we include these small terms in calculating the isotope shifts for the methane family we find a deviation from additivity in the ratio 0:3:4:3:0 for $n = 0$ to 4.[90] The isotope effects on the ^{13}C shifts in $CH_{4-n}D_n$ have been measured,[105] but the associated errors are not small enough to enable one to see these systematic deviations from additivity. On the other hand, excellent measurements have been carried out[107] for the ^{14}N shifts in the ammonium ion, $^{14}NH_{4-n}D_n^+$, with a precision of ±0.001 ppm.[107] Deviations are found from the strict additivity of −0.014 ppm, −0.020 ppm, −0.014 ppm respectively for $n = 1$, 2, 3 which are in a ratio of 0:2.8:4:2.8:0. Another example is the isotope shift of the ^{119}Sn nucleus in the $Sn(CH_3)_{4-n}(CD_3)_n$ system.[116] This system shows deviations from additivity in the same direction as those found for $NH_{4-n}D_n^+$, although the ratios are not 0:3:4:3:0 exactly. Only if we can consider the CD_3 and CH_3 groups as point masses can the centrifugal stretching contribution be neglected, as in $CH_{4-n}D_n$. It should be noted that the ratio 0:3:4:3:0 is strictly parallel to the results obtained[117] for deviations from additivity in zero-point energies in methanes using a model which treats the four bonds in $CH_{4-n}D_n$ as four coupled oscillators. The deviation from linear behaviour of the zero-point energy *vs.* n plot comes from the term in the energy which corresponds to the mutual motion of two atoms in different oscillators from their equilibrium position. In our case the deviations from additivity come from the small secondary effects δ on the mean bond displacements, which are again a result of the coupled atomic motions in molecular vibrations.

E. Contributions from bond angle changes and higher order derivatives of the shielding surface

So far we have truncated equation (5) after the linear term in order to calculate or estimate isotope effects on nuclear shielding in polyatomic molecules. It is shown in Table 6 that this assumption is not unreasonable for many diatomics. The terms connected with higher order derivatives of the shielding surface contribute significantly less to the isotope shift than the linear ones. In some cases, however, the neglect of the second derivative term leads to significant error.

TABLE 14

Individual contributions to the isotope shift in the water molecule, in ppm.[38]

Term in equation (5)	$^1\Delta^{17}O(^{2/1}H, ^{2/1}H)$	$^1\Delta^1H(^{18/16}O)$
$(\partial\sigma/\partial\Delta r)_e$	−2.57	−0.0021, −0.0003[b]
$(\partial\sigma/\partial\Delta\alpha)_e$	−0.01	+0.0003
$(\partial^2\sigma/\partial\Delta r^2)_e$	−1.31	+0.0010, −0.0002[b]
$(\partial^2\sigma/\partial\Delta\alpha^2)_e$	+0.45	−0.0001
Total[a]	−3.68	−0.00017

[a] Including also third and fourth derivatives of shielding.
[b] The same bond and other bond contributions, respectively.

In Table 14 we show Fowler's[38] results for the H_2O molecule, indicating the relative contributions of terms involving the first and second derivatives of nuclear shielding. Although the observed ^{17}O isotope shift is only −3.08 ppm, the relative values of the calculated contributions to the total *ab initio* value of −3.68 ppm should indicate the relative importance of the various terms. We see that the largest contribution does indeed come from the term $(\partial\sigma/\partial\Delta r)_e\Delta\langle\Delta r\rangle$. There is, however, an important quadratic contribution $(\partial^2\sigma/\partial\Delta r^2)_e\Delta\langle(\Delta r)^2\rangle$. There is a smaller but non-negligible term in $(\partial^2\sigma/\partial\Delta\alpha^2)_e\Delta\langle(\Delta\alpha)^2\rangle$ and the remainder is due to 3rd and 4th derivatives of ^{17}O shielding.

For ^1H isotope shifts, the terms involving the bond angle are even less important. For ^1H isotope shifts, the term involving the primary derivative $(\partial\sigma^{H_a}/\partial\Delta r_{OH_a})_e$ gives the largest contribution, as might be expected.

There are several important conclusions from these results. (a) Neglecting the higher order contribution leads to an underestimation of the total isotope effect. (b) On the other hand, it becomes more clear from these findings that the isotope effects involving the bond angles are extremely small. They do not contribute significantly to the isotope shift (less than 1% for H_2O). This justifies using the same definition of a reduced isotope shift even for molecules with non-vanishing $\langle\Delta\alpha\rangle$. (c) Notice also that the contribution due to the harmonic bond angle changes which are associated with the derivative $(\partial^2\sigma/\partial\Delta\alpha^2)_e$ can have an opposite sign to the term in $\langle\Delta r\rangle$ and in $\langle\Delta r^2\rangle$.

If a change in the bond angle away from the equilibrium configuration weakens the bond (as in a linear triatomic molecule like OCO or a bent triatomic molecule like HOH) then a trace on the shielding surface along the $\Delta\alpha$ coordinate, such as that shown in Fig. 8(a), will have a minimum close to the equilibrium bond angle. This trace will be a function which is concave upward, i.e. increased shielding of the nucleus at the vertex of the

angle accompanies the opening of the bond angle as well as the closing of the bond angle. Such a shielding surface will therefore have $(\partial^2\sigma/\partial\Delta\alpha^2)_e > 0$, giving a positive contribution to the isotope shift since $\langle\Delta\alpha^2\rangle$, like $\langle\Delta r\rangle$ or $\langle(\Delta r)^2\rangle$, is greater for the isotopomer with lighter end atoms. The term $(\partial^2\sigma/\partial\Delta\alpha^2)_e\Delta\langle\Delta\alpha^2\rangle$ is especially important in linear molecules with low frequency bending vibrational modes. For acetylene, for example, a $^{2/1}$H-induced effect on the ^{13}C shift over one bond is -0.223 ppm whereas the effect over two bonds is larger (-0.438 ppm).[118] The observed small $^1\Delta^{13}C(^{2/1}H)$ is probably due to the partial cancellation of the negative linear and quadratic terms in Δr by the positive $(\partial^2\sigma/\partial\Delta\alpha^2)_e\Delta\langle\Delta\alpha^2\rangle$ term. Of course we cannot rule out a π contribution to the secondary derivative $(\partial\sigma^{C_1}/\partial\Delta r_{C_2H})_e$.

There is very little else known about $(\partial\sigma/\partial\Delta\alpha)_e$ or $(\partial^2\sigma/\partial\Delta\alpha^2)_e$. The observed negative sign, additivity, and dependence on $(m'-m)/m'$, even for isotope shifts in apex nuclei in bent systems, support the assumption of neglect of bond angle deformation contribution to the isotope shifts. The same assumption cannot always be made in the interpretation of the temperature dependence in the zero-pressure limit. It has been suggested that the unusual temperature dependence of ^{15}N in NH_3 and ^{31}P in PH_3 is due to contributions of bond angle deformations to the temperature dependence of nuclear shielding.[14] Unfortunately it has not been possible to obtain a quantitative simultaneous fit to the isotope shift and the temperature dependent chemical shift in the case of PH_3.

In Fig. 16 we compare several calculated $^{13/12}$C-induced isotope shifts on ^{19}F shielding with experimental values for a series of halomethanes.[11] The isotope effects are calculated only from the linear term in equation (5), but this time the derivatives $(\partial\sigma/\partial\Delta r_{CF})_e$ are obtained from fitting the experimentally measured temperature dependence of the nuclear shielding at the zero-pressure limit to a function[13,11,94]

$$\sigma_0(T) - \sigma_0(300\text{ K}) \approx (\partial\sigma^F/\partial\Delta r_{CF})_{e,emp}[\langle\Delta r\rangle^T - \langle\Delta r\rangle^{300}]. \tag{88}$$

We can see that there is a systematic trend in the deviation of the calculated values from the experimental isotope shifts. When one or two heavier nuclei like Cl are attached to the carbon the calculated isotope shifts are in good agreement with experiment whereas hydrogens lead to underestimation (as expected). The higher the percentage of rotational contributions to the temperature dependence of $\langle\Delta r\rangle$, the more accurate the empirical $(\partial\sigma/\partial\Delta r)_e$ which results from fitting $\sigma_0(T) - \sigma_0(300\text{ K})$ data since the rotational term linearly dependent on temperature dominates the observed $\sigma_0(T)$. For CH_3F 65% of the temperature dependence of $\langle\Delta r\rangle$ is due to rotation,[11] so we expect to get a reasonably good empirical estimate of $(\partial\sigma/\partial\Delta r)_e$. For the others the rotational contribution to the temperature coefficient of $\langle\Delta r\rangle$

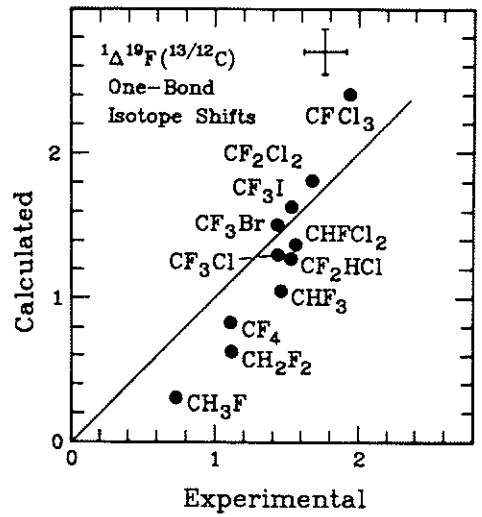

FIG. 16. Comparison of calculated (using equation (73)) and experimental ^{13}C-induced ^{19}F isotope shifts. From reference 11, with permission.

decreases with increasing masses of the other atoms attached to the carbon, down to only 10% rotation for $CFCl_3$.

Including the quadratic term in equation (88), we have

$$\sigma_0(T) - \sigma_0(300) \approx (\partial\sigma/\partial\Delta r)_e[\langle\Delta r\rangle^T - \langle\Delta r\rangle^{300}] + \tfrac{1}{2}(\partial^2\sigma/\partial\Delta r^2)_e[\langle(\Delta r)^2\rangle^T - \langle(\Delta r)^2\rangle^{300}] \tag{89}$$

In polyatomic molecules there are of course many more quadratic terms than this. For the purpose of estimating the discrepancies between experimental and calculated isotope shifts in Fig. 16 let us consider only the term in $\langle(\Delta r)^2\rangle$. Furthermore, we will use the diatomic molecule approximation for the relationship between $\langle\Delta r\rangle$ and $\langle(\Delta r)^2\rangle$ (equation (47)). Then

$$\sigma_0(T) - \sigma_0(300) = \{(\partial\sigma/\partial\Delta r)_e + (1/3a)(1-f_T)(\partial^2\sigma/\partial\Delta r^2)_e\} \times \{\langle\Delta r\rangle^T - \langle\Delta r\rangle^{300}\} \tag{90}$$

where f_T is that fraction of the total temperature dependence $[\langle\Delta r\rangle^T - \langle\Delta r\rangle^{300}]$ which is due to rotation. Thus the empirical derivatives $(\partial\sigma/\partial\Delta r)_{e,emp}$ obtained from fitting $[\sigma_0(T) - \sigma_0(300)]$ will be

$$(\partial\sigma/\partial\Delta r)_{e,emp} = \{(\partial\sigma/\partial\Delta r)_e + (1/3a)(1-f_T)(\partial^2\sigma/\partial\Delta r^2)_e\} \tag{91}$$

When the rotational contribution to $[\langle\Delta r\rangle^T - \langle\Delta r\rangle^{300}]$ is sizeable (i.e. $f_T \geq 0.3$), then $(\partial\sigma/\partial\Delta r)_{e,emp}$ should be very close to $(\partial\sigma/\partial\Delta r)_e$, because a is typically

around 2 $Å^{-1}$ and the second derivative is of the same order of magnitude as the first derivative, so the neglected terms are about a factor of $(1-f_T)/6$ smaller than $(\partial\sigma/\partial\Delta r)_e$. For much smaller rotational contributions the magnitude of the empirical first derivative is overestimated. In accounting for the ^{13}C-induced ^{19}F isotope shift using only the linear term in equation (5), we should expect to get values that are too small, since the $(\partial^2\sigma/\partial\Delta r^2)[\langle(\Delta r)^2\rangle-\langle(\Delta r)^2\rangle^*]$ terms have not been included. When using the empirical derivatives from the temperature-dependent shielding to calculate the isotope shift, we underestimate the magnitude of the isotope shift by an amount

$$(f_T-f_{iso})(1/3a)(\partial^2\sigma/\partial\Delta r^2)_e[\langle\Delta r\rangle-\langle\Delta r\rangle^*] \qquad (92)$$

where f_{iso} is the fraction of $[\langle\Delta r\rangle-\langle\Delta r\rangle^*]$ that is due to rotation. In diatomic molecules f_{iso} is identically zero, and in polyatomic molecules it is typically less than 0.01. The different magnitudes of f_T lead to the systematic deviations observed in Fig. 16. For the CH_nF_{4-n} series the discrepancies between the calculated and experimental isotope shifts correlate with f_T values 0.31 to 0.65,[11] indicating a more or less constant value for $(\partial^2\sigma/\partial\Delta r^2)_e$. On the other hand, in the $CF_{4-n}Cl_n$ series, in which f_T ranges from 0.10 to 0.18,[94] the agreements between calculated and observed values are within experimental errors. This indicates that, for molecules with smaller rotational contribution to the temperature dependence ($f_T \ll 0.2$), the overestimation of $(\partial\sigma/\partial\Delta r)_{e,emp}$ partially compensates the error associated with the neglect of quadratic and higher order derivatives in the shielding expansion. Where the empirical first derivatives are closest to the true values the calculated isotope shifts are underestimated.

F. Estimation of one-bond isotope shifts for end atom substitution

In this section we discuss the general magnitudes of observed one-bond isotope shifts and provide estimates of others. We have shown that it is possible to estimate the isotope effect on the mean bond displacement in the case of end atom substitution so that we can obtain a value within 10% of the value one would obtain from a full dynamical calculation using an anharmonic force field. We have also shown that, except for ^1H or ^7Li, the term $(\partial\sigma/\partial\Delta r)_e\Delta\langle\Delta r\rangle$ gives 70–88% of the total calculated isotope shift in diatomic molecules and 70% of the calculated ^{17}O isotope shift in H_2O. With empirical shielding derivatives we can obtain around 75% of the observed ^{13}C-induced ^{19}F isotope shift in fluoromethanes with this term only.[11,94] Therefore it should be possible to estimate a one-bond isotope shift not previously measured, by using only the $(\partial\sigma/\partial\Delta r)_e\Delta\langle\Delta r\rangle$ term in the shielding. When isotope shifts are used in applications where a special synthesis is necessary in order to "tag" the molecule of interest, it would

be very useful to know *a priori* if the expected isotope shift is observable under experimental conditions. An order of magnitude estimate is easily within reach when the particular observed nucleus-substituted atom pair has previously been observed in any compound. In such a case the correlations which are shown in Fig. 2, and further discussed below, can narrow down the estimate easily to within 20% uncertainty. When the isotope shift for a particular observed nucleus-substituted atom pair has not been previously observed, it would be very useful to have an order of magnitude estimate in order to know whether the observation of the isotope shift is feasible, given that an NMR spectroscopist can generally predict linewidths to be expected under experimental conditions. Therefore we show here a method of estimation for one-bond isotope shifts proposed earlier.[119] Let us do this in parts. We wish to show how to estimate a one-bond isotope shift in the following situations:

(A) If an isotope shift has been previously observed for the same nucleus in an analogous compound, e.g. $^1\Delta^{31}P(^{34/32}S)$ from $^1\Delta^{31}P(^{18/16}O)$.

(B) If an isotope shift has been observed in an analogous compound for a different nucleus belonging in the same column of the periodic table as the desired one, e.g. $^1\Delta^{31}P(^{m'/m}X)$ from $^1\Delta^{15}N(^{m'/m}X)$.

(C) If no previously measured isotope shifts in analogues are known, and in the most general sense for an arbitrary previously unobserved nucleus-substituted atom pair.

We have shown that to a first approximation the one-bond isotope shift can be expressed by equation (77). In this expression the experimentally observed isotope shift consists of the product of two factors. The electronic factor reflects the sensitivity of nuclear shielding to bond extension and the dynamic factor reflects the average change in the molecular geometry on isotopic substitution. Let us first consider the dynamic factor. There are practical implications of equation (77) for measurements of isotope shifts. Quite apart from the advantage of a large chemical shift range for heavier nuclei, the mass dependence alone favours the observation of the chemical shift of a heavy nucleus upon substitution of a light neighbouring atom with an isotope. The most favourable case is the $^{3/1}H$-induced shift of a heavy nucleus. The largest experimentally observed one-bond isotope effect so far is the $^{2/1}H$-induced effect on the ^{77}Se shielding, −7.02 ppm per D in H_2Se.[4] In addition to the favourable fractional mass changes in the factor $(m'-m)/m'$, the factor $m_A(m_A+m)$ is close to 1.0. It would be wise to calculate the mass factors prior to attempting an isotope shift measurement. For example, in the Se–C bond the $^{13/12}C$-induced ^{77}Se shift is easily observable, whereas the $^{80/77}Se$-induced ^{13}C shift is not. A shift of $^1\Delta^{77}Se(^{13/12}C) = -0.683$ ppm is observed in $NCSe^-$, whereas no shift due to the Se isotopes in the ^{13}C spectrum has been found.[58] The mass factor $\frac{1}{2}\cdot(m'-m)/m'\cdot m_A/(m_A+m)$ is equal to 0.033 in the first case and 0.003

in the second. For a mass factor greater than 0.01 it should be feasible to observe any one-bond isotope effect on nuclear shielding with a medium-field high resolution spectrometer when linewidths are favourable. We also introduce the reduced one-bond shift equation (54)[58,119] as a means of removing most of the dependence of the measured isotope shifts on the masses. Thus $^1\Delta^R$ for ^{31}P in PH_3 can be directly compared to ^{31}P in PO_4^{3-} or to ^{15}N in NH_4^+. The range of values of $^1\Delta^R$ for a given observed nucleus therefore reflects the variation of $(\partial\sigma/\partial\Delta r)_e\langle\Delta r\rangle$ with nuclear environment. We have already shown that $\langle\Delta r\rangle$ is $15\text{–}20\times10^{-3}$ Å for hydrides and $4\text{–}7\times10^{-3}$ Å for most other bonds, and that it is possible to estimate $\langle\Delta r\rangle$ involving an end atom by knowing only the bond length, the masses and the rows of the periodic table of the pair of atoms.

Case (A) is therefore easily handled with the appropriate mass factors. The one-bond isotope shift $^1\Delta^{31}P(^{81/79}Br)$ in PBr_3 can be estimated as follows. From $^1\Delta^{31}P(^{37/35}Cl)$ in PCl_3, which is −0.019 ppm,[120] we calculate the reduced isotope shift (equation (54)) which is −1.50 ppm, approximately identified with $(\partial\sigma/\partial\Delta r_{PCl})_e\langle\Delta r_{PCl}\rangle$. At this point we can make a rough estimate and simply assume that

$$\langle\Delta r_{PCl}\rangle \approx \langle\Delta r_{PBr}\rangle \text{ and } (\partial\sigma/\partial\Delta r_{PCl})_e \approx (\partial\sigma/\partial\Delta r_{PBr})_e$$

In other words, we are estimating $^1\Delta^R(P, Br) \approx {}^1\Delta^R(P, Cl)$ from which we then calculate the desired isotope shift as −0.005 ppm. This shift has been reported as −0.006 ppm.[120] Another application would be the estimation of $^1\Delta^{31}P(^{34/32}S)$ in P(v) compounds with a P=S bond. The one-bond $^{18/16}O$-induced shift has been measured (−0.0354 ppm).[121] From this, following the same procedure as for the PX_3 example, we would obtain a reduced isotope shift of −0.96 ppm from which $^1\Delta^{31}P(^{34/32}S) = -0.0140$ ppm. A slightly better estimate can be obtained if we know the P=O and P=S bond lengths. Then we can find the ratio $\langle\Delta r_{PS}\rangle/\langle\Delta r_{PO}\rangle$:

$$\frac{\langle\Delta r_{PS}\rangle}{\langle\Delta r_{PO}\rangle} = \left(\frac{\mu_{PO}}{\mu_{PS}}\right)^{1/2}\frac{(10^{-D})_{PS}}{(10^{-D})_{PO}} = 0.95$$

using $r_e = 1.86$ and 1.52 Å respectively for P=S and P=O and the values of the parameters in Table 7. Thus we only need to assume that $(\partial\sigma^P/\partial\Delta r_{PS})_e \approx (\partial\sigma^P/\partial\Delta r_{PO})_e$.

$$^1\Delta^R(P, S) \approx {}^1\Delta^R(P, O)\langle\Delta r_{PS}\rangle/\langle\Delta r_{PO}\rangle = -0.91 \text{ ppm}$$

Then, as previously, we get an estimate for $^1\Delta^{31}P(^{34/32}S) = -0.0132$ ppm. We can also estimate $^1\Delta^{31}P(^{36/32}S)$ to be approximately twice as large because of the factor $(36-32)/36$ instead of $(34-32)/34$. These isotope shifts have recently been measured and reported as −0.0097 ppm and −0.0184 ppm.[122]

Also, the $^{34/32}S$-induced ^{95}Mo isotope shift in MoS_4^{2-}, which should have roughly the same value of $^1\Delta^R$ as MoO_4^{2-} (−5.26 ppm), can be predicted

to be

$$-5.26 \text{ ppm} \times (34-32)/34 \times 1/2 \times 95/(95+32) = -0.11 \text{ ppm}$$

if electronic factors are about the same and $\langle\Delta r_{MoO}\rangle$ is comparable to $\langle\Delta r_{MoS}\rangle$. The measured value is −0.090 ppm.[123]

Let us now consider the electronic factor in more detail. The value of $(\partial\sigma/\partial\Delta r)_e$ for a given nucleus reflects the range of chemical shifts for that nucleus, since both are measures of the nuclear shielding sensitivity, the former to bond extension and the latter to changes in electronic structure. For example, the ratio of the *ab initio* theoretical ^{19}F shielding derivative $(\partial\sigma^F/\partial\Delta r_{HF})_e$ in HF to the empirical ^1H shielding derivative $(\partial\sigma^H/\partial\Delta r_{HH})_e$ in H_2 (−442 ppm Å^{-1}/−12.1 ppm Å^{-1})[43,70] is approximately the same as the ratio of the chemical shift ranges of ^{19}F and ^1H, about 800 ppm/20 ppm. Since the periodicity of the $\langle a_0^3/r^3\rangle$ of the valence p or d orbitals of the observed nucleus has been found to be generally reflected in the ranges of chemical shifts,[124] it is possible to use $\langle a_0^3/r^3\rangle$ in the same fashion (where $a_0 = 0.529$ Å). For example, the derivatives $(\partial\sigma^X/\partial\Delta r_{XH})_e$ for ^{11}B, ^{13}C and ^{15}N in BH_4^-, CH_4 and NH_4^+ have been estimated from observed $^{2/1}H$-induced isotope shifts; these are −27, −35 and −65 ppm Å^{-1} respectively,[58] or 0.76:1:1.85. These may be comapred with the values of $\langle a_0^3/r^3\rangle$ for free atoms which are in the ratio 0.5:1:2.0,[125,126] roughly the same ratio as the observed ranges of chemical shifts for these nuclei. In CN^- the ratio $(\partial\sigma^N/\partial\Delta r)_e$ to $(\partial\sigma^C/\partial\Delta r)_e$ is −872 ppm Å^{-1} to −473 ppm Å^{-1},[127,69] the same ratio as for the derivatives in NH_4^+ and CH_4 (1.85:1). In CO the ratio of $(\partial\sigma^O/\partial\Delta r)_e$ to $(\partial\sigma^C/\partial\Delta r)_e$ is −1150 to −456 ppm Å^{-1},[50] which is 2.5; this may be compared with the ratio of $\langle a_0^3/r^3\rangle$ for the atoms, which is 3.5.

When the values of $\langle\Delta r\rangle$ are comparable, the reduced isotope shifts will appear to be related to one another in the same way as chemical shifts in general. In the above example, the $\langle\Delta r\rangle$ values for BH_4^-, CH_4 and NH_4^+ are similar $(2\text{–}2.2\times10^{-2}$ Å), so the reduced isotope shifts are related in very nearly the same way as the respective $(\partial\sigma/\partial\Delta r)_e$. Note, however, that $\langle\Delta r\rangle$ for bonds involving hydrogen are different from all others. Although the mean bond angle deformation $\langle\Delta\alpha\rangle$ is non-zero for NH_3 and PH_3,[14] it has been found that the $^{2/1}H$-induced isotope effect on X is dominated by the change in $\langle\Delta r\rangle$. It is found[109,110] that the ratio

$$\frac{^1\Delta^R(P, H) \text{ in } PH_3}{^1\Delta^R(N, H) \text{ in } NH_3} = 1.26$$

is comparable to the ratio of $\langle a_0^3/r^3\rangle$ for the P and N atoms which is 1.4. Thus the trends relating magnitudes of isotope shifts to shielding sensitivity and the similarities of $\langle\Delta r\rangle$ for the bonds being compared lead to relationships between reduced shifts based on chemical shift ranges (or $\langle a_0^3/r^3\rangle$) if the isotope shift of one chemical analogue is known. The method of

estimation for case (B) now becomes clear. Given that $^1\Delta^{95}Mo(^{18/16}O) = -0.25$ ppm,[128] by using the ratio of $\langle a_0^3/r^3\rangle$ for the $3d_{3/2}$ and $4d_{3/2}$ states of the atoms,[126] we can estimate $^1\Delta^{99}Tc(^{18/16}O)$ as follows. Take

$$(\partial\sigma^{Tc}/\partial\Delta r_{TcO}) \approx \frac{\langle a_0^3/r^3\rangle_{Tc}}{\langle a_0^3/r^3\rangle_{Mo}} (\partial\sigma^{Mo}/\partial\Delta r_{MoO})_e$$

and for a rough estimate let $\langle\Delta r_{TcO}\rangle \approx \langle\Delta r_{MoO}\rangle$. Then

$$^1\Delta^{99}Tc(^{18/16}O) \approx \frac{\langle a_0^3/r^3\rangle_{Tc}}{\langle a_0^3/r^3\rangle_{Mo}} {}^1\Delta^{95}Mo(^{18/16}O) \frac{99}{99+16} \frac{95+16}{95}$$

$$= -0.34 \text{ ppm.}$$

This compares well with the experimental value of -0.44 ± 0.06 ppm.[129]

There are fewer data on analogous compounds which involve replacement of non-end atoms. It is interesting, however, that the relationship holds even in the case of $^{13/12}$C-induced ^{199}Hg and ^{111}Cd shifts in Me_2Hg and Me_2Cd. Here the isotope shifts are of unusual sign, +0.4 ppm and +0.14 ppm respectively.[130,131] Nevertheless the reduced isotope shifts, 11.0 and 4.0 ppm, are in the same ratio as $\langle a_0^3/r^3\rangle$ of Hg and Cd.

TABLE 15

Observed and estimated (in parentheses) $^{2/1}$H-induced one-bond isotope shifts in hydrides, in ppm per D.[119]

H_2	BH_4^-	CH_4	NH_4^+	NH_3	H_2O	HF
−0.0402	−0.138	−0.192	−0.307	−0.65	−1.54	−2.5
		SiH_4		PH_3	H_2S	HCl
		(−0.4)		−0.843	(−2.2)	(−2.8)
		GeH_4		AsH_3	H_2Se	HBr
		(−1.1)		(−2.0)	−7.02	(−5.6)
		SnH_4		SbH_3	H_2Te	HI
		(−1.6)		(−3.0)	(−10.6)	(−7.9)
		PbH_4				
		(−2.9)				

The above examples indicate that predictions to within a factor of 2 are possible when chemically analogous compounds are compared. In Table 15 we show $^{2/1}$H-induced one-bond isotope shifts for various nuclei where they have been observed, and our predictions of the magnitudes of $^1\Delta$ for yet unknown shifts in parentheses. We present similar values and predictions for $^{18/16}$O-induced one-bond isotope shifts in Table 16. The predicted values

TABLE 16

Observed and estimated (in parentheses) $^{18/16}$O-induced one-bond isotope shifts, in ppm per ^{18}O.[119]

CO_2	NO_2^- /	NO_3^-		O_3	
−0.019	−0.138	−0.056		(−0.26)	
		PO_4^{3-}	SO_2 /	SO_4^{2-}	ClO_4^-
		−0.019	(−0.27)	(−0.026)	(−0.03)
		AsO_4^{3-}	SeO_2 /	SeO_4^{2-}	BrO_4^-
		(−0.06)	(−0.72)	(−0.06)	(−0.09)
			TeO_2 /	TeO_4^{2-}	IO_4^-
			(−1.6)	(−0.14)	(−0.16)

in Tables 15 and 16 are based on calculations of $\langle\Delta r\rangle$ using methods described in Section IV.B, and estimates of $(\partial\sigma/\partial\Delta r)_e$ based on correlations of the type described above.

Estimates can also be made by comparing non-analogous compounds for different nuclei in the same group of the periodic table. Here the estimate will not be as good as in the analogous compounds which we have used for case (A) and case (B). However, even if no other information regarding analogous compounds is available, this can lead to an estimate within a factor of 2-3. For example, to estimate $^1\Delta^{15}N(^{2/1}H)$ in NH_4^+ from $^1\Delta^{31P}(^{18/16}O)$ in PO_4^{3-} (-0.019 ± 0.002 ppm) we proceed as follows:

$$^1\Delta^{15}N(^{2/1}H) \approx {}^1\Delta^{31}P(^{18/16}O) \frac{\langle a_0^3/r^3\rangle_N}{\langle a_0^3/r^3\rangle_P} \frac{\langle\Delta r_{NH}\rangle}{\langle\Delta r_{PO}\rangle} \frac{\frac{2-1}{2}\frac{15}{15+1}}{\frac{18-16}{18}\frac{31}{31+16}}$$

Using equation (74) to estimate $\langle\Delta r\rangle$, this gives a value of −0.72 ppm, to be compared with the measured value, −0.307 ppm.[107]

Finally, it would be useful to have a way of making an order of magnitude estimate of the isotope shift that may be expected for a nucleus in any bond, at least a prediction of the feasibility of the observation. The derivatives $(\partial\sigma/\partial\Delta r)_e$ vary with structural factors by as much as 2-fold even for the same bond (^{19}F in C-F bonds in various halomethanes for example).[11,94] There are other variations in electronic factors for a given nucleus which imply that the derivatives $(\partial\sigma/\partial\Delta r)_e$ should have a spread of about a factor from 2 to 10. (These are discussed below.) In Table 17 we show the known ranges of $^1\Delta^R$ for various observed nuclei and in parentheses our predictions for other nuclei in any electronic environment. These predictions are based on two measured isotope shifts, $^1\Delta^{31}P(^{18/16}O)$ in PO_4^{3-} and $^1\Delta^{15}N(^{18/16}O)$ in NO_2^-, and the $\langle a_0^3/r^3\rangle$ for the observed nucleus. From this table an

TABLE 17

Magnitudes of reduced isotope shifts observed for various nuclei, in ppm. Predicted[a,b] values for other nuclei are shown in parentheses.[119]

								H 0.375–0.81
								Li (0.006–0.1)
								Na (0.036–0.5)
								K (0.065–0.91)
								Rb (0.13–1.75)
								Cs (0.2–2.7)
Sc (2.1–5.2)	Ti (2.8–7)	V 4.5 (3.6–9)	Cr 10.3 (4–9.9)	Mn 13.7 (5.5–13.7)	Fe (6.7–16.6)	Co 28.6 (8–19.8)	Ni (9.4–23.3)	Cu (0.2–2.5)	Zn (0.4–5)
Y (2.7–6.7)	Zr (3.8–9.3)	Nb (4.1–10.2)	Mo 4.1–5.3 (5.3–13.1)	Tc 9.2 (7.1–17.5)	Ru (7.5–18.7)	Rh (8.8–21.9)	Pd (9.7–23.9)	Ag (0.4–5.2)	Cd 4 (0.7–9.5)
La (3.9–9.6)	Hf (7.5–18.7)	Ta (9.3–23)	W (11.1–27.4)	Re (13.1–32.4)	Os (15.1–37.3)	Ir (17.4–43.1)	Pt 3.2–7.3 (18.6–46)	Au (0.9–12.4)	Hg 4–11 (1.5–20.7)

[a] The predictions are based on P in PO_4^{3-} for the upper limit and N in NO_2^- for the lower limit for the main groups.

[b] For the transition elements the predictions are based on MoO_4^{2-} and MnO_4^- respectively, i.e. for highly symmetric environments only. Furthermore, the factor ΔE^{-1} in the chemical shift depends on the ligands, so the given ranges should be multiplied by the factor by which ΔE^{-1} varies for a given transition element in its complexes compared to ions of the type MO_4^{m-}. For example, the observed values for Pt in $PtCl_6^{2-}$ and $PtBr_6^{2-}$ are smaller, whereas that for Co in $Co(CN)_6^{3-}$ is greater.

estimate of $^1\Delta$ can be made for nucleus A due to substitution of an end atom ^{m}X by $^{m'}$X by multiplying the number in Table 17 by $(m'-m)/m'X_{\frac{1}{2}}^{\frac{1}{2}}m_A/(m_A+m)$. Given no further information these estimates predict the feasibility of observation of any given one-bond isotope shift. This is based on the assumption that $\langle\Delta r\rangle$ is approximately the same for an arbitrary bond as for the P–O or N–O bond. Because of the fact that $\langle\Delta r\rangle$ is significantly different for X–H bonds in comparison to others, Table 17 is not suitable for predicting $^{2/1}$H-induced isotope shifts. For this the use of Table 15 and a case (B) approach would be more appropriate.

As an example we predict from Table 17 a $^{18/16}$O-induced shift on the ^{51}V shielding of VO_4^{3-} in the range of −0.15 to −0.38 ppm, whereas the experiment yields −0.19 ppm.[132] For $^1\Delta^{19}F(^{34/32}S)$ we would predict −0.007 to −0.115 ppm. This may be compared with the experimental values which range from −0.0091 ppm to −0.0755 ppm for a variety of S–F bonds.[133–134] Equation (77) indicates that the least feasible observations are those of the shift in light nuclei A upon isotopic substitution of a heavy ligand X. The mass factors are unfavourable and the shielding derivative is expected to be small for the smaller chemical shift ranges typical of light nuclei.

G. Factors affecting $(\partial\sigma/\partial\Delta r)_e$

We have already seen that the dynamical factors in one-bond isotope shifts are fairly predictable and can even be estimated without a good force field because the mass-independent part of the dynamic factor is largely determined by the bond length and the rows of the periodic table of the pair of bonded atoms. In order to explain the correlations (a)–(d) which were noted in Section I, we look to the electronic factors $(\partial\sigma/\partial\Delta r)_e$. There are several systems for which these derivatives have been estimated. The results of dynamical calculations on a variety of molecules and the accompanying measurements of the temperature dependence of nuclear shielding in the zero-pressure limit provide empirical estimates of $(\partial\sigma/\partial\Delta r)_e$ according to equation (88). We use these as illustrative examples. Although most of the estimates of $(\partial\sigma/\partial\Delta r)_e$ which are now available are for ^{19}F shielding, the systematic trends which we have found for these derivatives are probably typical. In Table 18 we summarize the derivatives estimated from temperature-dependent shielding studies in the zero-pressure limit, from theoretical (*ab initio*) calculations, and from the reduced isotope shifts.

Examination of the derivatives in Table 18 reveals the following trends:

(a) $(\partial\sigma/\partial\Delta r)_e$ seems to be always negative, with rare exceptions, i.e. deshielding accompanies bond extension.

(b) $|(\partial\sigma/\partial\Delta r)_e|$ is smaller for nuclei in symmetric environments such as the octahedral, tetrahedral or trigonal planar nuclear sites.

(c) $|(\partial\sigma/\partial\Delta r)_e|$ generally increases with the chemical shift range of the observed nucleus, as we have already noted in the previous section.

TABLE 18

Derivatives of nuclear shielding with respect to bond extension, $(\partial\sigma^A/\partial\Delta r_{AX})_e$, and the absolute shielding σ_0^A (300 K).

		$(\partial\sigma^A/\partial\Delta r_{AX})_e$					
Nucl.	Mol.	theory[a]	temp. depend.[b]	isot. shift	Ref.	σ_0^A (300 K)	Ref.
^{1}H	H_2	−20.7		−12.1	43, 70	26.363	70
				−11.5	58		
	LiH	−4.19			43	26.213	43
	CH_4	−25.6		−38	135, 35	30.611	72
	H_2O	−35.3			76	30.052	72
		−40.7			136		
	HF	−41.8, −42.6			43, 135	28.8	104
^{11}B	BH_4^-			−26.7	58		
^{13}C	CO	−413.7, −535			53, 137	3.2	138
		−640		−456	74, 50		
	CN^-			−473	69		
	CO_2		−221	−214	34, 50	60.9	139
	CH_4	−30, −40		−35	140, 35	197.35	72
	CH_3—CH_3	−31, −50(CH)			140	183.1	72
		−15(C—C), −6.3			140, 135		
	CH_2=CH_2	−26, −32(CH)			140	66.76	72
		−252, −188(C=C), −187.7			140, 135		
	CH≡CH	−4.5, −19(CH)			140	121.35	72
		−206, −110(C≡C), −103			140, 135		
^{15}N	CN^-			−873	69, 135		
	N_2		−774	−910	67, 141	−61.6	142
		−640, −1090			54, 74		
	NH_4^+			−65	58	223.8	142
	NO_3^-			−410	143	−131.8	142
	NO_2^-			−990	143	−365	5
^{17}O	CO	−479		−1150	53, 50	−42.3	73
		−1240			74		
		−1077, −1166			137, 135		
	H_2O	−270.9		−294	76, 14	344.0	73
		−285, −275			136, 135		
	CO_2			−1641	143	243.4	73
^{19}F	HF	−411, −444			52, 135	410.0	104
		−441.7			43		
	F_2		−4530		135, 57	−232.8	144
	ClF	−2782	−2070		57	637.1	144
	BF_3		−1115		103	327.2	144
	NF_3		−2500		143	50.3	144
	PF_3		−1200		143	228.3	144
	SiF_4		−1170		103	363.2	144
	SF_6		−2200		146	139.6	144
	COF_2		−1146		33	221.6	144
	CF_4		−1180		11	259.0	144
	CF_3Cl		−1630		94	224.4	144
	CF_2Cl_2		−2000		94	202.6	144
	$CFCl_3$		−2400		94	195.7	145
	CF_3Br		−1850		94	213.8	145
	CF_3I		−1950		94	199.6	145
	CH_3F	−131	−338		135, 11	471.0	144
	CH_2F_2		−725		11	339.1	145
	CHF_3		−1274		11	274.1	144
^{31}P	PO_4^{3-}			−120	58		
	PCl_3			−310	143		
	PBr_3			−370	143		

TABLE 18 (*cont.*)

		$(\partial\sigma^A/\partial\Delta r_{AX})_e$					
Nucl.	Mol.	theory[a]	temp. depend.[b]	isot. shift	Ref.	σ_0A (300 K)	Ref.
^{55}Mn	MnO_4^-			−2490	58		
^{77}Se	H_2Se			−1273	14		
^{95}Mo	MoO_4^{2-}			−1400	58		
^{99}Tc	TcO_4^-			−2030	58		
^{119}Sn	Bu_3SnH			−367	58		
^{195}Pt	$PtCl_6^{2-}$			−2530	58		
	$PtBr_6^{2-}$			−1470	58		

[a] Derivatives of the shielding of various nuclei (B, C, N, F, Si, P) have also been calculated at the CNDO/S level using a sum over states method.[147] The results agree qualitatively with those shown in this table (all $(\partial\sigma/\partial\Delta r)_e < 0$) although, as might be expected at this level of approximation, the magnitudes are considerably smaller in some cases and larger in others. As we have seen in Section III.C, the paramagnetic term, which is most difficult to calculate accurately, dominates the change in shielding with molecular geometry.

[b] The derivatives obtained from the temperature dependence in the zero-pressure limit are overestimated in those cases where the rotational contributions are small; see text Section IV.E for discussion of this.

FIG. 17. Correlation of ^{19}F shielding derivatives with ^{13}C–F spin-spin couplings and the ^{19}F absolute shielding. From reference 11, with permission.

(d) $(\partial\sigma/\partial\Delta r)_e$ correlates with the absolute shielding σ_0. An example of this correlation is shown in Fig. 17 for ^{19}F in the C–F bond in fluoromethanes.[11] We have already seen in Section III that the theoretically calculated derivative of the paramagnetic term in the shielding has a larger magnitude than the derivative of the diamagnetic term. The more shielded nucleus has a smaller paramagnetic term. Thus the magnitude of $(\partial\sigma/\partial\Delta r)_e$ will be generally smaller for the more shielded nucleus. Another example is the ^{13}C shielding in CO, CN^-, CO_2, CH_4 in which the derivative is also smaller for the more shielded nucleus. The comparison is not as valid in this series because the bonds being extended do not involve the same atom. Nevertheless there is a clear trend. The consistently larger ^{13}C isotope shift upon D substitution in CH_2 groups compared to CH_3 groups is probably another example of the correlation of $(\partial\sigma/\partial\Delta r)_e$ with the absolute shielding; ^{13}C in CH_2 groups are generally less shielded than in CH_3 groups.

(e) $|(\partial\sigma/\partial\Delta r_{C\equiv O})_e|$ in CO (bond order ~3) is greater than $|(\partial\sigma/\partial\Delta r_{C=O})_e|$ in CO_2 (bond order ~2) for both O and C. Although there are not any other examples of $(\partial\sigma/\partial\Delta r)_e$ as a function of bond order, this particular example is illustrative. This also shows that $|(\partial\sigma/\partial\Delta r)_e|$ is greater for the shorter C≡O bond (1.128 Å) than the longer C=O bond (1.160 Å). Similarly, the magnitudes of $(\partial\sigma^F/\partial\Delta r_{CF})_e$ in CFH_3 and CF_4 correlate with bond lengths of 1.382 and 1.317 Å respectively. The shorter bond is associated with the larger derivative. We have already seen that the magnitude of the dynamic factor for a given bond type decreases with decreasing bond

length; therefore the electronic factor is responsible for the experimentally observed dependence of the isotope shift on bond/bond order.[3,134]

(f) $|(\partial\sigma^A/\partial\Delta r_{AX})_e|$ increases with increasing electronegativity of X, as for ^1H in the series HLi, H_2, H_4C, H_2O, HF, or ^{19}F in the series FH, F_4C, F_3N, FCl, F_2.

(g) $|(\partial\sigma/\partial\Delta r)_e|$ appears to be greater for nuclei with σ lone pairs, e.g. −990 for NO_2^- compared to −410 for NO_3^-, −310 and −370 for PCl_3 and PBr_3 respectively compared to −120 for PO_4^{3-}.

(h) $|(\partial\sigma/\partial\Delta r)_e|$ increases with increasing J. An example of this correlation is shown in Fig. 17 for ^{19}F shielding derivatives with respect to C–F bond extension and the corresponding J(CF) for the fluoromethanes.[11]

These systematic trends in the derivatives account for the observed dependence of isotope shifts on electronegativity of substituents, bond order, etc.[8] Thus the electronic factor is mainly responsible for the observed correlations between the magnitude of the isotope shift and the bond order (or bond length), the spin–spin coupling, and the chemical shift which have been noted (as illustrated in Fig. 2).

V. ISOTOPE EFFECTS OVER MORE THAN ONE BOND

Isotope shifts due to substitution with a heavier atom at a site remote from the observed nucleus show the same general trends as one-bond isotope shifts. (i) The sign is still generally negative although some are positive, with some alternation of signs being observed in the same molecule. (ii) The magnitude reflects the chemical shift range of the observed nucleus. (iii) The magnitude is related to the fractional mass change. (iv) The effect is additive.

In the theoretical interpretation of n-bond isotope shifts ($n>1$) we need to consider at least two contributions: (i) the secondary changes in shielding with extension of the remote bond due to a primary change in the mean bond length at the substitution site, and (ii) the primary change in shielding with extension of the bond directly involving the observed nucleus due to the secondary change in this mean bond length accompanying isotopic substitution at a remote site. We can write this as follows:

$$^n\Delta A(^{m'/m}X) = S\Delta + P\delta + \cdots \qquad (93)$$

where $S \equiv (\partial\sigma^A/\partial\Delta r_{XY})_e$ is a secondary shielding derivative, $P \equiv (\partial\sigma^A/\partial\Delta r_{AZ})_e$ is a primary derivative, Δ is the primary change in the X–Y bond length, $\Delta = \langle\Delta r_{XY}\rangle - \langle\Delta r_{XY}\rangle^*$ when ^mX is replaced by $^{m'}X$ and $\delta = \langle\Delta r_{AZ}\rangle - \langle\Delta r_{AZ}\rangle^*$ is the secondary change in the A–Z bond length due to $^{m'/m}X$ substitution. There are also quadratic and higher order terms which have not been included in equation (93), as well as secondary-secondary terms such as $(\partial\sigma^A/\partial\Delta r_{ZY})_e\delta'$ which should be generally smaller than the secondary-primary and primary-secondary terms shown in equation (93). The magnitudes of secondary second derivatives of the type $(\partial^2\sigma^A/\partial\Delta r_{XY}^2)_e$ are unknown for any molecule except water.[76] Therefore we will limit our discussion to terms shown in equation (93).

It is easy to see why n-bond isotope shifts are in general smaller than one-bond isotope shifts. While the latter involve a primary electronic factor and a primary dynamic factor, n-bond shifts ($n>1$) involve at least one secondary factor in each term. The further away the substitution site is from the observed nucleus, the smaller the secondary factor (either δ or S). In the water molecule in Fig. 8(d) it is clear that the change in the ^1H shielding upon extension of the other O–H bond is much less pronounced than the change upon extension of the immediate bond. The sign of the secondary shielding derivative or the secondary isotope effect on the bond length is not necessarily the same for most systems, because secondary effects are more dependent on the details of the electronic distribution and the potential surface. Thus positive signs for n-bond isotope shifts are quite possible.

The magnitude of the derivatives should still reflect the sensitivity of a given nucleus to its electronic environment, i.e. the secondary derivatives should be dependent on this sensitivity just as the primary derivatives have been shown to be. The dependence of Δ on fractional mass change has already been established in consideration of one-bond isotope shifts, whereas the dependence of δ on these factors has not. Finally, the additivity of 2-bond isotope shifts has also been established by the $CH_{4-n}D_n$ example.[90] This can be written as follows in terms of the primary (P) and secondary (S) derivatives of ^1H shielding:

$$\sigma^H(CH_{4-n}D_n) - \sigma^H(CH_{4-n'}D_{n'}) = (n'-n)\{S[\Delta - \theta(\delta)] + P\delta\}$$

neglecting rotational contributions. $\theta(\delta)$, the term of order δ, can be neglected relative to Δ, leading to $(n'-n)[S\Delta + P\delta]$, which is an isotope shift linearly dependent on the number of substitutions. Thus we see that the additivity extends to both terms in equation (93). The secondary change in the mean bond lengths is very small, e.g. for D substitution it is $\sim 1\times10^{-5}$ Å compared to the $\sim 5\times10^{-3}$ Å typical for a primary change as in $\Delta = \langle\Delta r_{CH}\rangle - \langle\Delta r_{CD}\rangle$. The numbers are of this relative order also for δ and Δ in H_2O.[76] Because of this, the term involving δ in equation (93) is usually much less important than the term involving Δ. It is possible to estimate the secondary shielding derivative S from a measured n-bond isotope shift if the primary shielding derivative P is known from other sources (such as the temperature dependence of shielding) and both Δ and δ are calculated with an adequate force field.

Some secondary derivatives obtained in this way are given in Table 19. We note that these are about one order of magnitude smaller than the values

TABLE 19

Derivatives of nuclear shielding with respect to extension of a remote bond $(\partial\sigma^A/\partial\Delta r_{XY})_e$.

Nucl.	Molecule	r_{XY}	$(\partial\sigma^A/\partial\Delta r_{XY})_e$	Ref.
^1H	H_2O	OH′	−4.6	76
	CH_4	CH′	−1.3	35
			−2.6	135
^{19}F	$CFCl_3$	CCl	−70	94
	CHF_3	CH	−84	11
	$S{=}CF_2$	CS	−284	102
	$F_2C{=}CFH$ (*trans*)	CH	−30	148
	(*cis*)	CH	−23	148
	(*gem*)	CH	−78	148
	$F_2C{=}CH_2$ (*trans*)	CH	−47	148
	(*cis*)	CH	−33	148
^{13}C	$H_3C{-}CH_3$	CH	−12.4	~~140~~ /35
	$H_2C{=}CH_2$	CH	+5.3	~~140~~ /35
	$HC{\equiv}CH$	CH	+12.5	~~140~~ /35
^{17}O	UO_2^-	UO′	−300	102

of primary derivatives in Table 18. These secondary derivatives of nuclear shielding correlate with the spin–spin coupling constants over the same bond path. For example, the *cis*, *trans* and *gem* HF coupling constants in trifluoroethene are −2, +10 and +72 Hz respectively, the magnitudes being in the same order as the magnitudes of the secondary derivatives in Table 19. The chemical shifts upon substitution of atoms *cis*, *trans* and *gem* away from the observed nucleus also are in this relative order.[148]

The correlations found between isotope shifts and the spin–spin coupling constants or substituent effects on chemical shifts indicate that the dominating electronic factor in isotope shifts involves the same electronic transmission path. Furthermore, two-bond isotope shifts are found to correlate with the bond length at the substitution site.[134] These imply that the term $S\Delta$ is the one of major importance in determining the isotope shift. This is fortunate, since the secondary dynamic effects are sensitive to the fine details of the force field and require a reasonably good vibrational calculation to get even the sign of δ right. On the other hand, the magnitude of Δ is fairly easy to calculate or estimate as we have seen in Section IV.B. This is of practical importance because this allows the estimation of secondary derivatives $S = (\partial\sigma^A/\partial\Delta r_{XY})_e$ directly from $^n\Delta A(^{m'/m}X)$ knowing only the X–Y bond length and the masses m_Y, m' and m. Like substituent shifts and spin–spin coupling constants, the secondary derivatives of the shielding tell us the extent to which the electron distribution at one point in the molecule

is affected by the perturbations that occur at a remote site. This information is transmitted through bonds and therefore carries information about molecular structure. There are some interesting examples of this. The dihedral angle dependence of the three-bond isotope shift,[149] $^3\Delta^{13}C(^{2/1}H) = -0.080$ ppm for $\theta \approx 0°$, -0.050 ppm for $\theta \approx 30°$ and $\gtrsim -0.020$ ppm for $\theta \approx 90°$, shows some dependence on proximity, not quite analogous to the Karplus relationship for vicinal coupling across the same electronic transmission path. The two- and three-bond isotope shifts in fluoroethanes show good correlations with couplings across the same transmission path:

$$|^3\Delta_{cis}{}^{19}F(^{2/1}H)| < |^3\Delta_{trans}{}^{19}F(^{2/1}H)| < |^2\Delta_{gem}{}^{19}F(^{2/1}H)|$$

in the same order as $^3J_{cis}(HF)$, $^3J_{trans}(HF)$ and $^2J_{gem}(HF)$ for several compounds,[148] which is also the same ordering as the magnitudes of the ^{19}F substituent shifts.

Long-range isotope shifts are observed in conjugated systems just as are coupling constants and substituent shifts. Some alternation of signs of isotope shifts is observed in such cases, as it is in the coupling over the same π system.[150] The same transmission of electronic information that gives rise to the shielding changes over many bonds in a π system upon chemical substitution also gives rise to the much smaller shielding changes upon isotopic substitution. The efficiency of the transmission of electronic information is indicated by the small secondary derivatives of shielding. These secondary derivatives are not easily calculated with *ab initio* methods since one needs to do calculations on fairly large molecules in order to study long-range effects. However, the semi-empirical methods which have been used for long-range couplings in conjugated systems may suggest a parallel approach for the calculation of secondary derivatives over the same pathways.

In the foregoing we have always implicitly assumed the Born–Oppenheimer approximation, i.e. that the rovibrational averaging occurs in the same potential energy surface and shielding surface for both isotopomers. The interpretation of the isotope shifts in terms of two factors, the dynamic and the electronic factor, is a consequence of the Born–Oppenheimer approximation and is not possible in cases where this separation is not valid, e.g. if Jahn–Teller effects occur. Other properties such as the electric dipole moment of HD or CH_3D are entirely due to a breakdown in the Born–Oppenheimer approximation. Although the observed effect, the chemical shift, is the same as that which would be observed if the hydrogen and the deuterium acted as if their electronegativities were different, it is not necessary to assume this. The NMR isotope shift data which have been reported so far can be interpreted with the foregoing theory without having to assume Born–Oppenheimer breakdown. Thus we would like to discourage the use of terms such as "isotope-induced inductive effect" of a deuterium

relative to a hydrogen,[151] or "hyperconjugation", which have been used in interpretation of some isotope shifts.[152] Both concepts imply that a Born-Oppenheimer breakdown is responsible for the observed isotope shift. In the cases when such models have been applied, the rovibrational averaging model within the context of the Born-Oppenheimer approximation is entirely sufficient.

VI. TEMPERATURE AND SOLVENT EFFECTS ON ISOTOPE SHIFTS

Figures 3 and 4 show that the rovibrationally averaged shielding changes with temperature in a parallel fashion for both isotopomers. Therefore, although the shielding temperature dependence may be large (e.g. it is calculated to be 1.56×10^{-3} ppm deg^{-1} for ^{19}F in HF in the range 100-500 K), the temperature dependence of the isotope shift will be very small, and probably very difficult to measure. In the case of the HD-D_2 system, Beckett and Carr[45] observed the temperature dependence of the isotope shift. Since the magnitude of the isotope shift at any one temperature can be used to obtain $(\partial\sigma/\partial\Delta r)_e$, and since this derivative can then be used to predict the temperature dependence of the shielding in both isotopomers, the magnitude and the temperature coefficient of the isotope shift are related to one another. Raynes and Panteli[70] have shown that the temperature dependence observed by Beckett and Carr is consistent in this way with the magnitude of the isotope shift at 300 K.

The temperature dependence of the isotope shift in diatomic molecules (other than H_2) is given by equation (40). The temperature dependent factor is $\{\coth(hc\omega/2kT)-(\mu/\mu^*)^{\frac{1}{2}}\coth[hc(\mu/\mu^*)^{\frac{1}{2}}\omega/2kT]\}$. For example, $^1\Delta^{19}F(^{37/35}Cl)$ in ClF has been calculated to be -0.0886 ppm at 300 K. In the temperature range 280-350 K the isotope shift in ClF changes from 1.027 to 0.93 times the value at 300 K.[39] The temperature factor shown above predicts that the magnitude of the isotope shift should decrease with increasing temperature for diatomic molecules. Similar factors for polyatomic molecules lead to the same prediction for these as well. This temperature dependence has been verified experimentally for $^1\Delta^{19}F(^{34/32}S)$ in SF_6 and $^2\Delta^{19}F(^{34/32}S)$ in $S{=}CF_2$. The isotope shifts are -0.0552 ppm (at 225 K), -0.0530 ppm (at 293 K) for SF_6 and -0.0138 ppm (at 210 K) and -0.0119 ppm (at 293 K).[134] Somewhat larger changes have been observed in several other ^{34}S-induced ^{19}F isotope shifts in SOF_2, SO_2F_2, SO_2ClF and $CF_3S(O)F$,[134] which could be partly attributed to the larger amplitudes of motion in these fluxional molecules.

When unusual sign and/or unexpectedly large isotope shifts are observed, the possible involvement of chemical or conformational equilibria should

be investigated. These would exhibit temperature dependence and solvent effects which are larger than are normally observed for intrinsic isotope shifts. An example might be the unusual positive isotope shifts of ^{67}Zn in various zinc salts. It has been pointed out that these shifts may be due to solvent dependent equilibrium positions between inner- and outer-sphere complexes. The tendency for a halogen to enter the first coordination sphere is more pronounced in D_2O than in H_2O so the large positive shifts in $ZnBr_2/D_2O$ may be traced to an effective removal of D_2O ligands by bromide.[153] In those cases where conformational or chemical equilibria can be excluded with some certainty, the effects of intermolecular interactions on isotope shifts have been found to be small. For example, a linear density dependence of $^1\Delta^2D(^{2/1}H)$ has been measured in gas samples having densities up to 840 amagat; the magnitude of the isotope shift decreases with increasing density. This observation has been explained as follows:[17]

$$\begin{aligned}\sigma^{HD}(T,\rho)&=\sigma_0{}^{HD}+\sigma_1{}^{HD}(T)\rho+\cdots\\ \sigma^{D_2}(T,\rho)&=\sigma_0{}^{D_2}+\sigma_1{}^{D_2}(T)\rho+\cdots\end{aligned}\tag{94}$$

$(\sigma_0{}^{D_2}-\sigma_0{}^{HD})$ is the isotope shift in the zero-pressure limit, and $(\sigma_1{}^{D_2}-\sigma_1{}^{HD})$ is the difference in the effects of binary collisions on the two species. Both σ_1 values are expected to be normal (i.e. negative). The greater magnitude of the σ_1 in D_2 molecules interacting with other (D_2 or HD) molecules is due to the more exposed deuterium nucleus in D_2 (where each D is $r_e/2$ from the centre of mass) compared to HD (where the D nucleus is $r_e/3$ from the centre of mass). A calculation using the nuclear site effect model gives -0.049×10^{-4} ppm amagat^{-1} for this difference, which compares favourably with the experimental result which is $-(0.059\pm0.026)\times10^{-4}$ ppm amagat^{-1}. For polyatomic molecules dissolved in a liquid the solvent effect on the isotope shift may be considered in terms of the smaller average volume of a D atom undergoing vibrational averaging; compared to an H atom in the same bond, the solvent molecules can get closer to the D atom. Since differences in site factors are small, the solvent effects on isotope shifts are expected to be small except when specific interactions such as hydrogen bonding are involved. This is very fortunate because this allows the determination of accurate isotope shifts in solution where conditions can be arranged so as to obtain favourable linewidths, as opposed to the very difficult zero-pressure limit measurements.

VII. CONCLUSIONS

We have presented the theoretical basis for isotope shifts in NMR. We find that the theory gives a good account of generally observed trends as well as some of the more specific correlations with electronic structure and

with other molecular properties. In some specific cases in which *ab initio* calculations have been carried out the theory gives semi-quantitative agreement with experiment.

Isotope shifts are due to rovibrational effects and can be described by an electronic factor multiplied by a dynamic factor. The nearly uniform sign (negative) which is observed in one-bond isotope shifts comes from the nearly uniform sign (negative) of the electronic factor (the shielding increases as the bond gets shorter) combined with the widely observed shortening of the average bond length upon heavy isotope substitution.

The dynamic factor depends on the masses of the atoms involved in the bond. It has been possible to express the change in the mean bond length upon isotopic substitution in a simple form depending on the masses of the atoms involved in the bond, so that it becomes possible to estimate the dynamic factor from the bond length. The mass factor confirms the observed dependence of isotope shifts on the fractional change in mass. It favours the observation of isotope shift upon substitution of light atoms while observing heavy nuclei.

Because the dynamic factor is easily estimated, the electronic factor can be directly extracted from the measured isotope shift to a first approximation. Thus the one-bond isotope shift serves as an index of the chemical bond. The correlations of isotope shifts with other properties such as spin–spin coupling, bond order, bond length or electronegativity of substituents are then interpretable as manifestations of the sensitivity of the shielding derivative $(\partial\sigma/\partial\Delta r)_e$ to these chemical parameters.

Based on what we have shown here about the nature of the dynamic and electronic factors, it is possible to predict the order of magnitude of one-bond isotope shifts for any combination of atoms. Thus it is possible to make an *a priori* estimate of the feasibility of observation of one-bond isotope shifts involving any two atoms.

The additivity of isotope shifts has been shown to be due to the additive nature of mean bond length changes and provides an easily recognizable pattern in the spectrum, i.e. equally spaced peaks corresponding to each isotopomer with substitution at equivalent sites.

The isotope shift over more than one bond is interpreted in a similar way. Although there are secondary effects on bond lengths at nuclear sites remote from the substitution site, the important contribution seems to come from the primary change in bond length at the substitution site combined with a secondary electronic factor, the derivative of nuclear shielding with respect to the extension of a remote bond. Thus, with the given estimation methods for the dynamic factor, it is possible to obtain the change in nuclear shielding upon extension of a remote bond to a first approximation. This serves as an index of the electronic transmission path just as the spin–spin coupling does, and is therefore a useful tool in characterizing molecular electronic structure.

Isotope shifts are thus understood in principle. However, the *ab initio* calculation of long-range isotope shifts has not yet been attempted. A suitable model for estimating the change in shielding upon remote bond extension would be very useful.

The unusual sign of a few one-bond isotope shifts is still to be explained, although some of these can be excluded from consideration because isotopic effects on chemical equilibrium may be involved.

The theoretical model discussed here has also been successfully applied to the primary and secondary effects of isotopic substitution on spin–spin couplings which are reported elsewhere.[154]

ACKNOWLEDGMENT

This review was written while the authors were visiting the Department of Theoretical Chemistry, Cambridge University, for which we thank Professor A. D. Buckingham.

REFERENCES

1. H. Batiz-Hernandez and R. A. Bernheim, *Progr. NMR Spectrosc.*, 1967, **3**, 63.
2. (a) P. E. Hansen, in *Annual Reports on NMR Spectroscopy*, Vol. 15 (G. A. Webb, ed.), Academic Press, London, 1983, p. 105. (b) D. A. Forsyth, in *Isotopes in Organic Chemistry*, Vol. 6 (E. Buncel and C. C. Lee, eds), Elsevier, Amsterdam, 1984, p. 1.
3. W. Gombler, *J. Am. Chem. Soc.*, 1982, **104**, 6616.
4. H. J. Jakobsen, A. J. Zozulin, P. D. Ellis and J. D. Odom, *J. Magn. Reson.*, 1980, **38**, 219.
5. K. K. Andersson, S. B. Philson and A. B. Hooper, *Proc. Nat. Acad. Sci. USA*, 1982, **79**, 5871.
6. J. M. Risley, S. A. Defrees and R. L. Van Etten, *Org. Magn. Reson.*, 1983, **21**, 28.
7. M. Cohn and A. Hu, *J. Am. Chem. Soc.*, 1980, **102**, 913.
8. C. J. Jameson, in *Specialist Periodical Report on NMR*, Vol. 10 (G. A. Webb, ed.), Royal Society of Chemistry, London, 1981.
9. S. G. Frankiss, *J. Phys. Chem.*, 1963, **67**, 752.
10. R. D. Sammons, P. A. Frey, K. Bruzik and M. D. Tsai, *J. Am. Chem. Soc.*, 1983, **105**, 5455.
11. C. J. Jameson and H. J. Osten, *Mol. Phys.*, ~~in press.~~ 1985, 56, 1083
12. J. R. Everett, *Org. Magn. Reson.*, 1982, **19**, 86.
13. C. J. Jameson, *Mol. Phys.*, 1985, **54**, 73.
14. H. J. Osten and C. J. Jameson, *J. Chem. Phys.*, 1985, **82**, 4595.
15. N. F. Ramsey, *Phys. Rev.*, 1952, **87**, 1075.
16. C. J. Jameson, *Bull. Magn. Reson.*, 1980, **3**, 3.
17. C. J. Jameson, A. K. Jameson and D. Oppusunggu, *J. Chem. Phys.*, 1984, **81**, 2313.
18. R. A. Hegstrom, *Phys. Rev.* (A), 1979, **19**, 17.
19. H. Wind, *J. Chem. Phys.*, 1965, **42**, 2371; **43**, 2956.
20. G. Riley, W. T. Raynes and P. W. Fowler, *Mol. Phys.*, 1979, **38**, 877.
21. P. W. Fowler, *Mol. Phys.*, 1981, **43**, 591.

22. P. W. Fowler, *Mol. Phys.*, 1982, **46**, 913; 1984, **51**, 1423.
23. E. B. Wilson, J. C. Decius and P. C. Cross, *Molecular Vibrations*, McGraw-Hill, New York, 1955.
24. A. R. Hoy, I. M. Mills and G. Strey, *Mol. Phys.*, 1972, **24**, 1265.
25. I. M. Mills, *J. Phys. Chem.*, 1976, **80**, 1187.
26. M. Toyama, T. Oka and Y. Morino, *J. Mol. Spectrosc.*, 1964, **13**, 193.
27. E. B. Wilson and J. B. Howard, *J. Chem. Phys.*, 1936, **4**, 260.
28. H. H. Nielsen, *Rev. Mod. Phys.*, 1951, **23**, 90.
29. G. Amat, H. H. Nielsen and G. Tarrago, *Rotation-Vibration of Polyatomic Molecules*, Dekker, New York, 1971.
30. R. W. James, *Physik. Z.*, 1932, **33**, 737.
31. L. S. Bartell, *J. Chem. Phys.*, 1963, **38**, 1827; 1979, **70**, 4581 (and references cited therein).
32. P. Ehrenfest, *Z. Physik* (Leipzig), 1927, **45**, 455.
33. C. J. Jameson and H. J. Osten, *J. Chem. Phys.*, 1984, **81**, 4915.
34. C. J. Jameson and H. J. Osten, *J. Chem. Phys.*, 1984, **81**, 2556.
35. H. J. Osten and C. J. Jameson, *J. Chem. Phys.*, 1984, **81**, 4288.
36. S. Cyvin, *Molecular Vibration and Mean Square Amplitudes*, Elsevier, Amsterdam, 1968.
37. K. Kuchitsu, in *Molecular Structures and Vibration* (C. J. Cyvin, ed.), Elsevier, Amsterdam, 1972, Ch. 12.
38. P. W. Fowler, private communications.
39. C. J. Jameson, *J. Chem. Phys.*, 1977, **66**, 4983.
40. J. L. Dunham, *Phys. Rev.*, 1932, **41**, 713, 721.
41. R. M. Herman and S. Short, *J. Chem. Phys.*, 1968, **48**, 1266; 1969, **50**, 572.
42. W. T. Raynes, A. M. Davies and D. B. Cook, *Mol. Phys.*, 1971, **21**, 123.
43. R. Ditchfield, *Chem. Phys.*, 1981, **63**, 185.
44. D. F. Evans, *Chem. and Ind.*, 1961, 1960.
45. J. R. Beckett and H. Y. Carr, *Phys. Rev.* (A), 1981, **24**, 144.
46. D. K. Hindermann and C. D. Cornwell, *J. Chem. Phys.*, 1968, **48**, 2017.
47. P. Morse, *Phys. Rev.*, 1929, **34**, 57.
48. A. D. Buckingham and W. Urland, Chem. Rev., 1975, **75**, 113.
49. L. S. Bartell, *J. Chem. Phys.*, 1955, **23**, 1219.
50. R. E. Wasylishen, J. O. Friedrich, S. Mooibroek and J. B. Macdonald, *J. Chem. Phys.*, 1985, **83**, 548.
51. R. M. Stevens and W. N. Lipscomb, *J. Chem. Phys.*, 1964, **40**, 2238.
52. R. M. Stevens and W. N. Lipscomb, *J. Chem. Phys.*, 1964, **41**, 184.
53. R. M. Stevens and M. Karplus, *J. Chem. Phys.*, 1968, **49**, 1094.
54. E. A. Laws, R. M. Stevens and W. N. Lipscomb, *J. Chem. Phys.*, 1971, **54**, 4269.
55. W. T. Raynes and G. Stanney, *J. Magn. Reson.*, 1974, **14**, 378.
56. A. Saika and H. Narumi, *Can. J. Phys.*, 1964, **42**, 1481.
57. C. J. Jameson, *J. Chem. Phys.*, 1977, **66**, 4977.
58. C. J. Jameson and H. J. Osten, *J. Chem. Phys.*, 1984, **81**, 4300. (Erratum: *J. Chem. Phys.*, 1985, **83**, 915.)
59. D. R. Herschbach and V. W. Laurie, *J. Chem. Phys.*, 1961, **35**, 458.
60. I. M. Mills, in *Theoretical Chemistry*, Vol. 1 (R. N. Dixon, ed.), Royal Society of Chemistry, London, 1974, p. 110.
61. C. J. Jameson and A. D. Buckingham, *J. Chem. Phys.*, 1980, **73**, 5684.
62. R. F. W. Bader and A. D. Bandrauk, *J. Chem. Phys.*, 1968, **49**, 1666.
63. W. H. Flygare, *J. Chem. Phys.*, 1964, **41**, 793.
64. N. F. Ramsey, *Phys. Rev.*, 1950, **77**, 567; **78**, 699.
65. J. Verberne, I. Ozier, L. Zandu and J. Reuss, *Mol. Phys.*, 1978, **35**, 1649.
66. D. K. Hindermann and L. L. Williams, *J. Chem. Phys.*, 1969, **50**, 2839.
67. C. J. Jameson, A. K. Jameson, S. Wille and P. M. Burrell, *J. Chem. Phys.*, 1981, **74**, 853.

68. W. T. Raynes and B. P. Chadburn, *J. Magn. Reson.*, 1973, **10**, 218; *Mol. Phys.*, 1972, **24**, 853.
69. R. E. Wasylishen, *Can. J. Chem.*, 1982, **60**, 2194.
70. W. T. Raynes and N. Panteli, *Mol. Phys.*, 1983, **48**, 439.
71. P. W. Fowler, G. Riley and W. T. Raynes, *Mol. Phys.*, 1981, **42**, 1463.
72. W. T. Raynes, in *Specialist Periodical Reports on NMR*, Vol. 7 (R. J. Abraham, ed.), Royal Society of Chemistry, London, 1978, p. 1.
73. R. E. Wasylishen, S. Mooibroek and J. B. Macdonald, *J. Chem. Phys.*, 1984, **81**, 1057.
74. M. Schindler and W. Kutzelnigg, *Mol. Phys.*, 1983, **48**, 781.
75. D. M. Chipman, W. E. Palke and B. Kirtman, *J. Am. Chem. Soc.*, 1980, **102**, 3377.
76. P. W. Fowler and W. T. Raynes, *Mol. Phys.*, 1981, **43**, 65.
77. B. Sredni and S. Pinchas, *J. Magn. Reson.*, 1972, **7**, 289.
78. O. Lutz and H. Oehler, *Z. Naturforsch.*, 1977, **32a**, 136.
79. P. W. Fowler, *Mol. Phys.*, 1983, **48**, 153; V. M. Mamayev and N. M. Sergeyev, *Chem. Phys. Lett.*, 1975, **34**, 317.
80. A. Chedin, *J. Mol. Spectrosc.*, 1979, **76**, 430.
81. Z. Cihla and A. Chedin, *J. Mol. Spectrosc.*, 1971, **40**, 337.
82. I. Suzuki, *J. Mol. Spectrosc.*, 1968, **25**, 479.
83. M. Lacy, *Mol. Phys.*, 1982, **45**, 253.
84. M. Lacy and D. H. Whiffen, *Mol. Phys.*, 1982, **45**, 241.
85. A. Chedin, C. Amiot and Z. Cihla, *J. Mol. Spectrosc.*, 1976, **63**, 348.
86. I. Suzuki, *J. Mol. Spectrosc.*, 1969, **32**, 54.
87. R. J. Mawhorter, M. Fink and B. T. Archer, *J. Chem. Phys.*, 1983, **79**, 170.
88. A. D. Kohl and R. L. Hilderbrandt, *J. Mol. Struct. Theochem.*, 1981, **85**, 325.
89. D. H. Whiffen, *Mol. Phys.*, 1980, **39**, 391.
90. C. J. Jameson and H. J. Osten, *J. Chem. Phys.*, 1984, **81**, 4293.
91. J. L. Duncan, in *Specialist Periodical Reports on Molecular Spectroscopy*, Vol. 3 (R. F. Barrow, D. A. Long and D. J. Millen, eds), Royal Society of Chemistry, London, 1975, p. 104.
92. T. Shimanouchi, *Pure Appl. Chem.*, 1963, **7**, 131.
93. H. C. Urey and C. A. Bradley, *Phys. Rev.*, 1931, **38**, 1969.
94. C. J. Jameson and H. J. Osten, *Mol. Phys.*, 1985, **55**, 383.
95. T. Shimanouchi, *J. Chem. Phys.*, 1949, **17**, 245.
96. K. Kuchitsu and L. S. Bartell, *J. Chem. Phys.*, 1962, **36**, 2460.
97. R. H. Boyd and L. Kesner, *J. Chem. Phys.*, 1980, **72**, 2179.
98. J. Kestin, S. T. Ro and W. Wakeham, *Physica*, 1972, **58**, 165.
99. L. S. Bartell, *J. Chem. Phys.*, 1963, **38**, 1827.
100. L. S. Bartell, S. K. Doun and S. R. Goates, *J. Chem. Phys.*, 1979, **70**, 4585.
101. W. Gombler, *J. Magn. Reson.*, 1982, **53**, 69.
102. H. J. Osten, unpublished calculations.
103. C. J. Jameson, *J. Chem. Phys.*, 1977, **67**, 2814.
104. D. K. Hindermann and C. D. Cornwell, *J. Chem. Phys.*, 1968, **48**, 4148.
105. M. Alei and W. E. Wageman, *J. Chem. Phys.*, 1978, **68**, 783.
106. O. Lutz, D. Nolle and D. Staschewski, *Z. Naturforsch.*, 1978, **38a**, 380.
107. R. E. Wasylishen and J. O. Friedrich, *J. Chem. Phys.*, 1984, **80**, 585.
108. B. E. Smith, B. D. James and R. M. Peachey, *Inorg. Chem.*, 1977, **16**, 2057.
109. W. M. Litchman, M. Alei and A. E. Florin, *J. Chem. Phys.*, 1969, **50**, 1897.
110. A. K. Jameson and C. J. Jameson, *J. Magn. Reson.*, 1978, **32**, 455.
111. M. R. Bendall and D. M. Doddrell, *Austral. J. Chem.*, 1978, **31**, 1141.
112. G. Herzberg, *Infrared and Raman Spectra of Polyatomic Molecules*, Van Nostrand Reinhold, New York, 1945.
113. H. J. Bernstein and A. D. E. Pullin, *J. Chem. Phys.*, 1953, **19**, 1409.

114. D. L. Gray and A. G. Robiette, *Mol. Phys.*, 1979, **37**, 1901.
115. P. Pulay, W. Meyer and J. E. Boggs, *J. Chem. Phys.*, 1978, **68**, 5077.
116. C. R. Lassigne and E. J. Wells, *J. Magn. Reson.*, 1978, **31**, 195.
117. J. Bigeleisen and P. Goldstein, *Z. Naturforsch.*, 1963, **21a**, 205.
118. Y. N. Luzikov and N. M. Sergeyev, J. *Magn. Reson.*, 1984, **60**, 177.
119. C. J. Jameson and H. J. Osten, *J. Am. Chem. Soc.*, 1985, **107**, 4158.
120. M. J. Buckingham, G. E. Hawkes, I. M. Ismail and P. J. Sadler, *J. Chem. Soc., Dalton Trans.*, 1982, 1167.
121. G. Lowe, B. V. L. Potter, B. S. Sproat and W. E. Hull, *J. Chem. Soc., Chem. Commun.*, 1979, 733.
122. C. Roeske, P. Paneth, M. H. O'Leary and W. Reimschussel, *J. Am. Chem. Soc.*, 1985, **107**, 1409.
123. O. Lutz, A. Nolle and P. Kroneck, *Z. Phys.* (A), 1977, **282**, 157.
124. C. J. Jameson and H. S. Gutowsky, *J. Chem. Phys.*, 1964, **40**, 1714.
125. R. G. Barnes and W. V. Smith, *Phys. Rev.*, 1954, **93**, 95.
126. T. A. Carlson, C. C. Lu, T. C. Tucker, C. W. Nestor and F. B. Malik, *Eigenvalues, Radial Expectation Values, and Potentials for Free Atoms from Z = 2 to 126 as calculated from Relativistic Hartree-Fock-Slater Atomic Wave Functions*, Oak Ridge National Laboratory, 1970, pp. 1-29.
127. R. E. Wasylishen, D. H. Muldrew and K. J. Friesen, *J. Magn. Reson.*, 1980, **41**, 341.
128. K. U. Buckler, A. R. Haase, O. Lutz, N. Muller, and A. Nolle, *Z. Naturforsch.*, 1977, **32a**, 126.
129. K. J. Franklin, C. J. L. Lock, G. B. Sayer and G. J. Schrobilgen, *J. Am. Chem. Soc.*, 1982, **104**, 5303.
130. J. Jokisaari and K. Raisanen, *Mol. Phys.*, 1978, **36**, 113.
131. J. Jokisaari, K. Raisanen, L. Lajunen, A. Passoja and P. Pyykko, *J. Magn. Reson.*, 1978, **31**, 121.
132. V. P. Tarasov, V. I. Privalov, Y. A. Buslaev and U. Eichhoff, *Z. Naturforsch.*, 1984, **39b**, 1230.
133. R. J. Gillespie and J. W. Quail, *J. Chem. Phys.*, 1963, **39**, 2555.
134. W. Gombler, *Z. Naturforsch.*, 1985, **40b**, 782.
135. D. B. Chesnut, private communications.
136. M. Schindler and W. Kutzelnigg, *J. Chem. Phys.*, 1982, **76**, 1919.
137. T. Weller, W. Meiler, H. J. Kohler, H. Lischka and R. Holler, *Chem. Phys. Lett.*, 1983, **98**, 541.
138. D. B. Newmann and J. W. Moskowitz, *J. Chem. Phys.*, 1969, **50**, 2216.
139. K. Jackowski and W. T. Raynes, *Mol. Phys.*, 1977, **34**, 465.
140. D. B. Chesnut and A. L. Helms, *Theoret. Chim. Acta* (Berlin), 1981, **58**, 163.
141. J. O. Friedrich and R. E. Wasylishen, *J. Chem. Phys.*, 1985, **83**, 3707.
142. C. J. Jameson, A. K. Jameson, D. Oppusunggu, S. Wille, P. M. Burrell and J. Mason, *J. Chem. Phys.*, 1981, **74**, 81.
143. C. J. Jameson and H. J. Osten, to be published.
144. C. J. Jameson, A. K. Jameson and P. M. Burrell, *J. Chem. Phys.*, 1980, **73**, 6013.
145. C. J. Jameson, A. K. Jameson and J. Honarbakhsh, *J. Chem. Phys.*, 1984, **81**, 5266.
146. C. J. Jameson, *Mol. Phys.*, 1980, **40**, 999.
147. B. T. Hamdi, D. J. Reynolds and G. A. Webb, *Org. Magn. Reson.*, 1984, **22**, 90.
148. H. J. Osten, C. J. Jameson and N. C. Craig, *J. Chem. Phys.*, 1985, **83**, 5434.
149. J. L. Jurlina and J. B. Stothers, *J. Am. Chem. Soc.*, 1982, **104**, 4677.
150. S. Berger and H. Kunzer, *Angew. Chem. Int. Ed. Engl.*, 1983, **22**, 321.
151. K. L. Servis and F. F. Shue, *J. Am. Chem. Soc.*, 1980, **102**, 7233.
152. J. R. Wesener and H. Gunther, *Tetrahedron Lett.*, 1982, **23**, 2845.
153. D. Rehder, *Magn. Reson. Rev.*, 1984, **91**, 125.
154. C. J. Jameson and H. J. Osten, *J. Am. Chem. Soc.*, ~~in press~~. 1986, 108, 2497